HYDRODYNAMIC STUDIES AND REACTOR MODELLING OF A THREE PHASE SLURRY REACTOR IN FISCHER TROPSCH APPLICATION

by

Juan Ricardo Inga

B.Sc. Chemical Engineering (Universidad Nacional de Ingenieria
Lima-Peru)

This dissertation is submitted in partial fulfillment of the
requirements for the degree Master in Engineering in the
Faculty of Engineering, Potchefstroom University for
Christian Higher Education.

Supervisor : Prof. R. C. Everson

Co-supervisor : Mr. A.P. Steynberg

Potchefstroom

October 1992

Declaration

I declare that the work hereby submitted is my own, except where otherwise stated. The work presented has not been presented to any other university for the qualification of a degree.

Juan R. Inga

Acknowledgement

I would like to express my gratitude towards the following persons and institutions for the assistance received:

* Sastech Research and Development for the opportunity to do this work based on the Sasol Slurry Bed project, specially to Dr. Ben Jager, Manager of Process Development department.

* The Slurry bed process development team for helping in the data adquisition and the performing of different tests required for this work.

Mr. Renus Kelfkens	Chief Process Engineer
Mr. Luis Dancuart	Senior Process Engineer
Mr. Francois Malherbe	Area Head
Mr. Jan van Antwerpen	
Mr. Dawie Stols	

* The colleagues who helped me with the spelling and gramma of this thesis

Mr. Mike Smith
Miss. Lindsay Dawes
Mr. Radleigh Hartford

* Professor R.C. Everson, who acted as Mentor for his motivation and encouragement.

* Mr. Andre Steynberg, as my supervisor and project leader guided me in this stage of the development of my carreer.

*My wife Janni and my son John for their patience and support during the preparation of this work.

* My parents who taught me the first steps in Chemistry

* Last but not least, God, without His help this thesis would not have been possible

ABSTRACT

HYDRODYNAMIC STUDIES AND REACTOR MODELLING OF A THREE PHASE SLURRY REACTOR IN FISCHER TROPSCH APPLICATION

In this study the hydrodynamic characteristics of the slurry bed reactor was investigated. This study was aimed to the understanding of the important parameters that describe the hydrodynamic regime and their quantification .

In order to determine the relevant parameters the use of a theoretical model was necessary. This model should include all the hydrodynamic parameters in form of correlations. A sensitivity study was done and the parameters which have great impact, were determined.

An extensive literature review was done in order to gather the experience of previous investigations. Unfortunately all the experience was obtained in a different hydrodynamic regime and therefore the published results could not be used directly in our study.

Hydrodynamic test were performed in the works pilot plant at the operating conditions. Unlike a laboratory, the instrumentation used was the one use in commercial reactors with the commercially aceptable range of accuracy. A mass balance was done around the reactor to ensure that the data was sound.

Heat balance was also performed and the study of the heat transfer coefficient was performed. Although this was beyond the scope of this study was here included due to its importance in the design of slurry bed reactors.

An existing computer model was adapted for the churn-turbulent regime and the hydrodynamic parameters were implemented. This reactor model was coupled with flashes subroutines in order to have a complete reactor train. This computed model was used for the design of the Slurry Bed Commercial Reactor to be commisioned on 1993 at Sasol One.

OPSOMMING

'n HIDRODINAMIESE STUDIE EN REAKTOR MODELLERING VAN 'N DRIE FASE FLODDERBED REAKTOR IN 'N FISCHER TROPSCH TOEPASSING.

In hierdie studie is die hidrodinamiese karakteristieke van die flodderbed reaktor ondersoek. Daar is gepoog om die belangrike parameters wat 'n invloed op die hidrodinamika van die reaktor het te beskryf.

'n Teoretiese model is ontwikkel om sodoende die relevante parameters vas te stel. Al die parameters is in die vorm van korrelasies in die model ingesluit. 'n Sensitiwiteits analise is op hierdie parameters gedoen ten einde te bepaal watter die grootste inpak het.

'n Literatuur studie van vorige werk in hierdie studie veld is gedoen. Die meerderheid van publikasies is van toepassing op hidrodinamiese kondisies anders as in hierdie studie. Resultate van die publikasies kan dus nie in hierdie studie gebruik word nie.

Hidrodinamiese toetse is gedoen op 'n loodskaal reaktor by normale bedryfskondisies. Die instrumentasie was egter nie akkuraat nie. Aanpassings is gemaak deur 'n massa balans uit te voer oor die reaktor.

'n Hitte balans oor die loodskaal aanleg is bereken om die hitte oordrag koëffisiënt te bepaal. Alhoewel dit buite die studie veld val was dit belangrik vir die ontwerp van die kommersiële skaal flodderbed reaktor.

'n Bestaande rekenaar model is aangepas vir turbulente vloei en die hidrodinamiese parameters is geïmplimenteer. Hierdie model is gekoppel met flits berekening om die volledige reaktor trein te simuleer. Hierdie rekenaar model is ook gebruik vir die ontwerp van die kommersiële skaal flodderbed reaktor wat in 1993 by Sasol in bedryf gestel gaan word.

TABLE OF CONTENTS

APPENDIXES

LIST OF TABLES

LIST OF FIGURES

LIST OF SYMBOLS

a	Gas liquid interfacial area (m^{-1})
a_s	Liquid solid interfacial area (m^{-1})
A	Cross sectional area of the column (m^2)
a_H	Heat transfer area (m^2)
A_o	Heat transfer area outside the coils (m^2)
A_i	Heat transfer area inside the coils (m^2)
A_{avg}	Average heat transfer area (m^2)
Bo	Bond number $= \frac{g d_c^2 . \rho_L}{\sigma_L}$ (2.2.9)
$C_{s,i}$	Concentration of solids at i level (Kg/m^3)
$C_{s,o}$	Concentration of solids at the bottom of the column (Kg/m^3)
$C^*_{L,i}$	Concentration of i in the liquid at saturation point (mol/l)
$C_{i,j}$	Concentration of i at j phase (mol/lt)
C_R	Total reactants concentration in the gas phase (mol/lt)
d_o	Gas sparger orifice diameter (m)
d_c	Column diameter (m)
d_b	Bubble diameter (m)
D_g	Gas dispersion coefficient (m^2/s)
D_L	Liquid dispersion coefficient (m^2/s)
D_s	Solid dispersion coefficient (m^2/s)
$d_{v.s}$	bubble Sauter diameter (m)
D_i	Molecular difusivity of i (m^2/s)
$ds,equiv$	Equivalent particle size (m)
Da	Damkoler number $=\frac{Lw(1-\epsilon_g)k_L}{U'_g}$
Fr	Froude number $= \frac{u_g}{(g.d_c)^{0.5}}$

$Ga =$	Galileo number = $\frac{g d_c^3 \cdot \rho_L^2}{\mu_L^2}$
g	gravity (m/s^2)
ΔH_r	Heat of reaction (J/mol)
h_o	Heat transfer coefficient from the slurry to the cooling coils $(W/m^2 \cdot C)$
h_i	Heat transfer coefficient inside the cooling coils $(W/m^2 \cdot C)$
K	constant used in 2.2.10, described in table 2.3
k_L	Liquid side mass transfer coefficient (m/s)
k_o	Overall rate constant for the Hydrogen consumption (s^{-1})
k_s	Solid liquid mass transfer (cm/s)
k_c	reaction rate constant for Hydrogen consumption per unit of catalyst $(m^3/s.kg)$
L	Bed level (m)
Mo	Morton number = $\frac{g \mu_L^4}{\rho_L \sigma^3}$ used in 2.2.9
m	constant used to correlate actual solid concentration by the sedimentation model (2.4.3)
m_i'	Henry's law coefficient for i
MW	Molecular weight (g/mol)
m_i''	modified Henry's law coefficient = $\frac{m^i}{RT}$
$N_{g,i}$	Stanton Number for gas = $\frac{k_{L,i} \cdot a}{m_i \cdot U_g^o}$
$N_{L,i}$	Stanton number for liquid= $\frac{k_L . a . L}{u_L}$
Pe_g	Peclet number for the gas phase $\frac{u_g . L}{D_g}$
P	Pressure absolute (bar)
Pe_s	Peclet number for the solid phase $\frac{U_g \cdot d_c}{D_s}$
Q_g	Volumetric gas flow (m^3/s)
Q_L	volumetric liquid flow (m^3/s)
$R_{g,L}$	ratio between the liquid and gas slip velocities $\frac{\frac{U_L}{(1-\epsilon_g)}}{\frac{U_g}{\epsilon_g}}$
$Re_{o,L}$	Reinolds number for the orifice $\frac{\rho_L \cdot v_o \cdot d_o}{\mu_L}$

R	Radious of the column (m)
r	radial position in the column
$Re_{p,L}$	Reinolds number for the particle $\frac{\rho_p u_L}{\nu}$
$Re_{p,\infty}$	Reinolds number for settling particles $\frac{\rho_s d_p \cdot u_{p,s}}{\mu_L}$
Re_s	Reinolds number for a particle in three phase $\frac{d_s \rho_L \cdot u_{s,\infty}}{\mu_L}$
R_{FT}	Kinetic rate of the Fischer Tropsch synthesis (mol/m^3.s)
R	Gas ideal constant (Chapter 2.5)
R_i	Reaction rate of i
r_w	heat transfer resistance of the cooling coils wall (m^2.C/W)
r_i	fouling of the coils from inside (m^2.C/W)
r_o	fouling of the coils from the outside (m^2.C/W)
Sc	Schimt number $\frac{\mu_L}{\rho_L \cdot D_l}$
St_g	Stanton number $\frac{k_o \cdot R.T.L}{\dot{m}_H \cdot U_g^l}$
t_{mix}	mixing time for homogeneous distribution (s)
T	Temperature absolute (°K)
T_w	Temperature of the cooling coils (°K)
U	velocity (m/s)
$u_{L,r=i}$	liquid velocity at radial position i (m/s)
$U_{b,slip}$	Slip bubble velocity $U_b - u_L$ (m/s)
U_p	settling velocity of the particle (m/s)
U_o	Overall heat transfer coefficient (W/m^2·C)
$V_{c,s}$	liquid circulation velocity due to gas sparging (m/s)
V	volume of the reactor bed (2.5) (m^3)
We	Weber number of the nozzle $\frac{u_{g,o}^2 \cdot d_o \cdot \rho_g}{\sigma_L}$
w	catalyst mass per unit volume of slurry (kg/m^3)
X_{H_2+CO}	Hydrogen and Carbon monoxide conversion
X_s	mass percent of solid in slurry (fraction)
X_H	Hydrogen conversion
z	axial position (m)

Greek Letters

α	gas contraction
β	stoichiometric coefficient
γ	reaction stoichiometric coefficient
ϵ	holdup fraction of a phase
θ_i	dimensionless concentration of i with respect to Hydrogen at inlet
$\lambda_{a,x}$	effective heat conductivity of slurry (J/s. m^2 °K)
ξ	dimensionless axial position
ρ	density Kg/m^3
τ	mean residence time (s)
υ	solid - liquid contact angle
υ_i	stoichiometric coefficient (5.2.1)
υ	dimensionless gas velocity
$\phi_{s,o}$	volumetric fraction of solids kept constant along the column
x_s	catalyst concentration in mass fraction
ψ	sphericity
ω	mass of catalyst per unit of slurry volume (Kg/m^3)

Subscripts

b	bubble
c	column
eff	effective
f	feed
g	gas
L	liquid
o	orifice
p	particle
t	top of the bed
s	solid
sl	slurry
∞	terminal velocity

Superscript

e	exit
i	inlet
w	wall
–	average

1 INTRODUCTION

1.1 General

New technology in the synthesis of fuels has always been a field of investigation around the world. This has become of special importance in countries that do not have sufficient local oil resources or cannot obtain them in an economic way. Since 1973, with the energy crisis, the search for appropriate technology which can achieve the production of fuels at competitive prices has been emphasised. Many countries realized their great dependence upon imported crude oil made them vulnarable to unpredictable and often sudden fluctuations in international prices. The last event that threatened the world supplies of oil was the invasion of Kuwait by Irak in December 1990. This event ended with the military intervention of the USA and their allies. This showed the great dependance of the developed countries on the cheap and abundant oil supply.

The Fischer Tropsch synthesis is one route to the production of hydrocarbons. Currently there are several technologies available. A comparison of the required capital cost for a commercial unit was done by Fujimoto and Kunugi 1982:173) and can be seen in table 1.1. As can be seen the slurry technology (three phase fluidized bed reactor) is the cheapest alternative.

Another comparative study was done by Mills (1991). He concluded that the best alternative for indirect liquefaction of coal was the use of Shell gasification process and the Slurry Fischer Tropsch process for the hydrocarbon synthesis (table 1.2).

Table 1.1 : Comparative studies of Fischer Tropsch reactors

Reactor Type	**Relative Equipment Investment**	**Catalyst Cost** (10^3 \$/year)	**Heat Recovery as Steam (%)**
Entrained CFB	**100**	**6720**	**36+30**
Tube - Wall	**208**	**14200**	**85**
Slurry	**45**	**3420**	**91**
Ebullating	**65**	**14400**	**-**

Only a few countries were successful in their effort to produce synthetic fuels starting from coal or natural gas. The first successful experience working in three fluidized phases was in Germany just before World War II. Kolbel was working with a Rheinsprussen catalyst for the production of fuels.

Table 1.2: Improvements in Indirect Liquefaction of coal

Processes plant Output Bpsd	Lurgi + Arge	Shell + Arge	Shell + Slurry
Alcohols	1762	1836	1954
Propane	4467	4037	4207
Butane	5403	5522	5560
Gasoline	36450	32494	33953
Diesel	35419	39617	37828
Total	83501	83505	85503
Energy Efficiency %	48	53	59
Required selling price \$/Bbl	55	48	42

Sasol, in their continuous effort to develope better technologies has already gained knowledge in the HTFT (High Temperature Fischer-Tropsch) reactor systems. In place of the CFB (Circulating Fluidized Bed), a new reactor has been developed, the SASR (Sasol Advanced Synthol Reactor). And for the LTFT (Low Temperature Fischer-Tropsch), the proposed alternative to the standard fixed bed reactor (ARGE), would be the SSB (Sasol Slurry Bed) process. This is the commercial name for the three phase fluidized bed reactor. In both cases the capital cost is tremendously reduced, therefore the recuperation period is shorter.

The same approach was taken for both processes ie. trying to keep the same product distribution for the non-disturbance of the stabilised market and also aiming for the reduction of down time. This was done by including online catalyst withdrawal and addition facilities.

The three phase fluidized process is a flexible technology which can be used for different applications. One of the more recently applications is in biotechnology and waste water treatment.

1.2 Scope of work

The scope of this work is the study of all the hydrodynamic parameters that can affect the reactor performance in a three phase fluidized reactor.

To understand what happens inside the reactor, it is necessary to bear in mind the number of mechanisms resistances that limit the reaction rate of the process concerned. Since three phases are involved, the understanding of each of them separately as well as their combined effects are necessary to be able to model the process. One of the difficulties that Sasol has faced in the attempt to model the reactor is the lack of data that can be applied to our system.

One unique aspect of the SSB process is the gas space velocities used . No previous experience is known in this turbulent regime. Most of the data, correlations and operating experience have been obtained from work in the bubbly regime and with "easy to handle" systems, like air/water/glass beads, which give results that in fact cannot be used for design purposes in other systems.

The lack of data had to be overcome by the performance of experimental tests in a ?works pilot plant. One parameter very important from the operating point of view is the heat transfer coefficient. The determination of this parameter for our system was included in the scope of this work due to its dependancy on the hydrodynamics of the system

The results of this investigation were to be appropiate for incorporation into a computer model which could reproduce and predict reactor performance. This model would be as theoretical as possible in order to incorporate the effect of the different variables. no tests

The ultimate aim of this study was to predict the performance of the slurry bed commercial reactor to be built at Sasol One.

2 LITERATURE SURVEY

2.1 Classification of three phase reactors

Due to the great number of variables, an extensive literature survey was done. Bearing in mind that with three phases there are a number of systems that can be obtained by only varying the fluid flows or the particle sizes, it was necesary to focus on a system in which the three phases were fluidized.

L.S.Fan (1989 :3) proposed a comprehensive clasification based on the relative velocities of the liquid and the terminal settling velocities of the particles in gas-liquid media. The stages of fluidization are shown in figure 2.1 and can be described as follows:

When the drag force on the particles induced by the gas-liquid mixture is smaller than the effective weight of the particles, these particles would stay settled. This regime is called fixed bed.

If the gas-liquid velocity increases up to a point where the drag force is equal to the effective weight, it is said that the system is at the minimum fluidization velocity.

A further increase in the gas-liquid mixture velocity would produce an expanded bed regime until the gas or liquid velocity reaches the terminal velocity of the particle in the gas-liquid media. Beyond this point it is said that the system is in the transport regime.

Figure 2.1: Hydrodynamic regime for three phase systems

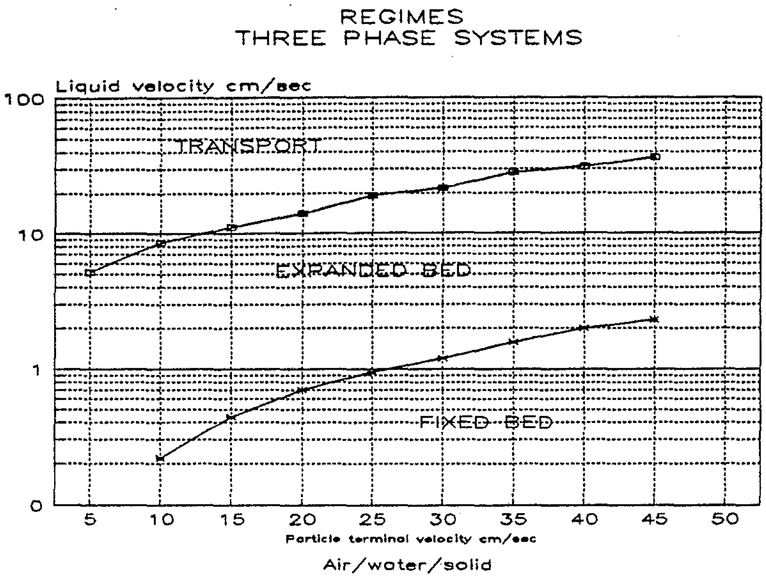

Table 2.1: Clasification of three phase reactors

Mode	Description	
E-I-a-1	Light particles, solid concentration profiles depending on liquid velocities	
E-I-a-2		
E-I-b	Particles in the bed are supported by the gas	
E-II-a-1	Inversed fluidized bed	Liquid higher density than solid.
E-II-a-2		Solid higher density than liquid phase.
E-II-b	Gas phase is the continuous phase (turbulent bed contactor)	
E-III-a	Solid loaded	Liquid continuous phase (Sasol SSB)
E-III-b	batch wise	Gas continuous phase (Sasol SAS)
T-I-a-1	Solids and gas are transported by liquid	
T-I-a-2	The gas is only used to make the particle size distribution uniform	
T-I-b	Gas is the continuous phase (liquid as droplets, carried by the gas)	
T-II-a	Slurry flows downwards	The gas passes through bubbling
T-II-b		The gas passes via an anular flow
T-III-a	Liquid as continuous phase	
T-III-b	Gas as continuous phase (liquid as droplets)	

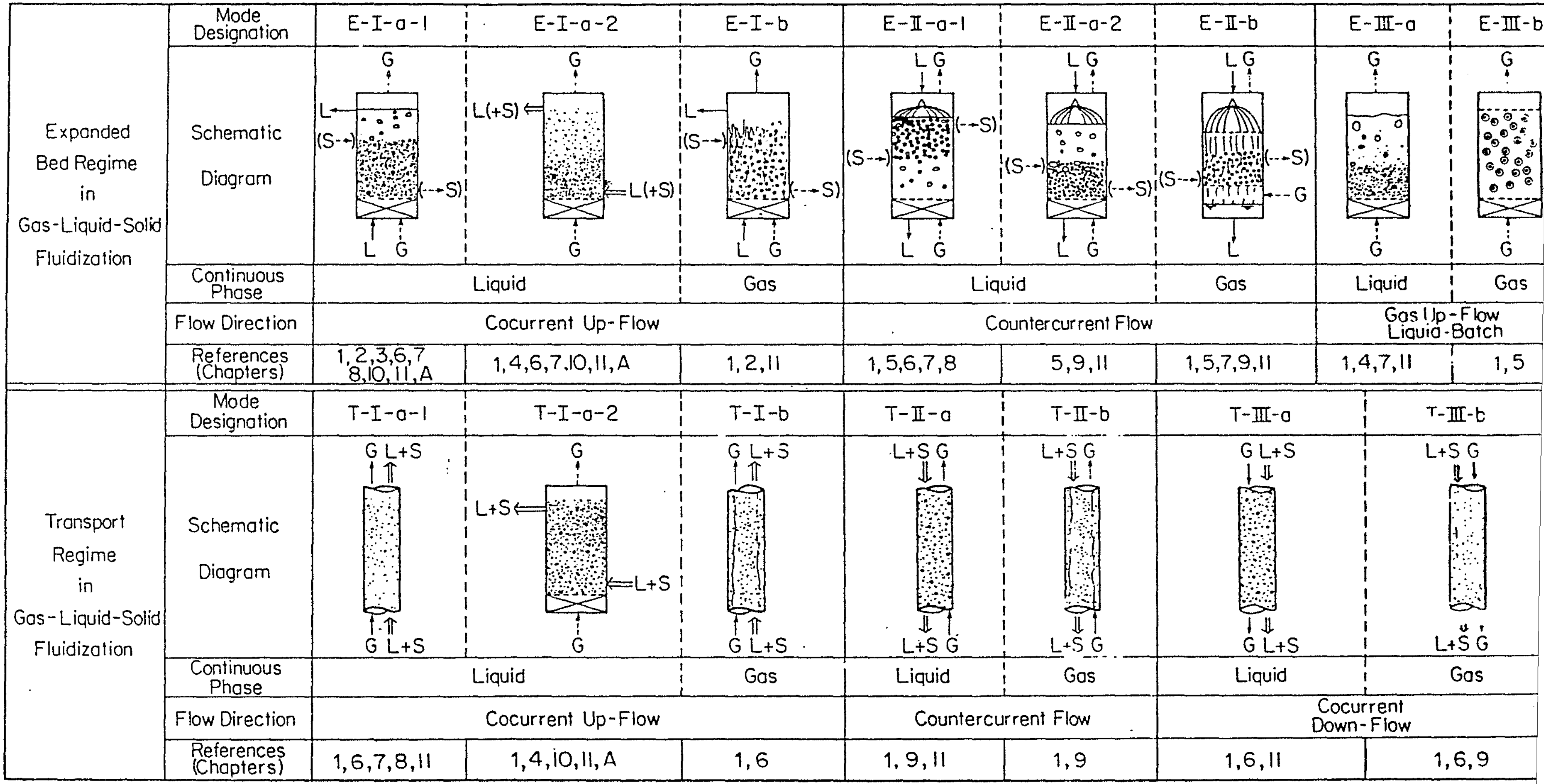

	Mode Designation	E-I-a-1	E-I-a-2	E-I-b	E-II-a-1	E-II-a-2	E-II-b	E-III-a	E-III-b
Expanded Bed Regime in Gas-Liquid-Solid Fluidization	Schematic Diagram								
	Continuous Phase	Liquid		Gas	Liquid		Gas	Liquid	Gas
	Flow Direction	Cocurrent Up-Flow			Countercurrent Flow			Gas Up-Flow Liquid-Batch	
	References (Chapters)	1,2,3,6,7 8,10,11,A	1,4,6,7,10,11,A	1,2,11	1,5,6,7,8	5,9,11	1,5,7,9,11	1,4,7,11	1,5

	Mode Designation	T-I-a-1	T-I-a-2	T-I-b	T-II-a	T-II-b	T-III-a	T-III-b
Transport Regime in Gas-Liquid-Solid Fluidization	Schematic Diagram							
	Continuous Phase	Liquid		Gas	Liquid	Gas	Liquid	Gas
	Flow Direction	Cocurrent Up-Flow			Countercurrent Flow		Cocurrent Down-Flow	
	References (Chapters)	1,6,7,8,11	1,4,10,11,A	1,6	1,9,11	1,9	1,6,11	1,6,9

(S--→) Independent Charge of Solids from Fluid (--→S) Independent Discharge of Solids from Fluid (+S) Charge or Discharge of Solids with Fluid
A : Appendix A

Figure 2.2 Basic classification of gas-liquid-solid fluidization systems.

The Sasol slurry bed process belongs in the gas-liquid-solid fluidized regime. Figure 2.2 shows the different regimes that can be obtained with the same material, just changing their velocities, the solid density or the particle size distribution.

The present study is related basically to modes E-III-a and E-I-a-2 from figure 2.2.

2.2 Gas phase hydrodynamic

2.2.1 Gas holdup

The gas holdup is the fraction which the gas phase occupies in the fluidized slurry.

Theoretically the gas holdup is defined as the relation of the gas linear velocity and the mean bubble velocity

$$\epsilon_g = \frac{u_g}{u_b}$$

There are two principle component of the gas holdup distribution. This distribution is the result of the behaviour of the gas bubbles. The most common circulation pattern assumes that the nett transport of the gas is held in the middle of the column, while in the section near the walls, the liquid returns to the bottom of the reactor carrying with it gas in the form of small bubbles (Molerus 1986:2686). This portion of the holdup produces most of the gas liquid interfacial area available.

Figure 2.3:Variation of gas holdup

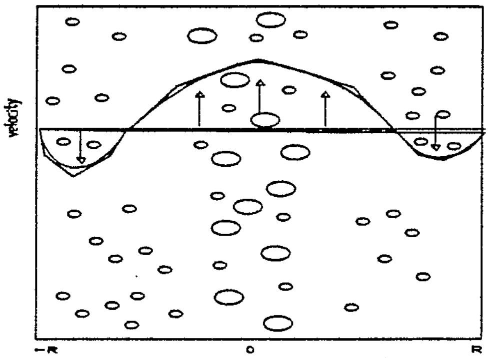

Small bubbles recirculate carried by the backmixing liquid

This concept is based on the transient response of the bed level measurements when the gas flow is suddenly stopped. The first gas to disengage from the bed is in the form of big bubbles (greater than 5 cm diameter). This can be seen from studies done in the CSIR with Sasol Arge wax (Van Vuuren 1988a, 1988b). The disengagement of the remaining gas from the bed takes more time. This portion is mainly bubbles with diameters smaller than 1 cm.

Figure 2.4: Dynamic disengagement in bubble columns

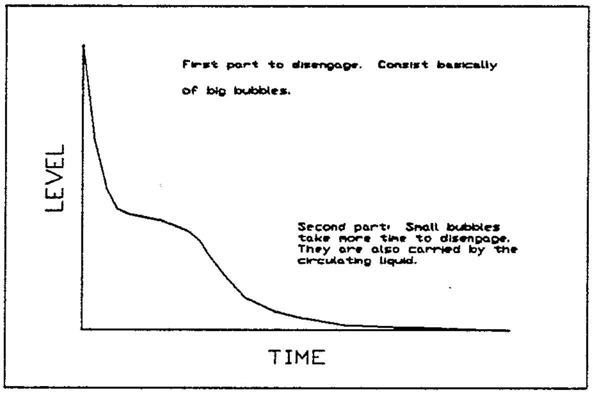

First part to disengage. Consist basically of big bubbles.

Second part: Small bubbles take more time to disengage. They are also carried by the circulating liquid.

2.2.2 Gas holdup hysteresis

This effect is commonly observed when the working velocities are very low (less than 10 cm/s) and when the gas velocity is increased or decreased. This phenomenon was reported by Bukur et al(1987:1088), Ueyama et al(1989:524), Maruyama et al (1985: 354) Prakash and Briens (1990: 204) and many other authors. Above a critical point the effect disappears and the holdup obtained at a certain gas velocity is the same whether it was obtained increasing the linear velocity or decreasing it. Ueyama, working with tap water and Nitrogen, found that this effect was produced by the impurities of the water and the oil that the gas carried over from the compressor. Bukur and Daly (1982: 2967) working with different waxes tried to explain this effect by the ageing of the waxes and the operational procedures.

Figure 2.5: Hysteresis effect in gas holdup

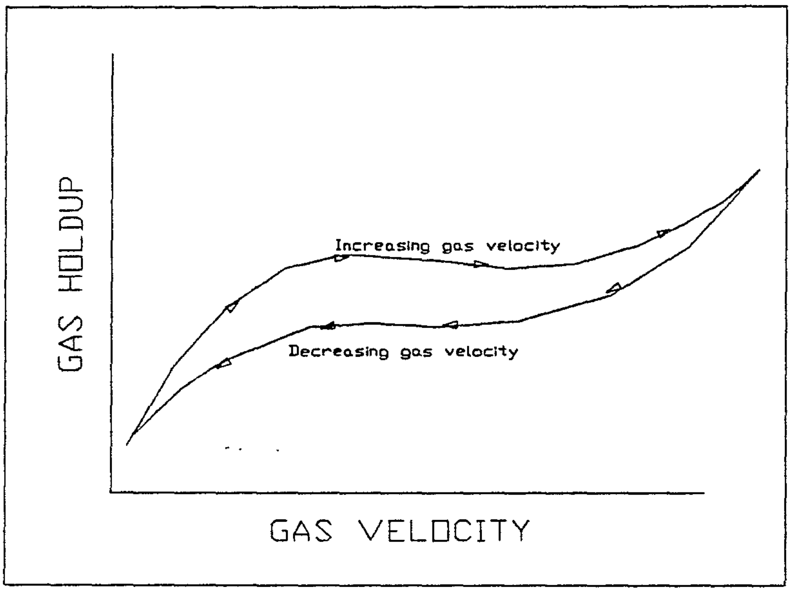

2.2.3 Effect of gas sparger on gas holdup

The type of sparger has an important role in the gas holdup when the system is working at low gas velocities (less than 15 cm/sec) (Khare and Joshi 1990:15). Most of the studies done in this field concluded that at higher velocities the effect of the sparger in the gas holdup becomes marginal. Also these effects decrease with increasing bed height. Guy et al (1986:33) presented in his publication a correlation including the orifice diameter.

$$\epsilon_g = 0.386 N_{Ga}^{0.025} Fr_o^{0.84} \left(\frac{d_o}{d_c} \right)^{2.075}$$

Because the gas distributor is usually placed in the middle of the bottom of the reactor, a radial velocity profile is created inside the reactor, with a maximum value in the middle (fig. 2.3). The same profile is followed by the gas holdup, as would be expected form the previous theory of the different portions the gas holdup. Because of this fact it is necessary to define a gas "slip velocity".

$$u_{slip} = \frac{u_g}{\epsilon_g}$$

which can be understood as the gas flow passing through an empty pipe.

Figure 2.6: Gas holdup radial profile

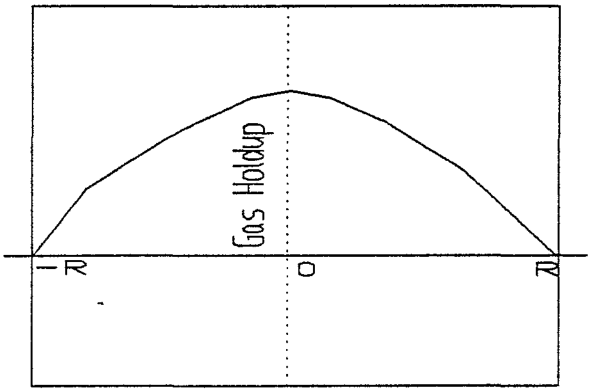

2.2.4 Effect of solids in gas holdup

Many investigations were made using different types of solids and in different concentrations. The gas holdup is sensitive to the presence of solids. Studies have been done using different particles distributions. Kim et al (1987:266) found, working in a air/water system and using glass beads, that there is a relationship between the gas holdup and the particle size. Khare and Joshi (1990:12), working in similar conditions, achieved the same results.

Figure 2.7: Effect of particle size on gas holdup

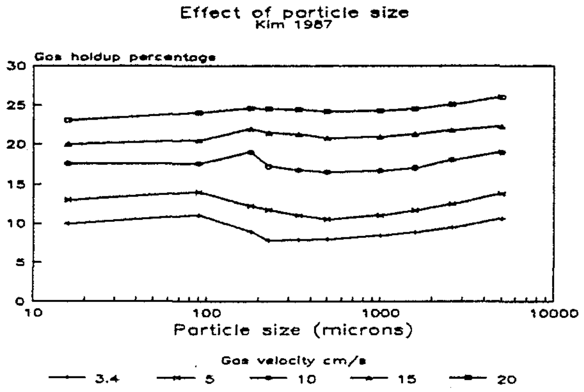

Most of the correlations published are not corrected for the presence of solids. This limits their application to only gas/liquid bubble columns. Matsumoto et al (1989: 1702) is one of the few authors that includes the solids holdup and the liquid velocity in his correlation:

$$\epsilon_g = U_g \frac{(1-R_{g,L})}{0.29(1+0.25\Phi_{s,o}^{0.85})+1.8U_g(1-R_{g,L})}$$

Figure 2.8: Effect of solids concentration in gas holdup

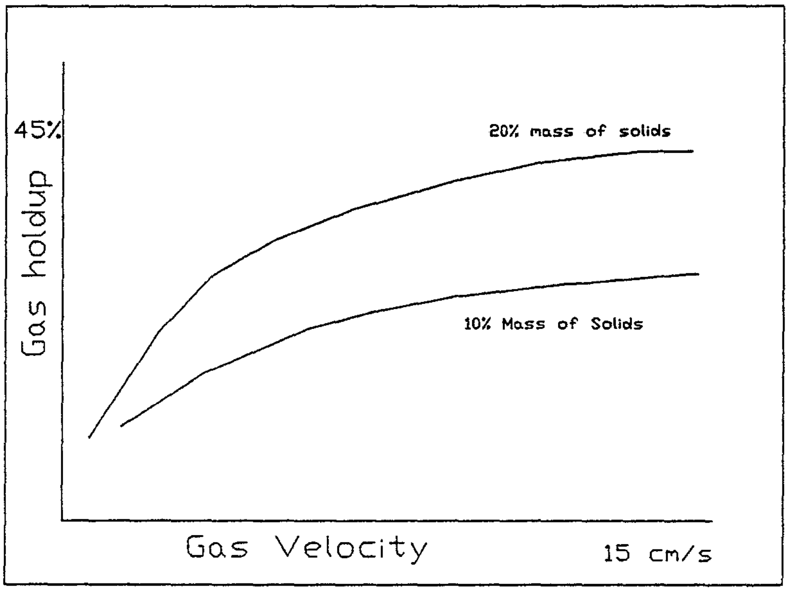

2.2.5 Effect of internals on gas holdup

The presence of internals (heating or cooling coils, filters, or baffles) has been investigated in order to understand the differences of the results obtained working with an empty column and with a column containing internals. Some of the research was aimed to determine the heat transfer coefficient in bubble columns (Saxena et al 1991a:97).

The first consideration is that the hydraulic diameter decreases. The cross sectional area decreases and therefore, at the same gas flowrate, the linear velocity increases. The radial profile of the gas velocity changes as well as the radial profile of the gas holdup. O'Dowd et al (1987: 1963) found higher gas holdup values for a baffled column than for an unbaffled column.

Figure 2.9: Effect of internals on gas holdup

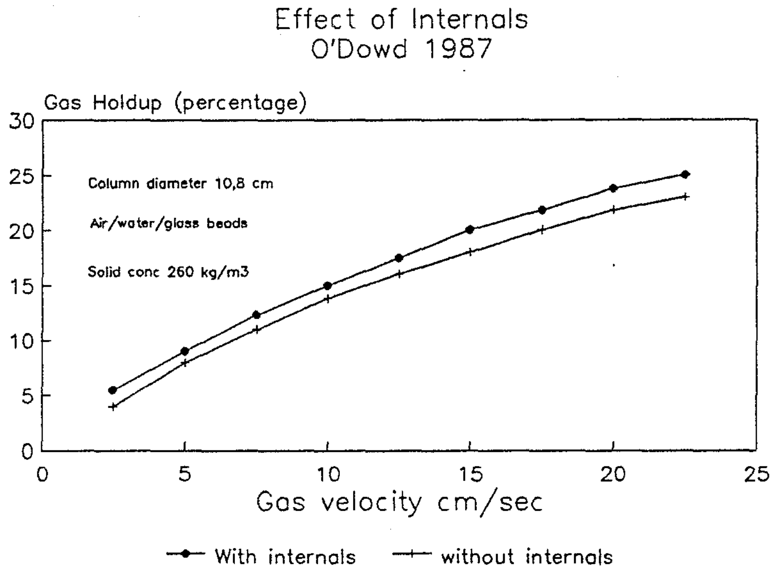

2.2.6 Bubble Sauter Diameter

The bubble size is an important factor. It limits the transport of reactants from the gas phase to the liquid phase, as well as that of the product from the liquid to the gas phase. In most of the cases, the controlling step in the process is the gas/liquid mass transfer. The difference in diameter of the bubbles (0.1- 10 cm) and the solid particles

(4-150 microns) indicates that the resistance between the liquid and solid is negligible when compared with the gas and liquid interfacial area.

The Sauter mean bubble diameter $d_{v,s}$ is commonly used to represent the bubble size distributions for mass transfer studies in two phase systems. It is a volume to surface ratio and together with the gas holdup value ϵ_g determines the specific gas-liquid interfacial area.

Figure :2.10: Flow Regimes in bubble columns

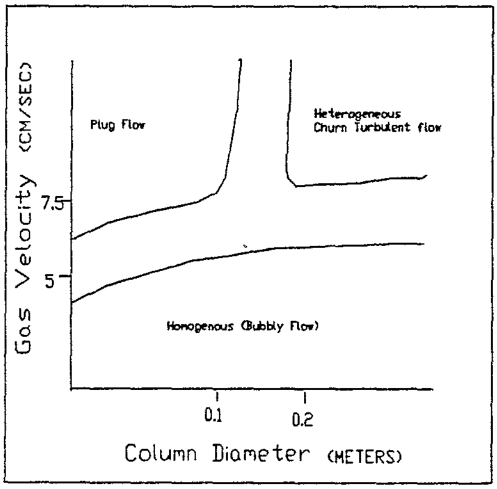

Figure: 2.11: Gas and Liquid motion at different hydrodynamic regimes

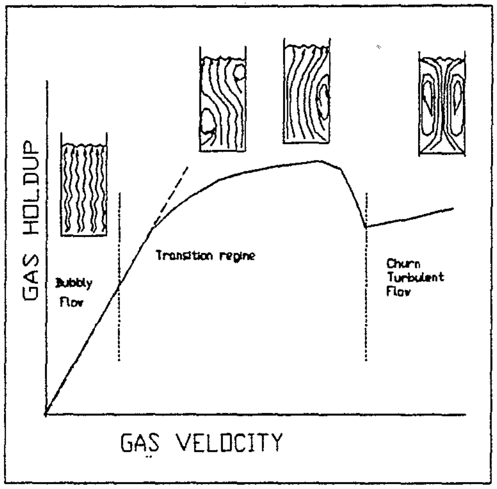

The bubble size distribution is mainly a function of the regime. The sparger plays an important role in this field. Maruyama et al (1985:352) studied the critical velocity required to pass from one regime to another.

Figure 2.12: Physical characteristics of the hydrodynamic regimes

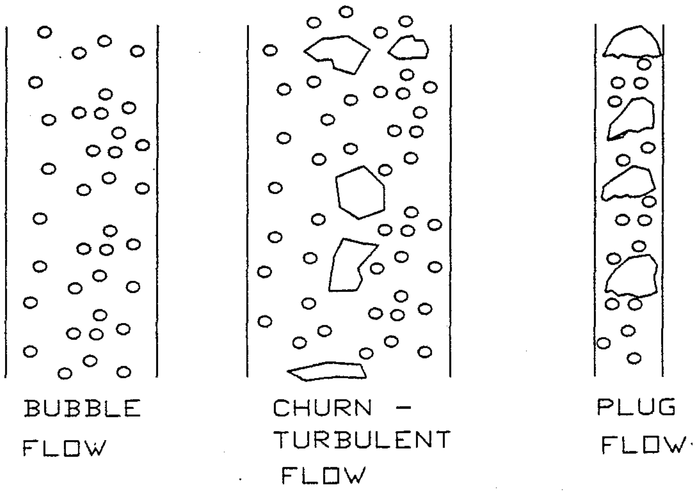

As noted previously, the gas sparger loses its influence in the gas holdup at high gas velocities (> 15 cm/sec), but this is not true with regard to it's effect on bubble size. The regime within the column is mainly determined by the column diameter and the gas linear velocity .

Guy et al(1986:33) presented a correlation for the bubble diameter which includes the nozzle diameter. This correlation was obtained working with low gas velocities (about 1.2 cm/sec).

$$d_b = 2.92 Re_{ol}^{-0.1} Fr_o^{0.42} d_o$$

Recently, comparative studies were done in order to determine the influence of the gas velocities and column diameter with the bubble size (Saxena 1990:159). The studies revealed that in smaller columns the mean bubble size is smaller.

Figure 2.13:Effect of column diameter on bubble size distribution

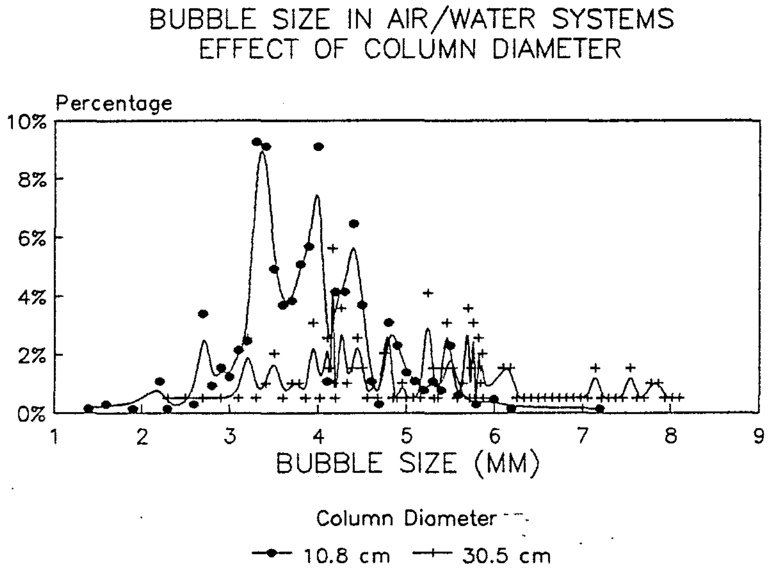

Usually the investigators measured the bubble size distribution in three different ways. The first one, and also easier is using a camera. This technique gives smaller bubble sizes because the picture contains only the bubbles near the wall and does not include those in the middle of the column. The second one involves a probe (electrical or optical), the third option is to estimate bubble size indirectly by the dynamic disengagement method.

As it can be seen in figure 2.10, there is a transition zone between the flow regimes. There are no fixed boundaries, these mainly depend on the liquid physical properties.

2.2.7 Effect of internals on bubble size

The presence of internals also has an influence on the bubble size. O'Dowd (1987: 1965) found that the sauter mean diameter in unbaffled slurry columns are smaller than that in the baffled columns when working at velocities less than 12 cm/sec. Above this velocity the effect is the reverse.

2.2.8 Coalescence and breakage

Blass (1990:210) working with high speed photography showed that single bubbles are still formed at higher gas throughputs, but after rising from the nozzle, the single bubbles are still connected to the gas supply by a neck (fig 2.14). As soon as the neck tears away, it jerks the bubble and sucks with it a small bubble and, more significantly, liquid having momentum which may split the bubble into two parts. This is the definition of the jet regime for bubble formation.

Figure 2.14: Bubble formation during high gas throughputs

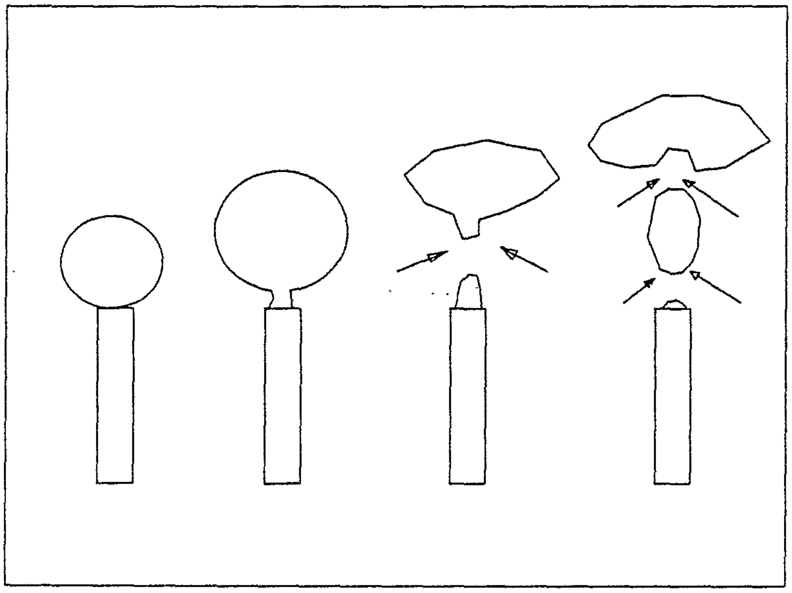

The jet regime is obtained at We > 2. This criterion is confirmed by Neubauer (1977) up to pressures of 300 bar. Using distributor plates with several holes the bubble diameter remains practically the same from We=6.

$$We = \frac{u_{g,o}^2 \rho_g d_n}{\sigma}$$

This points to another mechanism of dispersion: the shear field produced by neighbouring streams of bubbles in the liquid. Due to the strong buoyant force, these large bubbles tear off without a neck. Afterwards, they are split in the shear field produced by the streams of bubbles. However, if the distance between holes is less than 15 mm, the bubbles originating in neighbouring holes coalesce before they tear off.

Figure 2.15: Bubble size and Weber number

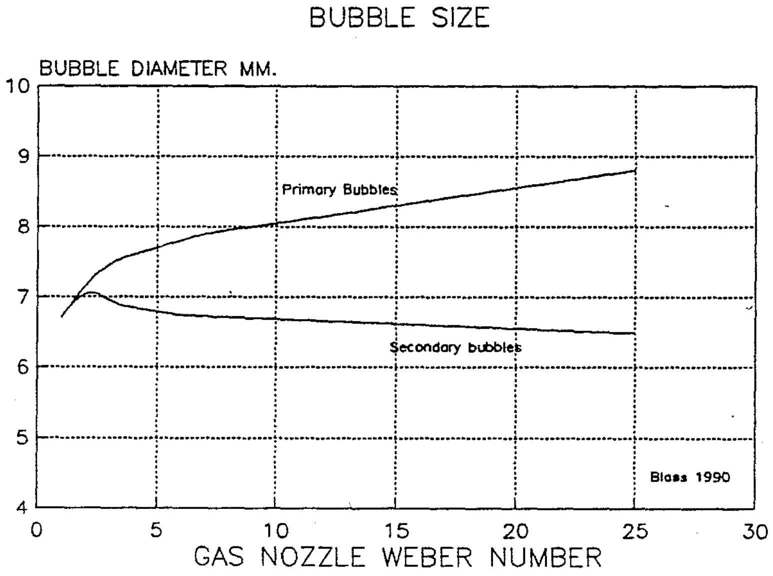

The limit of 2 for the Weber number is not always in accordance with other studies. Zahradnik (1982:266) found a stable operation of the sparger from Weber number of 2 to 4, and for large orifice diameters at 3 mm, a Froude number higher of 0.37.

$$Fr_o=\left(\frac{\rho_g}{(\rho_l-\rho_g)}\right)^{1.25}\left(\frac{u_o^2}{d_o g}\right)$$

There is general agreement that the coalescence tendency depends on the physical properties of the system. Some studies have been done introducing surface tension reduction agents in order to prove this theory. Godbole (1984,1990) postulated that the surface tension agents tend to accumulate between the bubble and the liquid phase, and when the bubble moves through the liquid, the absorbed material is swept to rear, creating a concentration gradient and hence a surface tension gradient which opposes the tangential shear stress. This phenomenon increases the drag effect on the bubble and hence reduces the rise velocity. Thus, the higher gas holdup values obtained with these agents were not due to low surface tension, but were rather a result of an increase in the surface activity of the bubble.

The presence of solids also affects the bubble size. Many studies have been done using different systems, most of them aqueous, and using different types of solids. The authors concluded that because of the increment of the liquid viscosity, the coalescence tendency increases and therefore the gas holdup decreases as the small bubbles leave the circulating behaviour to be included in the nett transport of the gas. Guy (1986:23) disagrees with this conclusion and bases his studies on the performance of inelastic and slightly elastic liquids

Another explanation of the change in the coalescence tendency due to the loading of certain solids is that the surface wettability of the particles tends to increase the breakage or the coalescence effect.

Figure 2.16: Effect of solids on the Sauter diameter: Air/water system

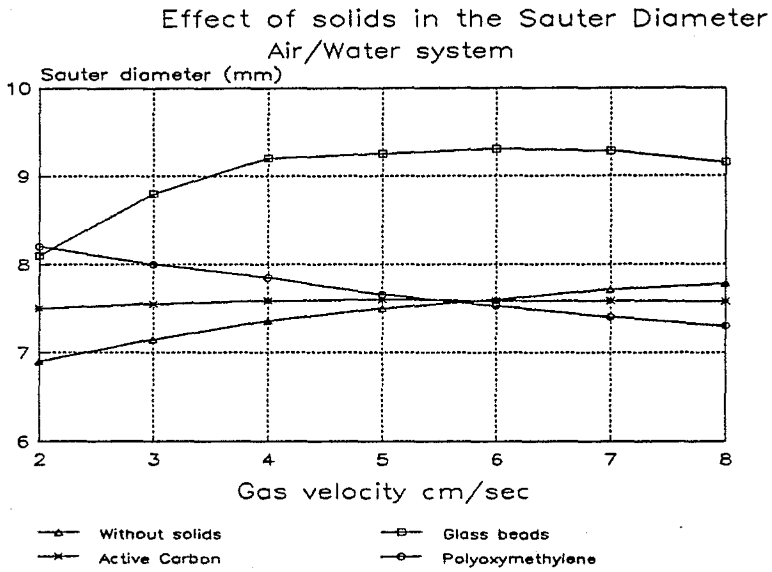

2.2.9 Bubble terminal velocity

The mean bubble rise velocity is very difficult to calculate, even theoretically, due to the fact that it depends on the bubble terminal velocity, which depends on the bubble diameter, column geometry and bubble-bubble interactions.

Taking this into consideration, Wallis (1969) proposed for the intermediate regimes the following expressions

$$Regime\ I: Re_b < 2, \quad (Stokes\ law) \quad u_{b,\infty} = \frac{\rho_l g d_b^2}{18\mu_L}$$

$$Regime\ II\ :\ 2 < Re_b < 4.02 Mo^{-0.214}$$

$$u_{b,\infty} = 0.33 g^{0.76} \left(\frac{\rho_l}{\mu_l}\right)^{0.52} \left(\frac{d_b}{2}\right)^{1.28}$$

$$Regime\ III: \ Re_b \gg 1 \ \text{and} \ Re_b > 4.02 Mo^{-0.214} \ \text{and} \ Bo\left(\frac{d_b}{d_C}\right)^2 \ll 2$$

$$u_{b,\infty} = \left(2\frac{\sigma_L}{\rho_l d_b}\right)^{0.5}$$

$$Regime\ IV: \ Re_b \gg 1 \ \text{and} \ Re_b > 4.02 Mo^{-0.214} \ \text{and} \ 2 < Bo\left(\frac{d_b}{d_C}\right)^2 < 8$$

$$u_{b,\infty} = 1.53\left(g\frac{\sigma_L}{g_l}\right)^{0.25}$$

$$Regime\ V: \ Re_b \gg 1 \ \text{and} \ Re_b > 4.02 Mo^{-0.214} \ \text{and} \ Bo\left(\frac{d_b}{d_C}\right)^2 \gg 8$$

$$u_\infty = \left(g\frac{d_b}{2}\right)^{0.5}$$

where the Morton number **(Mo)** is the ratio of the forces of viscosity and surface tension.

2.2.10 Gas dispersion coefficient

The gas dispersion coefficient is a parameter to indicate the degree of mixing inside a reactor. Usually due to the complexity of its measurement, the degree of mixing is expressed by a dimensionless number, in this case, the Peclet number.

$$Pe_g = \frac{u_g L}{D_g}$$

In the different papers most of the authosr refer to one another. Four publications are discussed here. The difference in their measurements and expressions can exceed two orders of magnitude. Towell et al (1965:97) worked with air/water systems and used 40 and 106 cm diameter columns. The maximum velocities they used were 13.1 and 1.3 cm/sec for the gas and liquid respectively.

Mangartz and Pilhofer (1980:40) presented the result of their work with different gases and liquids, in a column of 14 cm diameter and 2.5 m height. Their maximum velocities were 13 and 0.6 cm/sec for gas and liquid.

Field and Davidson (1980:228) present the results of working with a column of 3.2 m diameter and a 5.2 cm/sec maximum gas velocity. These results are mainly applicable to biotechnological reactor because the high residence times.

Wachi and Nojima (1990:901) worked with air/water systems and used two columns one of 0.2 m diameter and the second one of 0.5 m. The maximum gas velocity used was 0.456 m/sec.

Table 2.3 Correlation of the gas dispersion coefficient

$D_g = K u_g^{\exp 1} d_c^{\exp 2} \epsilon_g^{\exp 3}$				
Author	**K**	**Exponents:**		
	m2/s	**Exp 1**	**Exp 2**	**Exp 3**
Towell & Ackerman 1965	**19.7**	**1**	**2**	**0**
Mangartz & Pilhofer 1980	**50**	**3**	**1.5**	**-3**
Field & Davidson 1980	**54.6**	**3.56**	**1.33**	**-3.56**
Wachi & Nojima 1990	**20**	**1**	**1.5**	**0**

2.2.11 Gas - liquid interfacial area

Most of the studies done in this field are based on aqueous systems. Some of them are based on the solubility of a gas tracer in the liquid phase, while others include chemical reactions.

The specific gas-liquid interfacial area is the total surface area of all bubbles in the dispersion divided by the volume of the dispersion V_T .

$$a = \frac{\sum \pi d_i^2}{V_T} = \frac{6\epsilon_g \sum d_i^2}{\sum d_i^3} = 6\frac{\epsilon_g}{d_{v,s}}$$

where $d_{v,s} = \frac{\sum d_i^3}{\sum d_i^2}$

The interfacial area as it can be seen, follows an inverse trend with the sauter diameter. Because the easier way to calculate the interfacial area is by determining $ak_{L,i}$ (i=tracer) and then relate it to any other factors by the

Wilke - Chang relation, most of the studies have been directed in this way.

$$k_l Sc^{2/3} = 0.31\left(\frac{\mu \quad \Delta\rho \quad g}{\rho_l^2}\right)^{1/3} \qquad (*)$$

where

$$Sc = \frac{\mu}{\rho D_l}$$

The presence of solids has an influence on the bubble size and therefore on the interfacial area. O'Dowd et al (1987:1962) found that by increasing the solids concentration, the interfacial area decreases, due to the fact that the solids increase the coalescence tendency. Bruck (1986:388) does not agree totally, showing in his publication that he found that certain solids do not increase the bubble size. Moreover they decreased the coalescence and showed a tendency to break the bubbles, producing smaller ones and therefore increase the interfacial area.

2.2.12 Gas critical velocity

Imafuku et al (1968;154) found that there is a minimum gas critical velocity at which all the solids present in the column are fluidized. Below this point, there is solid matter that remains sedimented.

This critical velocity was found to have no dependence with the type on distributor and slightly dependence on the total amount of solids, but it is strongly influenced by the shape of the bottom of the column. As an example Imafuku showed that a 20 cm diameter column with a conical shape equipped with a sparger of 5 cm diameter at its bottom gave the same

* $k_L = cm/s$, $\rho = gr/cm^3$, $\mu = g/cm\text{-}s$

critical velocity (based on the sparger cross sectional area) as a 5 cm diameter column. Therefore the complete solid suspension can be achieved with smaller gas flowrates for conical bottomed columns than for columns with flat bottoms. He also emphasized that the position of the gas distributor is very important for the complete suspension of solid particles .

Figure 2.17: Effect of the shape of the bottom of the column on the critical gas velocity for solid suspension

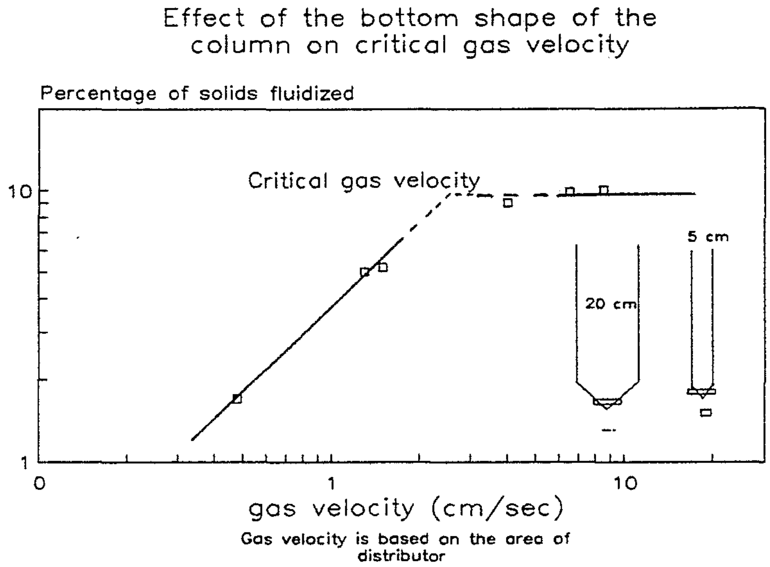

Another study was done by Abraham et al (1992). His conclusion about the gas critical velocity were that the sparger plays an important role in the suspension performance (unlike to Imafuku). The gas critical velocity decreases with increasing number of holes of the sparger. It is also dependant on the L/D ratio and on the liquid properties with regards to the coalescence tendency. His proposed correlation includes the effect of the column diameter, the solid concentration and the terminal velocities of the solids.

$$U_{g,c} = 0,54 u_{p,l}^{0.46} \epsilon_g^{0.66} \epsilon'^{0.39}_s d_c^{0.27} \qquad (*)$$

where ϵ'_s is the volume of solids per unit cross sectional area.

2.3 Liquid Phase

2.3.1 Backmixing

The moving of the liquid phase induced by the rising of the bubbles is known as the backmixing effect. The direct consequence of this effect is the circulation of small bubbles along the reactor. This provides the necessary residence time for the bubbles with a higher interfacial area to react.

2.3.2 Effect of the sparger

The effect of the sparger is highly noticable in the circulation regime (fig. 2.18). A few studies were made investigating this effect. One of the indications of the sparger efficiency, is the so called "mixing time".

Guy et al (1986:26) presented the results of three different spargers. He studied the efficiency of mixing by measuring the time taken to achieve a homogeneous mixture from a non disturbed system. He concludes that the mixing time increased as the viscosity or the shear-thinning properties increased.

* ϵ'_s = mm

Figure 2.18: Effect of the sparger on the liquid circulation pattern

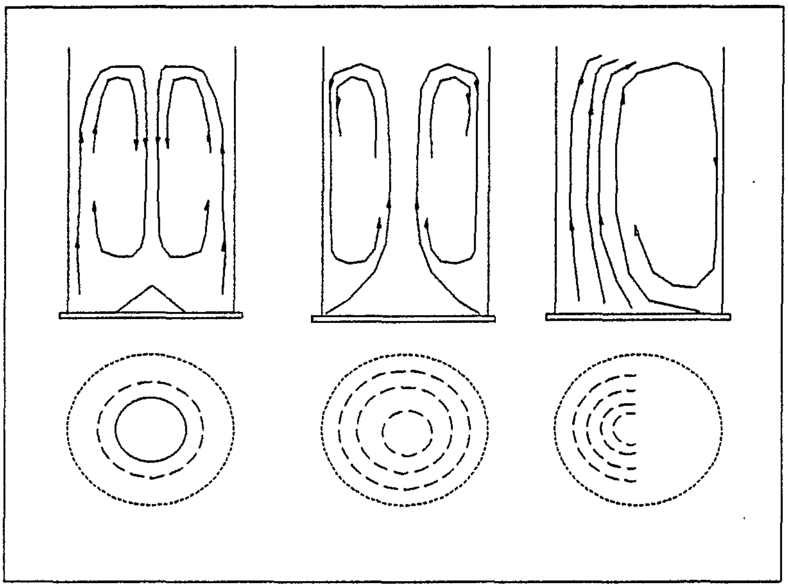

The mixing time is defined as the time between the beginning of a mixing operation and the moment when the fluid reaches a required degree of homogeneity and is related to a cell time, which is the mixing time for a single circulation cell. This "cell time" depends on the average of the liquid circulation velocity due to gas sparging and on the reactor geometry.

$$t_{mix} = t_{mix\ cell}\left(1 - 0.174\left(\frac{L}{d_c} - 1\right) + 0.0179\left(\frac{L}{d_c} - 1\right)^2\right)$$

$$t_{mix\ cell} = 7.5\frac{d_c}{V_{c,s}} \qquad V_{c,s} = 2\left(\frac{u_g}{\epsilon_g}\right)d_c^{1/3}$$

Working with the third sparger of fig 2.18, he achieved higher holdup values, due to solely to the strong circulation induced.

2.3.3 Liquid velocity

Kawase and Moo Young (1986:1970) found that the radial profile of the liquid velocity at high Reynolds numbers is satisfactorally approximated by

$$\frac{u_{L,r}}{u_{L,r=0}} = -2\left(\frac{r}{R}\right)^2 + 1$$

and the velocity in the column axis is defined as

$$u_o = 0.737 g^{1/3} d_c^{1/3} U_g^{1/3}$$

2.4 Solid Phase

2.4.1 Solid surface wettability

The presence of solids has a very important role in slurry reactors. In catalytic reactions such as the Fischer Tropsch , the solid phase represents the catalyst suspended in the liquid phase.

Bruck (1986:382), worked with an air/water system and different types of solids, he also added ethanol to vary the liquid surface tension. He found that when using particles of polyoxymethylene, the sauter diameter instead of increasing with the increase of the gas linear velocity, decreases (fig. 2.16). Therefore the interfacial area increases. He found that in air/water systems, with the addition of polyoxymethylene particles, it is possible to increase from 10 to 45 % the gas-liquid interfacial area. He concluded that the extent of bubble disintegration increases with the sphericity of the solid particles as well as with decreasing the wettability of the solid surface and surface tension of the liquid. However the wettability increases with declining surface tension, for solids which are not completely wetted.

The parameters which influence the occurrence of bubble disintegration can be described by a critical Weber number.

$$We_{crit} = \frac{(1-\sin\nu)\rho_{SL}(1-\epsilon_g)d_{p,equiv}u_{b,slip}^2\psi}{\sigma} = 2.5, \qquad 0° \leq \nu \leq 90°$$

if We >2.5 bubble disintegration may occur.

2.4.2 Solid dispersion coefficient

There is general agreement that the solid dispersion coefficient has the same value as the liquid dispersion coefficient. This is valid only over a certain range. Matsumoto et al(1989;1707), measured both coefficients and determined a relationship between them:

$$\frac{E_p}{E_l} = 1 - \frac{\frac{100}{Re}}{\left(1+\frac{100}{Re}\right)\exp\left(30\frac{k}{Re^2}\left(\frac{E_l}{\nu}\right)\left(\frac{\rho_l}{\rho_p}\right)\right)-1}$$

O'Dowd et al (1989:1966), working with baffled and unbaffled columns, concludes that for baffled columns the solid dispersion coefficient is higher than that for empty columns. The different expressions he quoted are:

for the baffled column

$$Pe_p = 7.4\left(\frac{Fr_g^6}{Re_g}\right)^{0.115} + 0.019Re_{p,\infty}^{1.1}$$

for the unbaffled columns

$$Pe_p = 7.7\left(\frac{Fr_g^6}{Re_g}\right)^{0.098} + 0.019Re_{p,\infty}^{1.1}$$

Figure 2.19: Effect of internals on the solid dispersion coefficient

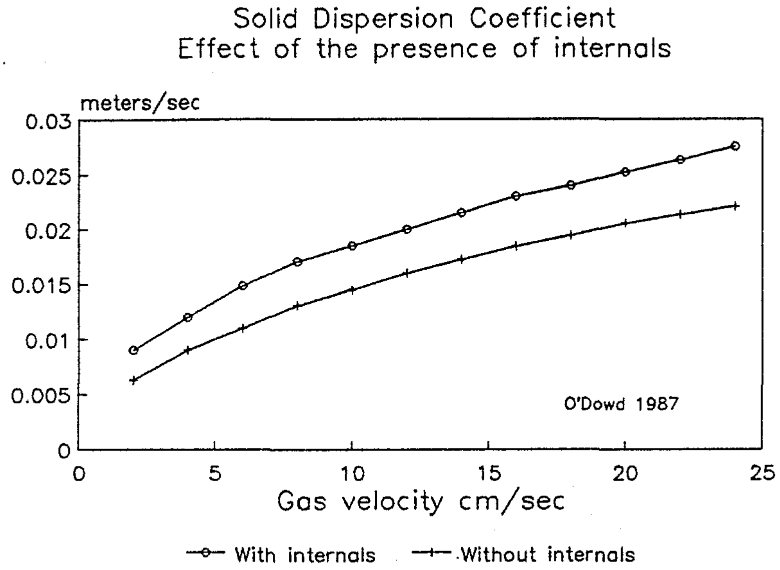

2.4.3 Axial Concentration Profile

Many investigators (Deckwer 1982:232), (Katoet al 1972:12), (Imafuku 1968) have successfully used the sedimentation-dispersion model expressed as an equation of the form:

$$\frac{C_{s,i}}{C_{s,o}} = \exp(-mL\xi)$$

to describe the solids concentration profile in a bubble column operating in batch mode. The slope m is defined as the relation between the mean particle settling velocity and the solid dispersion coefficient . Some authors use this equation also when a liquid velocity is present, due to the fact that this parameter is very low for bubbling columns.

Matsumoto (1989:1703) in his study concludes that by working at certain set of gas and liquid velocities, the solid holdup can be kept constant throughout the column. He does not agree with the previous authors and include the liquid velocity in all his considerations.

2.4.4 Exit discontinuity of the solid concentration profile

The exit discontinuity in a slurry bubble column, is the difference between the solid concentration at the top of the column and the concentration of the effluent when the level is running just above the exit point. There is a drop in the solid concentration for a very thin layer (foaming) at the gas/liquid interface (Bruijn et al 1989:283.

Figure 2.20:Exit discontinuity in air/varsol system

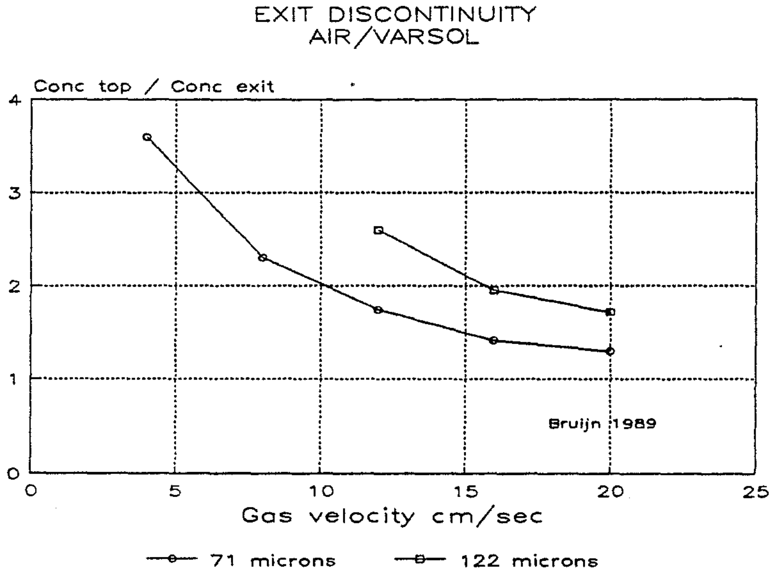

The solid distribution as quoted before depends highly on the liquid circulation velocity. The liquid velocity in the circulation cell is larger than the net liquid velocity.

If one follows the simple settling model

$$\frac{C_{s,i}}{C_{s,o}} = \exp\left(-\left(\frac{u_p}{D_s}\right)L\xi\right)$$

the only parameters that are require to determine the solid profile is the mean settling velocity and the solid dispersion coefficient. But when the solid exit discontinuity exists, the measurement of the solid concentration at the top of the column becomes necessary to calculate the solid concentration profile.

In the steady state the concentration in the feed must be the same as in the exit stream. So the discontinuity can be expressed in terms of the feed concentration. Kato et al (1972:114) gives the following relationship:

$$\frac{C_t}{C_f} = 1 + 0.5\left(\frac{U_g}{V_t}\right)^{-0.4}$$

The conclusion of these studies was that the exit discontinuity decreases as the gas velocity increases due to the increase of the backmixing effect. The effect of antifoaming agents was to decrease the amount of foaming present, thus eliminating the semi-stagnant layer and hence the discontinuity.

Figure 2.21: Bubble layer at the top of the column

— Free interface in water at $U_g = 0.023$ m/s and $U_l = 0.001$ m/s.

When liquid is withdrawn below the interphase or when gas and liquid are forced out of the system together, no free interface exists at the liquid exit and the discontinuity disappears.

2.5 Existing Models for the slurry bed reactor in Fischer Tropsch synthesis

2.5.1 Introduction

The limitations of any model are determined by its set of assumptions. By increasing this set of assumptions, the model gets closer to describing the so-called ideal situation and therefore becomes easier to handle mathematically. This is being done at the expense of the applicability of the model since it tends to move away from describing the real situation.

On the other hand by decreasing the set of assumptions, the model becomes more general. Such a general model is in many

Solid Concentration Profile
Air/Varsol with foamer agent

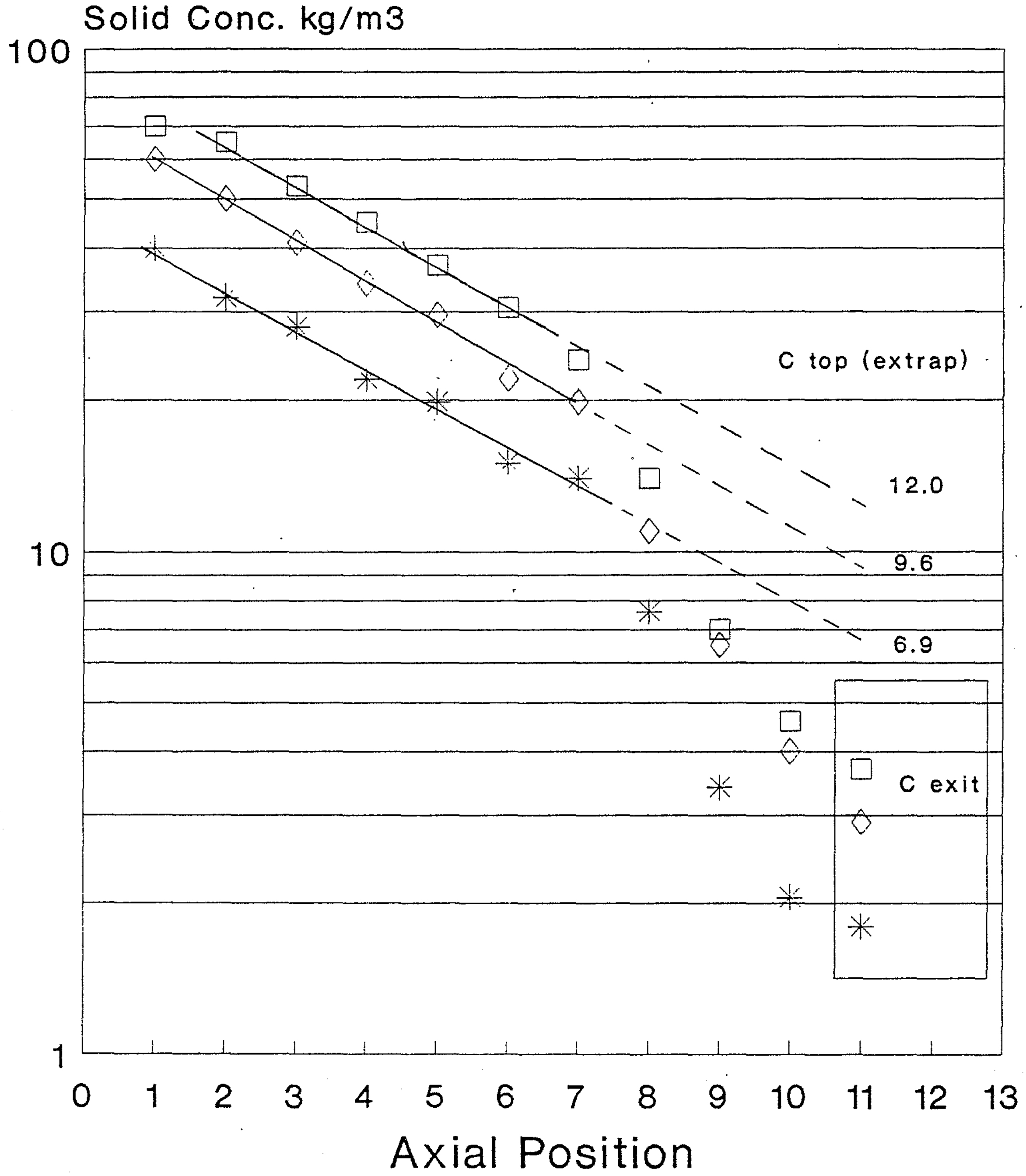

cases very difficult to handle mathematically and is also severely hampered by a large number of parameters which are very difficult to estimate.

In choosing a model for a specific application a balance will have to be found between the accuracy of the model on the one side and its case of application in terms of the number of parameters needed by its model and its mathematical simplicity on the other.

For describing the Fischer Tropsch synthesis in three phase fluidized beds, the following set of assumptions has to be made:

a. Steady state.
b. The gas phase obeys the ideal gas law.
c. Mass transfer resistance is controlled by the liquid interphase area.
d. The concentration of CO and H2 in the products are negligible.
e. The solubility of the reactants obeys Henry's law.
f. The resistance of diffusion through the liquid and through the liquid/solid interphase is negligible.
g. The mass transfer resistance of the products is negligible.

In the following models these common expressions is been used.

For the kinetic expression:

$$R_{FT} = K_0 w k_c C_{s,H_2}(1 - \epsilon_G)$$

And for the mass transfer expression:

$$R = a k_{L,H_2}(C_L^* - C_L)$$

2.5.2 Model I : Proposed by Calderbank (1961, 1963)

The additional assumptions are:

1. The gas holdup value is negligible.
2. Both phases are in plug flow, no axial mixing is present.
3. Bubble size is constant.
4. Holdup value is constant along the reactor.
5. The inlet H2/CO ratio remains the same in all the phases.
6. There are no inert gases present.
7. The catalyst is uniformly mixed.
8. The pressure and temperature are the same longitudinally down the reactor.

The general rate equation is expressed as:

$$R_{H_2} = \frac{C_{H,G} R T}{m'_H \left(\frac{1}{a k_{L,H}} + \frac{1}{k_L w k_{H_2}} \right)}$$

And the mass balance equation is:

$$\frac{k'_o \epsilon_G}{Q} dV = \left(1 + \frac{\gamma X_{H_2+CO}}{1 - X_{H_2+CO}} \right) d X_{H_2+CO}$$

Giving a final expression

$$\frac{V}{\left(\frac{m_H'}{RT}\right)\dot{Q}\left\{(1-\gamma)X^e_{H2+CO}+\gamma\ln\left(\frac{1}{1-X^e_{H_2+CO}}\right)\right\}}=\frac{1}{ak_{L,H}}+\frac{1}{k_C w K_{H_2}}$$

The characteristic of this model is its simplicity. Because of its large number of assumptions, it is unrealistic. As a matter of fact, the assumption that the bubble size does not change through the reactor means that there is very little reaction taking place. This limit this model to systems when the conversion per pass is very low.

The assumption of no inerts present in the feed, does not allowed the use of recycle gas.

2.5.3 Model II : Proposed by Deckwer (1981)

Some additional assumptions are:

1 The phases are in plug flow.

2 Holdup value is constant along the reactor.

Deckwer combines the adsortion constant of the catalyst and the equilibrium constant in one

k_C'.

The stoichiometric equation used is:

$H_2+U\ CO\rightarrow\gamma$ Products

The general rate equation is defined as:

$$R_{H_2}=\frac{C_{H,G}RT}{m_H'\left(\frac{1}{k_{H_2}'w(1-\epsilon)}+\frac{1}{ak_{L,H}}\right)}$$

The mass balance equation:

$$\frac{k_o RT}{m'_H U^i_G} dz = \frac{1+\alpha^* X_H}{1-X_H} dX_H$$

where: $\alpha^* = \frac{Q\left(X_{H_2+CO}-1\right)-Q')}{Q'} \frac{(1+U)}{(1+I)}$

Giving the final expression:

$$(\alpha^*+1)\ln(1-X^e_H)+\alpha^* X^e_H = \frac{k_o RTL}{m'_H U^i_G} = -St$$

Deckwer made his model more realistic than Calderbank (1961,1963). It seems that this model included all the restrictions of Calderbank without adding unnecessary complex expressions. It is based on the Hydrogen conversion. One of its limitations is that the gas holdup is considered constant through the reactor and the experimental work by Bukur had demonstrated that it is a function of the space velocity. Another questionable assumption is the perfect distribution of the catalyst along the reactor.

2.5.4 Model III: Proposed by Satterfield and Huff (1980)

Additional assumptions for this model are that the slurry phase is considered to be completely mixed while the gas phase is in plug flow and that the gas holdup is constant.

Satterfield and Huff defined a kinetic constant for the comsumption of Hydrogen and Carbon Monoxide refered to the catalyst loading in the reactor k''_C.

The general rate equation is defined as:

$$R_{H_2}=\frac{C^{i}_{H,G}RT}{m'_{H}\left(\frac{1}{\dot{m}_{H}\frac{Q}{V}\left(1-\exp\left(-\frac{aK_{L,H}L}{\dot{m}_{H}U_{G}}\right)\right)}+\frac{1}{\dot{k}_{C}w(1-\epsilon_{G})\frac{C^{i}_{H,G}-C^{*}_{H,G}}{C^{i}_{R,G}-C^{*}_{H,G}}}\right)}$$

Where $\dot{m}_{H}=\frac{m'}{RT}$ and $\alpha_{H}=\frac{ak_{L,H}}{\dot{m}_{H}U_{G}}$

This was the first model that considered the slurry to be completely mixed. Because of this consideration the Hydrogen concentration in the slurry phase is obtained by a total mass balance. This model considers the effect of the inlet H2/CO ratio. It could be considered complete if the Water Gas Shift reaction was included as well as an expression for the distribution of the solid phase.

2.5.5 Model IV : Proposed by Bukur (1983)

The additional assumptions for this model are:

The slurry phase is considered completely mixed.
The catalyst charge is not considered.
The bubble size decreases with conversion.

Bukur includes the absortion-equilibrium constant and catalyst loading into one constant k'_{C}.

When backmixing is considered the concentration of Hydrogen in the liquid phase is expressed as:

$$C_{H,L}=\frac{X^{e}_{H}U^{i}_{G}AC^{i}_{H,G}}{k'_{C}(1-\epsilon_{G})V_{L}}$$

The mass transfer resistance is defined as:

$$R_M = \frac{\dot{m}_H}{a k_{L,H}} \text{ and } N_m = \frac{L}{U_G^i R_m}$$

and the kinetic resistance as:

$$R_k = \frac{\dot{m}}{k_c'(1-\epsilon_G)} \text{ and } N_R = \frac{L}{U_G^i R_k}$$

giving the final expression

$$N_m = -\frac{1}{1+\frac{\alpha^* X_H^e}{N_R}} \left\{ \alpha^* X_H^e + \left(1+\alpha^* \frac{1-\frac{X_H^e}{N_R}}{1+\alpha^* \frac{X_H^e}{N_R}} \right) \ln \left(1 - X_H^e \frac{1+\alpha^* \frac{X_H^e}{N_R}}{1-\frac{X_H^e}{N_R}} \right) \right\}$$

This model is similar to Satterfields ones but differs in the gas contraction expression. Also, the expression for the Hydrogen concentration in the liquid phase is not obtained by a total mass balance but by the assumption that the mass of gas phase Hydrogen converted is equal to the mass of Hydrogen reacted at the catalyst surface. Also this model does not include any expression for the Water Gas Shift reaction or the catalyst distribution.

2.5.6 Model V : Proposed by Stern (1983)

The additional assumptions used are:

The slurry phase is considered completely mixed.
The bubble size decreases with conversion.

Stern defined the following parameters

m_i = Henry's law coefficient for each component (H2,CO, CO2,CH4 and CO2)

$k_{L,i}$ = Liquid side mass transfer coefficient for component i.

The mass balance expression is defined by :

$$Vak_{L,i}\left(\overline{C}^{*}_{L,i}-\overline{C}_{L,i}\right)= \qquad Vw(1-\epsilon_G)R_i \qquad + \quad \dot{Q}_L C_{i,L}$$

Moles that enter by diffusion

Moles that react

Moles that exit

Because of the backmixing, $\overline{C}_{i,L}$ is an average value

$$\overline{C}_{i,L}=\frac{1}{Vm_i^{*}}\int_0^V C_{i,G}\,dV$$

All the mathematics make use of dimensionless expressions. The concentrations are referred to the Hydrogen concentration at the inlet. Other parameters are referred to inlet conditions.

$$\theta_{i,G}=\frac{C_G}{C^{i}_{G,H}} \qquad \theta_{i,L}=\frac{C_{i,L}}{C_{H,L}} \qquad \tau_G=\frac{L}{U^{i}_{G}} \qquad St_i=\frac{ak_{L,i}L}{m_i^{*}U^{i}}$$

$$\xi=\frac{z}{L} \qquad \nu=\frac{U_G}{U^{i}_{G}} \qquad \tau_L=\frac{V}{Q_L}$$

Deifining the Damkohler number as:

$$Da=\frac{Lw(1-\epsilon_G)k_L}{U^{i}_{G}}$$

So the mass balance expression becomes:

$$St_i m_i^*\left(\frac{\tau_L}{\tau_G}\right)(\bar{\theta}_{i,G}-\theta_{i,L})-\gamma_i Da\left(\frac{\tau_L m_i^*}{\tau_G m_H^*}\right)\theta_{H,L}-\theta_{i,L}=0$$

And the differential equations that must also be solved are:

$-\frac{d}{d\xi}(v\theta_{i,G})=St_i(\theta_{i,G}-\theta_{i,L})$ The gas contraction expression.

$-\theta_G\frac{dv}{d\xi}=\sum_{i=1}^{n}St_i(\theta_{i,G}-\theta_{i,L})$ Change of gas space velocity

$\bar{\theta}_{i,G}=\int_0^1\theta_{i,G}\,d\xi$ Average value of the concentration in the liquid.

Stern (1983) gets a value for the Hydrogen concentration by taking an average along the reactor. One of the advantages of this model is the dimensionless treatment.

The use of variables for the catalyst concentration as well as the reaction rate makes it possible to includes sedimentation models and also the Water gas shift equation.

2.5.7 Model VI: Proposed by Deckwer (1982)

This model is one of the most general. It does not consider the reactor to be isothermal, nor the catalyst homogeneously distributed. It also takes into account the mass transfer resistance between the liquid and the solid surface. The degree of mixing depends on the extent of the axial dispersion.

The mass balance expression for the gas phase is:

$$D_G \epsilon_G \frac{d^2 C_{H,G}}{dz} - \frac{d}{dz}(U_G C_{H,G}) = a k_{L,H}(C^*_{H,L} - C_{H,L})$$

Axial Dispersion - Total Change = Moles incorporated in the liquid phase.

The mass balance is the liquid phase is expressed as:

$$D_L \epsilon_L \frac{d^2}{dz^2} C_{H,L} - k_s a_s (C_{H,L} - C_{H,S}) = -a k_{L,H}(C^*_{H,L} - C_{H,L})$$

Axial dispersion-moles to the solid phase= moles entering the liquid phase.

Deckwer is the first to assume that isothermal behaviour is not achieved. and provides an expression for the Heat balance across the reactor :

$$\lambda_{a,x} \epsilon_L \frac{d^2 T}{dz^2} \quad + (-\Delta H_r) R_{H_2} \quad = \quad h a_H (T_{sl} - T_w)$$

Heat conducted + Heat generated = Heat Removed

The catalyst concentration profile is determined by axial dispersion and by its hindered settling velocity. The expression for the solid phase is:

$$D_s \frac{d^2 w}{dz^2} \quad + U_T \frac{dw}{dz} \quad = 0$$

Axial dispersion + Settling = Accumulation

Another equation that has to be solved simultaneously is the one that describes the total transport of Hydrogen:

$$A U^i_G C^i_{H,G} + A D_G \epsilon_G \frac{d C_{H,G}}{dz} = A U_G C_{H,G}$$

Deckwer mentioned that there is uncertainty in the estimation of the parameters required. One of the observation was that the temperature profile seems very flat. The largest temperature difference was 5 deg C. This indicates that the assumption of an isothermal reactor is not far from reality.

The consideration of the liquid-solid interface resistance is unique. Deckwer also concluded that the reactor performance is insensitive to variations in the gas-liquid mass transfer rates.

2.5.8 Model VII: Proposed by Kuo (1983)

Workers at Mobil developed two models for the Slurry Bed Reactor. A single component model and a multi-component model have been described with different grades of complexity. The first simpler one, only considered kinetics and mass transfer resistance. The other included the Water Gas Shift reaction and the species Hydrogen, CO, CO2 and Water.

Both assumed axial dispersion and catalyst settling but assumed that the axial mixing of the gas is negligible. The Fischer - Tropsch reaction is defined as:

$$CO + \left(1 + \frac{m}{2}\right) H_2 \rightarrow -(CH_m)- + H_2O$$

They presented three cases for the liquid phase:

Plug Flow:

$$a k_{L,H}\left(\frac{C_{H,G}}{\tilde{m}_H}-C_{H,L}\right)=k''' w_{Fe}\phi_s(1-\epsilon_G)C_{H,L}\frac{w}{\overline{\overline{w}}}$$

Gas/liquid diffusion = Kinetic dissipation.

Backmixed Flow:

$$\int_0^L a k_{L,H}\left(\frac{C_{G,H}}{\tilde{m}_H}-C_{H,L}\right)dz=k''' w_{Fe} phii_s C_{H,L} L$$

Axially dispersed flow:

$$D_L(1-\epsilon_G)\frac{\phi_s^2}{dz^2}C_{H,L}=a k_{L,H}\left(C_{H,L}-\frac{C_{H,G}}{\tilde{m}_H}\right)+k_c''' w_{Fe}(1-V_C)\phi_s C_{H,L}\frac{w'}{\overline{\overline{w}}}$$

Dispersion in liquid = gas/liquid diffusion + kinetic dissipation.

The catalyst distribution is described in a similar form as that in the Deckwer model.

Using the first two cases for the slurry phase, it is possible to produce an explicit analytical solution, while for the axial dispersion model it needs to be solved by numerical methods.

The final expression for the case of plug flow is:

$$L=-U_G^i R_m(\alpha_H^* x_H^e+(1-\alpha^*)\mathrm{Ln}(1-x_H^e))-\frac{D_s}{v_T}\mathrm{Ln}\,B_1$$

where

$$B_1=\frac{B_{OC}+B_Z\{1-\exp(-B_{OC})\}}{B_{OC}-B_Z\{1-\exp(B_{OC})\}}$$

and

$$B_2 = \frac{a k_{L,H}}{k_C''' w_{Fe}(1-\epsilon_G)\phi_s} \quad \text{and} \quad B_{OC} = \frac{U_T L}{D_s}$$

For the multi-component model all the expressions are related to each component (Hydrogen , CO , CO2, water, etc).

Gas phase mass balance:

$$-\frac{d(U_G C_{i,G})}{dz} = a k_{L,i}\left(\frac{C_{i,G}}{m_i} - C_{i,L}\right)$$

Liquid phase mass balance:

$$-a k_{L,i}\left(\frac{C_{i,G}}{m_i} - C_{i,L}\right) = (1-\epsilon_G)(1-V_C) w_{Fe} \sum S_{ij} r_j$$

Mobil experience was that the catalyst desintegration into particles of 5 microns during normal operation. Under these conditions homogenous distribution is expected.

2.5.9 Model VIII: Proposed by Stern (1984, 1985a, 1985b)

This updated model keeps the same mathematical treatment as that proposed by Stern (1983), but assumes axial dispersion and a non-uniform distribution of the catalyst.

A detail description is presented in chapter 5.

3 SLURRY BED PILOT PLANTS AT SASOL ONE

3.1 Introduction

A typical development of a project involves different departments from the start of the project. One of the first to be involved is the Laboratory, where the reaction kinetics for the alternative catalysts is determined. The main emphasis is on the product distribution related to each catalyst composition. Although the use of highly specialized equipment for analisis is extensive, the measured yields are meaningless for scaleup purposes. A once through operation is typical in this case. The purity of the reactants is very high and the operation is done by highly skilled manpower.

The bench scale pilot plant is where the operating conditions are evaluated. The main objective here is to gather operational data. Yields can now be obtained and the effect of different variables studied. An attempt to reproduce a "typical cycle" of load, conditioning, deactivation, catalyst addition /removal /regeneration can be studied. Economic considerations are not addressed here. The limitation of the applicability of the results depends on the physical similarity of this plant to the commercial design.

The final step to the proof of concept is the use of a semi-commercial reactor. The main emphasis is placed in the study of the most economical route to follow in the plant operation and equipment selection. The cycle to be followed by the commercial route, can now be defined as well as the operating limits. Upsets during normal operation, trouble shooting, startup and shutdown procedures are addressed here. Due to the size of the production, market tests can be performed.

The philosophy of the instrumentation is defined here and new instrumentation tested. Heat removal is studied as well as the flexibility of the process. The reliability for scale up purposes of the obtained data is very high.

Optimization is not generally done in a semi-commercial reactor. A bench scale unit could be used for that purpose. The trial-error approach in a demonstration unit tends to be an expensive exercise but is very useful for confirming the results found on the bench scale.

3.2 Description of the micro-reactor

As mentioned previously, the objective of this reactor is the determination of the kinetic equation and the testing of alternative catalysts in respect of performance and product distribution.

The reactor vessel has a capacity of 500 ml and is made of 304 SS. The mixing inside the reactor is done by impellers and baffles. The gas that is introduced is Arge Pure Gas and its composition can be varied with the addition of gas from cylinders. The Arge Pure Gas is **"cleaned"** by a sulphur guard bed, to avoid sulphur breakthroughs.

The gas is introduced below the impellers and the impeller speed used is sufficient to ensure that a CSTR is obtained. The product (gas and liquid) leaves the reactor through a porous metal filter of 5 microns rating. To achieve the success of the filter operation, the catalyst needs to be sieved prior to loading between to be 38 and 150 microns.

Figure 3.1: Basic Catalysis Microreactor

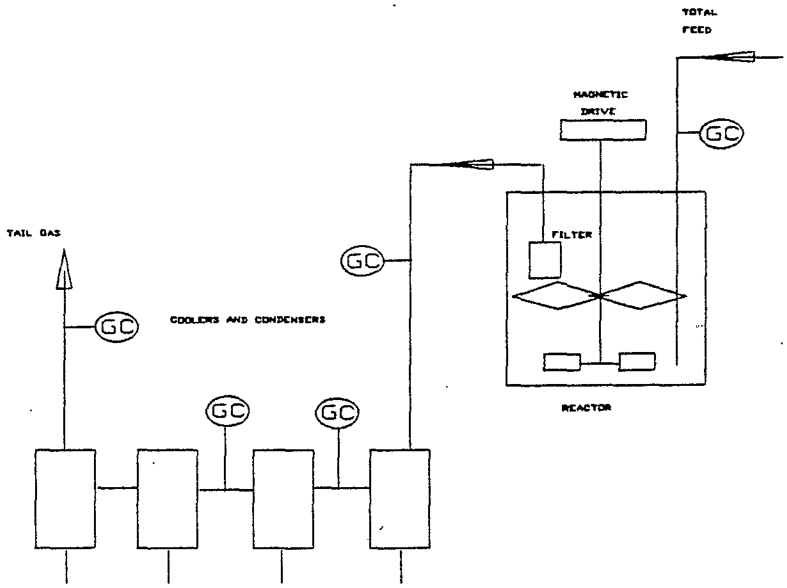

The gas liquid mixture is passed through a series of coolers and the different fractions are collected. Basically all the vessels have draining facilities and are linked to GC ports. A more detail description of this system was done by Van Berge (1989).

3.3 Bench scale pilot plant

This bench scale reactor consists of a circulating system. The products are carried out of the reactor by the ascending gas to a gas/liquid separation vessel. After the separation of phases, the slurry passes through a settler. In this settler the slurry is concentrated and sent back to the bottom of the reactor, while the overflow of the settler represents the reactor wax.

Basically, the reactor is a 12 meter jacketed tube of 46 mm internal diameter. Temperature control of the reactor is provided by means of a pressurized boiling water jacket. The gas is introduced at the bottom of the reactor through a single nozzle. The gas passes through the reactor in a plug flow regime.

Figure 3.2: Research bench scale pilot plant

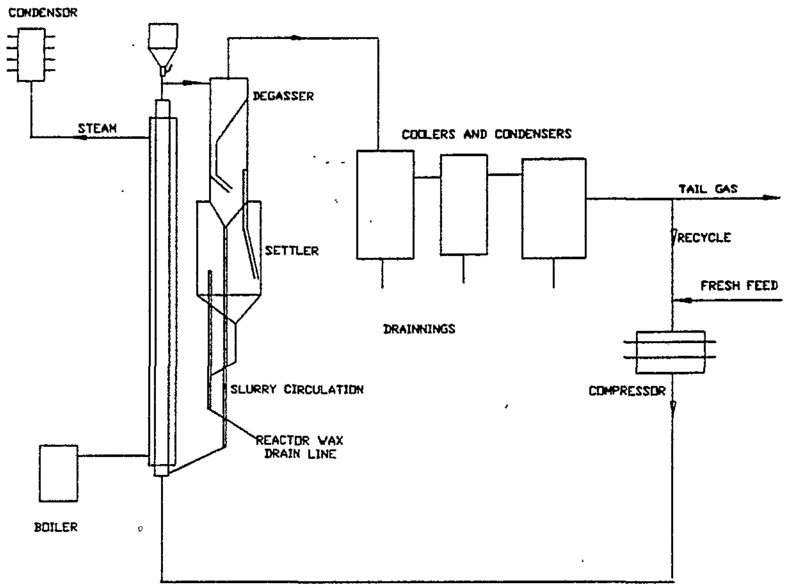

The slurry is carried out of the tube and discharged to the first stage of the settler. The gas velocity is reduced about 16 fold allowing a good separation of the gas/slurry mixture. The slurry is concentrated and returned to the reactor. An open line is used as a control level in the first stage of the settler and wax, which still contains some catalyst, overflows into a storage vessel. In the second stage the catalyst has more time to settle. Typically the solid content after this stage is about 500 ppm.

The reactor exit gases are directed to a set of two knock out vessels and coolers where the heavier hydrocarbons are knocked and the lighter ones condensed as well as the reaction water. The dried gas is then split into two streams, the recycle and tail gas. The tail gas is flared and the recycle gas is mixed with the fresh feed and its pressure boosted in a compressor before being sent back to the reactor.

3.4 Works pilot plant

The Works Pilot Plant, as it is called, was designed initially as a Fixed Fluid Bed (SFFB) for high temperature Synthol application. The construction material used was intended to be able to resist up to 350 C as normal operating temperature over a Hydrogen rich environment. Since gas/solid separation devices were required (cyclones), the internals were accommodated in such a way as to make provision for the cyclones dip legs. Several modifications have been done in order to make the reactor suitable for the slurry operation.

The reactor is a 86.6 cm column diameter with a length of 24 meters. It has three different sections. In the first 2,7 meters (from the bottom) there are no internals. The second section contains cooling coils of 3" SCH 160. There are 16 coils in a square pitch of 6 inches. The space left by the cyclones dip legs were at one stage filled with filters (runs 1 to 5) and, since run 6, by dummy coils. The total number of coils is 21. This section covers from 2,7 meters to 9,3 meters height.

The rest of the reactor is empty but for the filter section located between 11,2 and 12,2 meters of the column heigth. The set of filters consists of 4 banks, each capable of accommodating 4 filters. These filters are candle type filters of 1 meter long and 60 mm diameter.

Until now different positions for the filters have been tested and it is intended since run 7 to reproduce the position of the commercial design. This last section covers from 9,3 meters up to the bed level. The design bed level is 18 meters, leaving 5,3 meters for disengagement.

Figure 3.3: Process Development works pilot plant

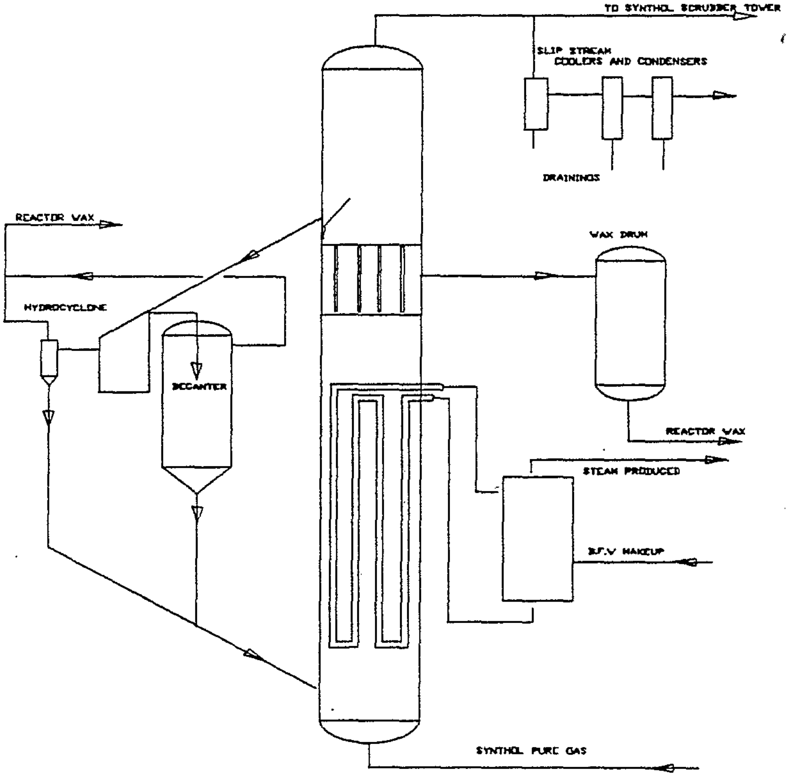

The operation of the Demonstration unit is as follows. The gas is taken from the Synthol train (Synthol Pure Gas) or the Arge train (Arge Pure Gas or Arge Tail Gas). The gas is fed at the bottom of the reactor through a proprietary gas distributor. A detail drawing can be found in Drawing Office of Sasol One under Drg. No. 700/2H, Reg. A-16-9747.

The gas is bubbled through the bed and as it rises, it induces liquid circulation (figure 2.11). The liquid velocity inside the column could reach up to 2 m/sec as described in 2.3.3 this high degree of liquid circulation would be responsible for the high level of mixing and the high heat transfer coefficient observed.

The gas/slurry separation is very sharp. Gamma ray scanning showed that the actual gas/slurry separation takes place in less than 25 cm. One can therefore said that if foaming is present, it should be in a thin layer at the top of the bed (around 15-20 cm).

The light products leave the reactor with the unconverted reactants from the top of the reactor while the wax produced is removed through the filters. Different kind of filters are being tested and evaluated. The selection of the filters will be based in their reliability and service period rather than their efficiency. Typically the filtered wax contains about 100 ppm Fe. The filters are backwashed with filtrated wax with a predetermined frequency.

The reactor gas is discharged to enter the Synthol loop at the Scrubber tower of the existing Synthol train (A,B or C) or sent to flare by directing it to E201 (wash tower).

In order to have information of the product and gas analysis, a slip stream is taken from the main gas reactor exit line. The gas from the slip stream is sent to a series of knock pots and coolers where the heavy and lighter hydrocarbons and water are condensed. The first vessel is kept at the same temperature as the reactor and is only used to determine the extent of slurry or catalyst entrainment. The second vessel is kept at about 170 C and the "hot condensate" collected from it. A set of two coolers follows and their drainings are called cold condensate. The remaining gas is measured and analysed before it is flared.

How the works pilot plant fits into the Sasol One gas loop is shown in figure 3.4.

Figure 3.4: Slurry Bed works pilot plant in the Sasol One Gasloop

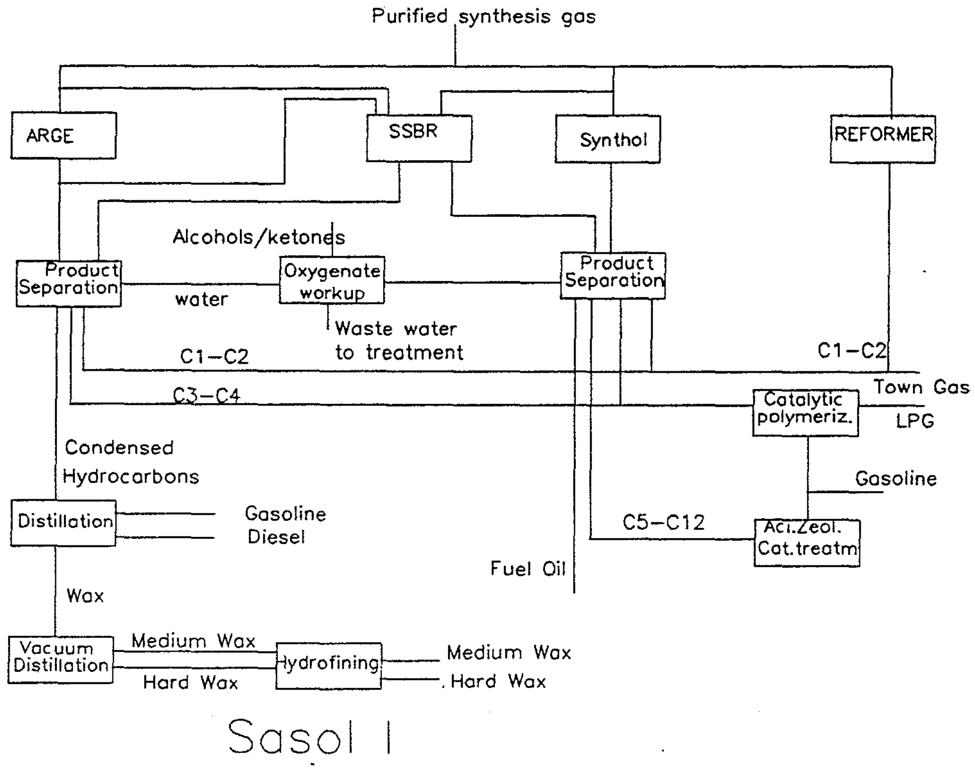

3.5 Pilot Plants Comparison

Due to the difference in sizes and objectives, a direct comparison of the different pilot plants cannot be made. However, when assessing some results obtained in these plants, one has to bear in mind their similarities and differences to judge their applicability.

Table 3.5: Size comparison of the Slurry bed reactors

Variable	Units	**MICRO-REACTOR**	**BENCH SCALE**	**WORKS PILOT PLANT**
Diameter	cm	7.85	4.56	86.6
Bed height	cm	8	1200	1800
Cat.Inventory	kg	0.015-0.03	6-12	800-2000
Total Gas Flow	n L/h	48-180	35000	8'800,000
Wax Product.	kg/day	0.2	10-16	5000
Wax Loading	kg	0.32	20	2100

Table 3.6: Comparison of Reactor Operating Conditions

Variable	Units	**MICRO-REACTOR**	**BENCH SCALE**	**WORKS PILOT PLANT**
Gas/catalyst	nm3/h. kg	1.6-12	2.9-5.8	3-25
Gas Velocity	cm/sec	0.065	42-46	36-44
Liquid Veloc.	cm/sec	0	4	0.01
Gas Turnaround	sec	101.5	21.45	46.14
Cat. Concentr.	%	5	35	35
Pressure	bar	20	22-26.5	20
Temperature	Deg C	240	240-246	240-250
Hydrodynamic Regime		CSTR	Plug Flow	Liquid: Circulating Flow Gas:Backmixed

Indicative	Performance related to:	**MICRO-REACTOR**	**BENCH SCALE**	**WORKS PILOT PLANT**
Conversion per pass	Fresh Feed	30-70	16-18	30-32
kmol/h.kg cat.	Catalyst	0.267	0.13	0.392
kmol/h.L vol	Reactor	0.0138	0.0796[1]	0.037
Wax Turnaround (day)	Production	1.6	1.5-2	1-1.4

4 EVALUATION OF THE HYDRODYNAMIC PARAMETERS ~~IN~~ for THE SLURRY BED REACTOR

4.1 Introduction

Most of the studies from which the correlations were obtained were air/water/glass beads and were presented in chapter 2. The gas linear velocities were below 10 cm/sec in most of the cases and, because of the high cost of the experimental equipment, the column diameters were limited to 15 cm. Within this range of conditions, the homogeneous and plug flow regimes are mainly present. So most of the correlations are only applicable in these regimes.

The use of correlations determined for a different system would not be able to predict the actual situation in our system. This is because of their dependance on the following factors:

---

[1] Considering only the reactor section, not the circulating system.

Table 4.1: Hydrodynamic parameters that can affect the hydrodynamic properties

Gas	density, molecular weight, solubility and composition.
Liquid	density, vapor partial pressure, viscosity, surface tension, foaming tendency, capilarity.
Solid	surface wettability, particle size distribution, sphericity, porosity.
Operating Conditions	Pressure, temperature, gas and liquid velocities, solid concentration, gas inlet temperature
Reactor Geometry	Height, Diameter, Internals (cooling coils, filters, supports), bottom shape and gas sparger.

Due to the great number of variables and their combined effect, a selection was made in terms of the unknown effect or unquantified effects that can affect the reactor performance. The correlations for the estimation of these parameters were found to be adecuate only for the regime in which it was produced. Most of them were innadequate for the turbulent regime with which we are concerned.

4.2 Interfacial area

The present model used the product of the interfacial area and the mass transfer coefficient for the CO_2. The other products are calculated with the Wilke Chang equation.

The effect of gas linear velocity determine the validity of the expression used. Below gas linear velocities of 4 cm/sec a simple equation such as $k_l a = cU_g$ can be used. But for higher velocities which produce a turbulent regime the equation change. Godbole (1984:444) working with Sotrol-130 (a mixture of C9 + iso paraffins) and with gas velocities up to 24 cm/sec found the following relationship:

$$k_l a = 0.31 U_g^{0.603}$$

Stern (1985) used Godbole's data in order to have a relationship that will also cover the low gas velocity regime, producing:

$$k_{l,co} a = \frac{0.12}{1 + 11 U_g}$$

The studies more relevant to our system are listed here:

Table 4.2: Techniques used for the determination of the gas-liquid mass transfer coefficient

Author	Column Diameter cm	Liquid	Gas	Gas Velocity cm/sec	Technique
Godbole 1984	35	Sotrol-130	Air	3-24	O2 conc
Akita 1973	15.2	Water	Air	0.4-33	Na2SO3
Kastanek 1977	30-100	Water	Air	0.2-20	Na2SO3
Towell 1965	40-105	Water	CO2	4.5-30	CO2 abs.

After considering the gas velocities used, the column diameter and the liquid media, it was decided to use the correlation of Godbole (1984:444).

With this initial value, it is possible to calculate the other components ak_l using the Calderbank and Moo Young correlation for bubbles smaller than 2.5 mm

$$k_l Sc^{2/3} = 0.31 \left(\bar{\mu} \Delta \rho \frac{g}{\bar{\rho}^2} \right)^{1/3} \qquad (*)$$

The relation is reduced to

$$k_{L,i} a = k_{L,co} a \left(\frac{D_i}{D_{co}} \right)^{2/3}$$

* k_L = cm/s , ρ = gr/cc , μ = gr/cm-s

4.3 Gas holdup

Some studies were made using Fischer Tropsch wax. Bukur (1982, 1983, 1987, 1989, 1990) made a very complete study using different waxes but their results are of limited applicability due to the fact that he worked in very low velocity ranges and at atmospheric pressure.

Most of the correlations developed by different studies are in the form:

$$\epsilon_g = K_1 U_g^{K_2}$$

Due to the importance of this hydrodynamic parameter, the CSIR was contacted to do some research work in the determination of the gas holdup. The characteristics of the equipment used were:

Table 4.3 : Characteristics of the columns used by the CSIR

Col. N.	Diam. cm	Height meters	Gas cm/s	Gas	P Bar	Liq.	Temp	Solid	Conc
1	45	8	30	N2	4	Wax	240	Fe	40%
2	15	8	20	N2	10	Wax	240	Fe	40%

The results of their studies indicated the effect on the gas holdup of the following conditions:

Table 4.4: Gas holdup trends found by the CSIR

at higher	temperature	higher	gas holdup
	pressure		gas holdup
	Solid concentration		gas holdup
	gas velocity		gas holdup
at bigger	column diameter	no effect in	gas holdup

Although Van Vuuren (1987:7) did not found foaming tendency in our wax, inhouses tests reveals that this effect is most probably to exists.

Considering the equipment limitation of the CSIR, several test were done also in the Demonstration unit. The reactor has dp cells to measure the density of the fluidized slurry as well as the height of the slurry bed. These are gas tight systems and are often purged to avoid blockages. The gas holdup was calculated from the drop in the level of the slurry bed after the gas supply was shut off. Allowing enough time for the gas to dissengage, the reading of the bed before and after the cut of the gas is considered reliable. The exact position of these dp cells in the demonstration reactor is shown in figure 4.1.

4.3.1 Effect of Temperature

No studies have attempted to correlate the effect of temperature on the gas holdup expression. This parameter was not taken into consideration in most of the studies which were done at ambient conditions. In our case in which the

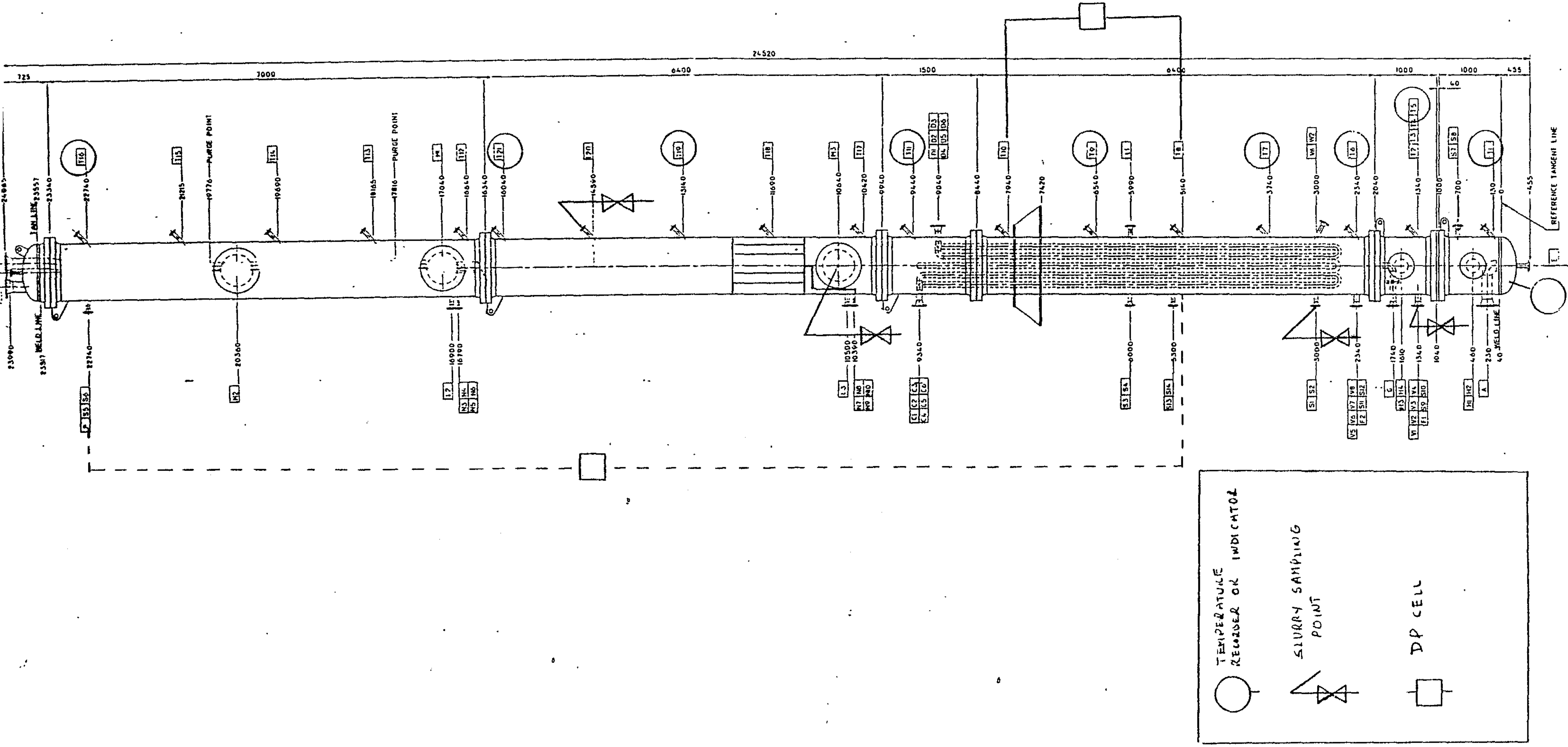
24520
725
7000
6400
1500
6400
1000
1000
455
40
PURGE POINT
PURGE POINT
TAN LINE
WELD LINE
WELD LINE
REFERENCE TANGENT LINE
TEMPERATURE RECORDER OR INDICATOR
SLURRY SAMPLING POINT
DP CELL

temperature can rise to 260 C and decrease to 200 C along the run, it is necessary to introduce this parameter into the general expression.

CSIR results are shown in figures 4.2. The results of the Works Pilot plant did not reflect a great difference when operating temperatures differing by 10 or 20 deg C. This is because the temperature of the bed is not homogeneous and the whole effect is balanced out.

Figure 4.2: Temperature effect on gas holdup

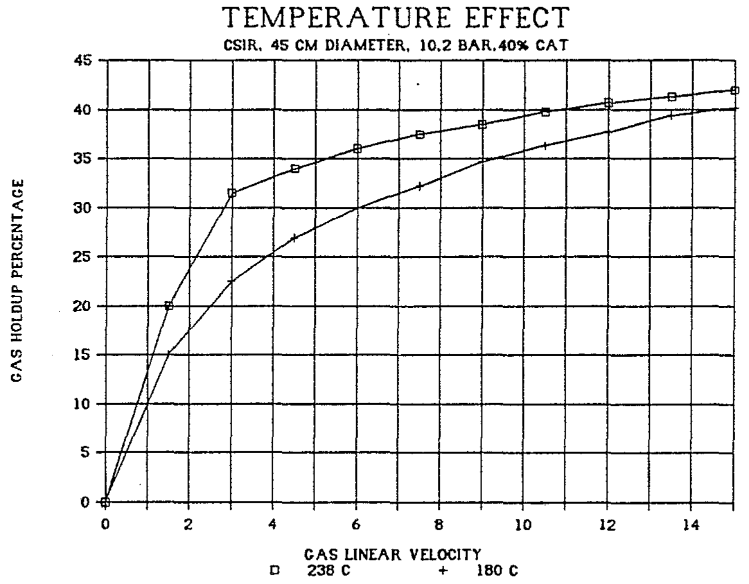

4.3.2 Effect of Pressure

In this field there is ongoing discussion between researchers. While Bukur (1987:1087) found no dependance in the range of 1-15 bar, other researchers (Clark 1990:2301, Kojima 1991:115, Wilkinson 1991:128) did.

CSIR studies found pressure dependence. Our inhouse tests reveal the pressure dependance as well. Moreover, the gas hold up was investigated with different gases. This was done in order to be able to assess the effect of the gas density as well. Results can be seen in figures 4.4.

Figure 4.3: Pressure effect on gas holdup: CSIR data

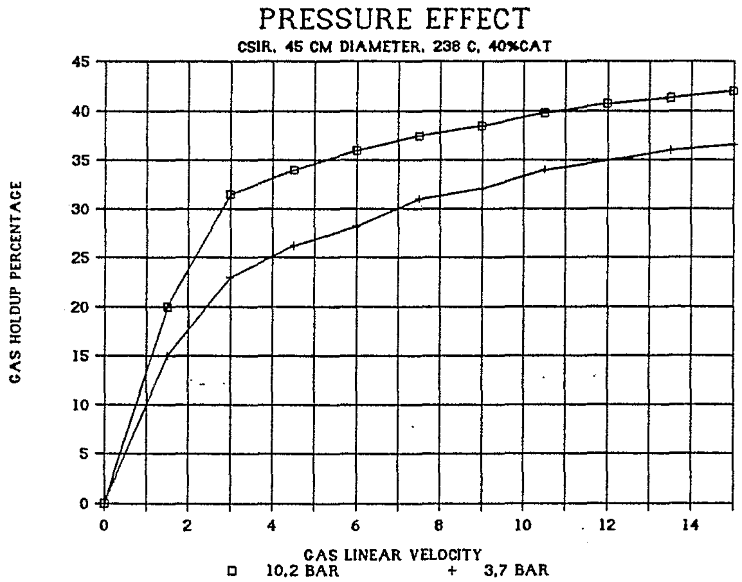

Figure 4.4: Pressure effect on gas holdup : Works Pilot Plant

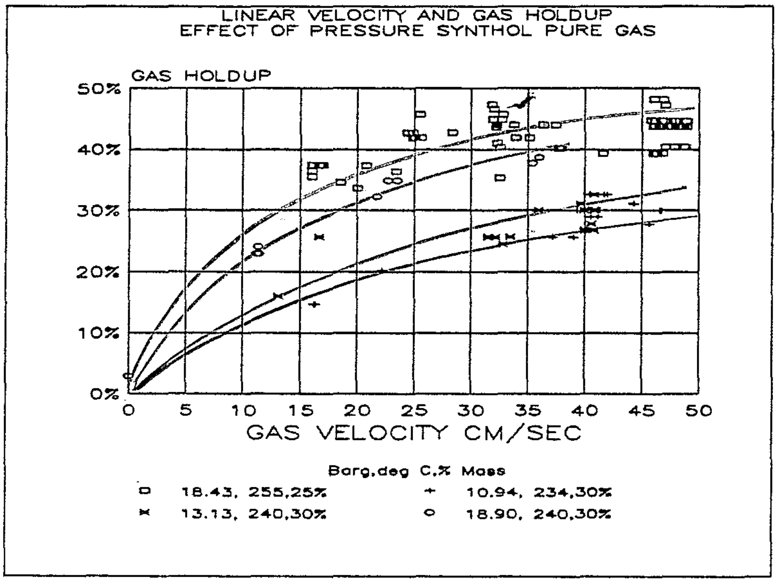

Results obtained using Nitrogen showed that the main contribution to the gas holdup is the gas density. This information is useful when designing a column for different gases (eg. recycle).

4.3.3 Effect of Catalyst concentration

On this particular point, much disagreement among researchers can be found. Some of them maintain that, at higher solid concentrations the gas holdup should increase, while others claim the opposite. It is believed that both opinions are correct, but only in the systems in which they were measured. Many factors can contribute to the difference in behavior.

Only a different composition of the solid particle would change the surface wettability properties. A poorly wettable surface would increase the gas holdup. The reason that the gas holdup decreases with the addition of solids in other systems is the effect of solids on viscosity and on the surface tension and the resulting effect of these two in the tendency to foam.

The CSIR results agrees with Bukur (1990) that in case of the Sasol Arge Reactor wax working with Fe oxide, the higher the solid concentration the higher the gas holdup. Bukur found that above 30 % mass of solid concentration, the gas holdup drops.

Results obtained in the demonstration reactors also showed that at higher solid concentration the gas holdup increases. This has been proven for concentrations up to

30 % mass. Above this limit circulation problems were experienced and this was also reflected in the drop of the heat transfer coefficient, discussed under 4.11.3.

4.3.4 Correlation

The correlation obtained includes the effect of gas density, pressure, solid concentration and gas velocity. This was obtained by the use of the data from the CSIR.

$$\epsilon_g = 3.4436 U_g^{0.2682} \left(\frac{\rho_g}{P} \right)^{0.53} X_s^{0.1703}$$

The same expression in terms of its primary physical properties is:

$$\epsilon_g = 0.10285 U_g^{0.2682} MW^{0.4375} P^{1.0925} T^{-0.4375} X_s^{0.1703} \qquad (*)$$

The parity plot obtained with this correlation is shown in figure 4.5.

Figure 4.5: Gas holdup correlation: Parity plot

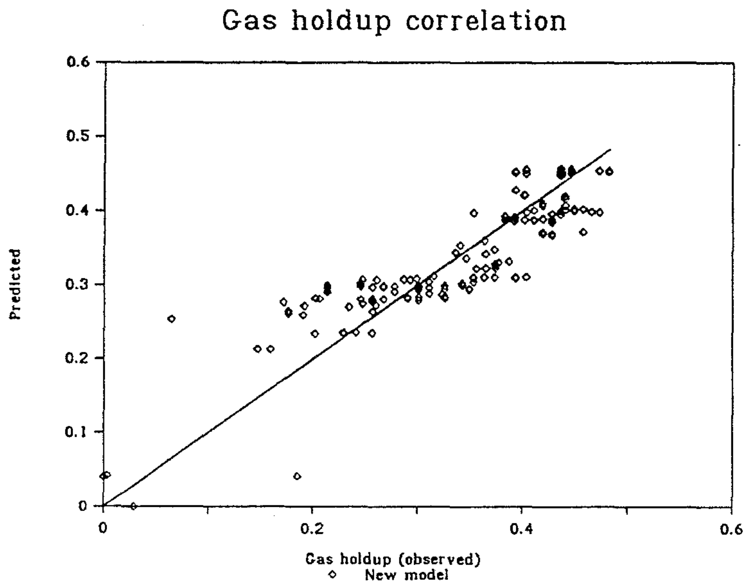

* U_g = cm/s , T = °C

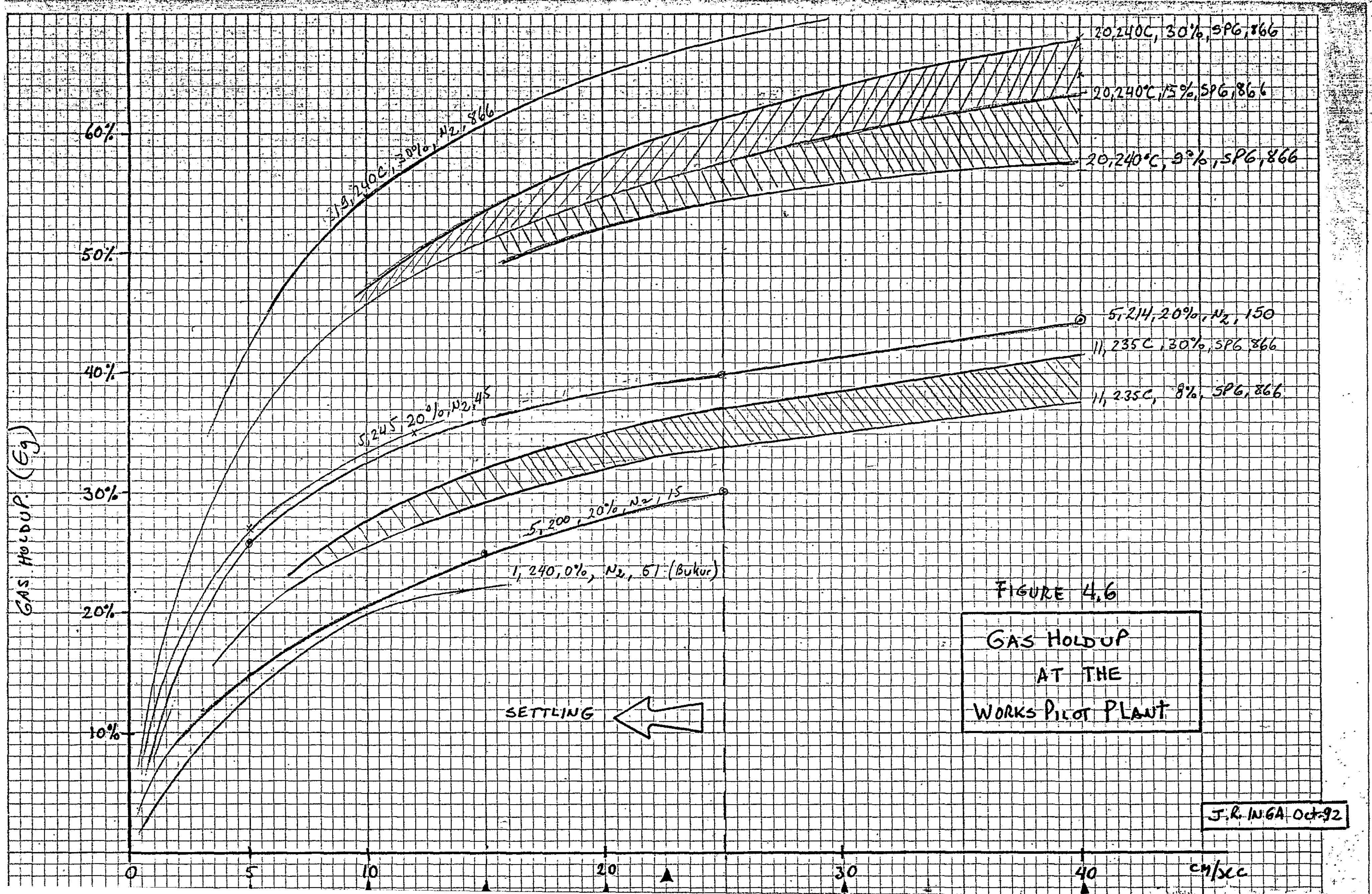

FIGURE 4.6

GAS HOLDUP
AT THE
WORKS PILOT PLANT

J.R. INGA Oct-92

The data from the works pilot plant is presented in figure 4.6 .

4.4 Gas dispersion coefficient

The four equations listed in table 2.3 were considered and compared with our inhouse tests. As can be seen in figure 4.6, the discrepancy between the predicted values and the observed are considerable.

The degree of mixing in the demonstration unit was done by means of a radioactive tracer. Monitoring the concentration at the exit of the reactor, the Peclet number can be calculated.

Figure 4.6: Gas dispersion coefficient: Comparison betweee predicted and observed

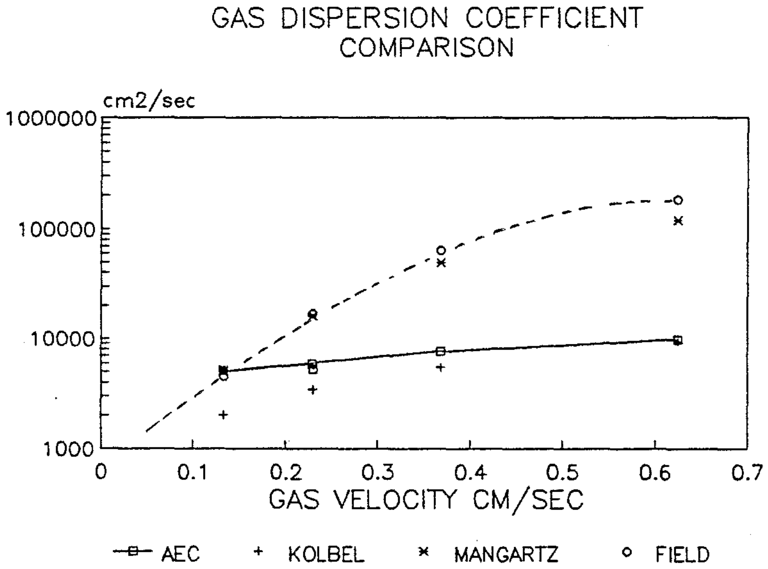

This experiment was done with help of AEC (Atomic Energy Corporation) and the use of Argon 41. The tracer gas was injected in gas inlet in the form of an impulse by means of

Nitrogen pressure. Different gas velocities were investigated. The actual results and the calculations followed are presented in Appendix 1.

Table 4.5: Operating conditions used for the determination of the gas dispersion coefficient

Gas Inlet Flow nm3/h	Gas Outlet nm3/h	Gas[1] Velocity cm/sec	Peclet Number	Gas Dispersion Coefficient cm2/s
4892	3790	23	26.7	4394
4924	3808	23	23.8	4921
3071	2042	13	19.1	4231
6760	5658	37	26.6	6393
7681	6756	62	28.2	8114

Figure 4.6 shows the comparison with the published correlations. It was decided to use an exponent of two for the column diameter, obtained by Towell and Ackerman (1965) and correlate the effect of the gas velocity.

The results obtained gave a new correlation, with a $r^2 = 91.7\%$

$$D_G = 1.9 d_c^2 U_G^{5/11} \qquad (*)$$

It can be argue why the difference in the gas velocity exponent compared with the values listed in table 2.3. The main difference between our system and the bubble column that the previous correlation was developed for the presence of internals. The presence of cooling coils behaves in a similar

---

[1] Calculated in the cooling coils region.

$*$ $d_c =$ cm, $U_g =$ cm/s, $D_G =$ cm^2/s way as a draft tube, this would increase the mixing. The effect of the gas velocity in the turbulent region is not a drastic as in other hydrodynamic regimes.

Another analysis that can be done to express the degree of mixing is in terms of a number of CSTRs in series. A plug flow regime would be described as an infinite number of CSTR in series, while a complete mixed reactor would be represent by only one. This means that the higher number of CSTRs in series the closest to a plug flow behaviour .

Figure 4.7: Number of CSTR in series

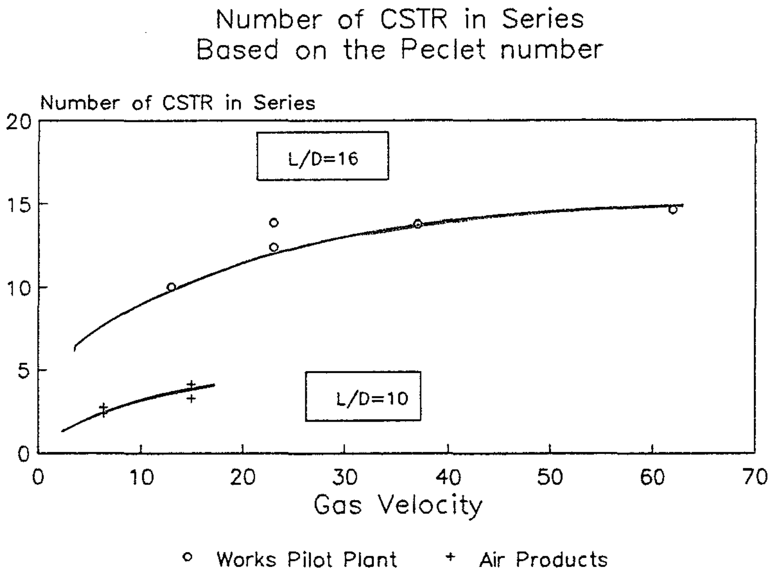

A similar analysis was done by Air Product and Chemicals (1990), and their results are shown in figure 4.7. It is important to note that the degree of mixing in the works pilot plant is much lower than the Air Products experience. This can be expected, considering that the gas holdup obtained with our system is lower than the Air Product experience for a similar set of conditions, which means that the slip velocity (defined in 2.2.3) would be lower. This would increase the residence time of the gas and therefore the degree of mixing would be much higher.

The procedure used for this calculation is presented in appendix 2.

4.5 Bubble Size

4.5.1 Bubble size distribution

Due to the characteristics of our system, light and conductivity probes can not be applied to measure bubble sizes. Other techniques such as photography and video recording are also not suitable for dark systems. Another method to asses the bubble sizes is the dynamic disengagement method (see 2.2.1). This method relates the rate of the drop in the bed level to the bubble sizes.

The CSIR did several tests in order to evaluate the effect of gas velocities and pressure. The table of results are listed in Appendix 3. No definetely trend could be found with gas velocity, but it was with pressure. This confirms results presented in the literature, in which at high pressures, the bubble sizes tend to decrease.

Figure 4.8 presents the fraction of the small bubbles of the total gas volume in the expanded bed as a function of pressure.

Dynamic disengagement tests were done in the works pilot plant. Limitations of this method are related to the reliability of the density measurement and the effect of the induced circulation rates. The dynamic disengagement test is done by monitoring the level drop rate after a sudden cut of the gas. Due to settling during this period, the density measured by the bottom dp cell (figure 4.1) indicates a higher density than the one expected along the reactor. This effect produces a systematic error for a certain period. Nevertheless the method can be applied if this period can be identified and corrected. An example of the calculation procedure followed is presented in appendix 4. Figure 4.9 shows the results obtained with this method.

Figure 4.8: Effect of pressure on the bubble size distribution

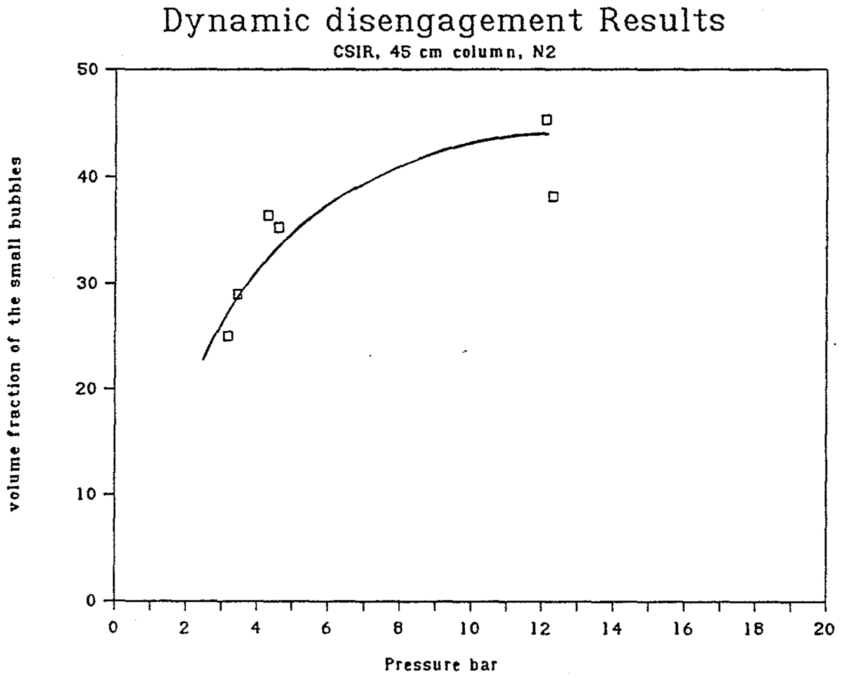

Figure 4.9: Bubble size distribution calculated by the dynamic disengagement method.

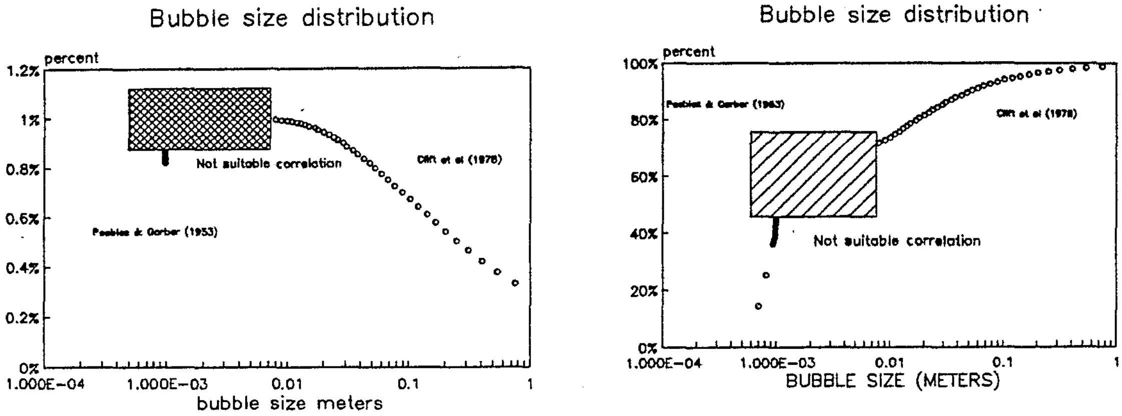

4.5.2 Maximum bubble size

In order to determine if big bubbles were present, gamma ray scanning was used. Probes and detectors were placed at different levels outside the reactor. Any disturbance noticed on a the detector was correlated with the readings of the detector. Special efforts were made to compare statistically if the same shape of the disturbance was observed in the upper detector. If it was the case, the confirmation of the passing of a big bubble was made. The time that the disturbance (bubble) took to travel from one detector to the other and the distance between them set the bubble velocity. The magnitude of the disturbance, expressed in the decreased density, determine its size.

The determination of the bubble size is still a point of discussion. Basically there can be two cases: The first assumes that at any time there is a bubble size distribution at that bed level. The moment a big bubble passes through, it displaces the same volume of gas/liquid upwards.

The second theory states that as the bubble passes through, only the liquid is pushed upward while the bubbles are pushed towards the wall.

The first theory gives more conservatives results (bigger bubbles). The maximum bubble size found with this method was about 25 cm diameter (Steynberg 1991). These bubbles were detected above the coil section. Due to the interference of the coils to the gamma ray, it was not possible to identify any specific disturbance in this section.

Some of the detected bubbles collapsed in the filter region, while others passed all the way through. An example of this analysis is presented in appendix 5.

4.6 Catalyst Concentration

Because of catalyst settling, different catalyst profiles can be found inside the reactor depending on the phase velocities. Matsumoto (1989:1701) showed that the solid concentration can reach a point in the reactor that is almost null. Therefore all the bed volume above this point is not used during reaction.

As it was pointed out in **2.4.2**, the presence of internals enhance the circulation and therefore the mixing. O'Dowd (1987:1959) reported a better homogeneous distribution of solids in columns with internals than in empty ones.

The solid distribution depends in our case mainly on the solid dispersion coefficient, which is a function of the gas velocity.

The catalyst concentration profile was measured in the Works pilot plant at different levels of the reactor. Correlating these results, one can see that there is definetely a concentration profile. Whilst large drops in concentration along the reactor length are presented in the literature, this is not our experience, due to the high gas velocity and the effect of the cooling coils which enhance the liquid circulation and therefore the mixing of the solids. Other evidence of this concentration profile is that the density profile along the reactor, as measured by Atomic Energy Corporation (Smith 1991a, 1991b), showed a declining trend.

Figure 4.10 : Density profile in the works pilot plant

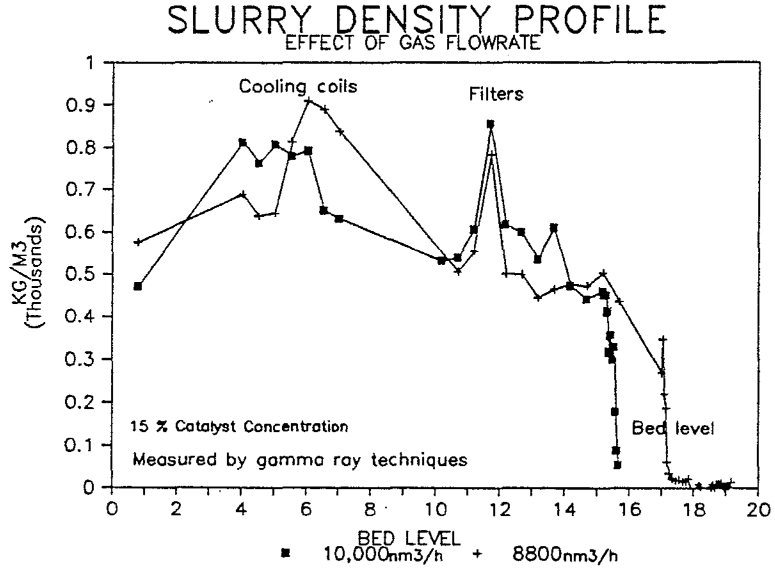

The proposed sedimentation model by Matsumoto (1989) was used for the prediction of the catalyst concentration profile. Figure 4.11 shows the prediction compared with the actual results.

Figure 4.11: Solid concentration profile in the works pilot plant

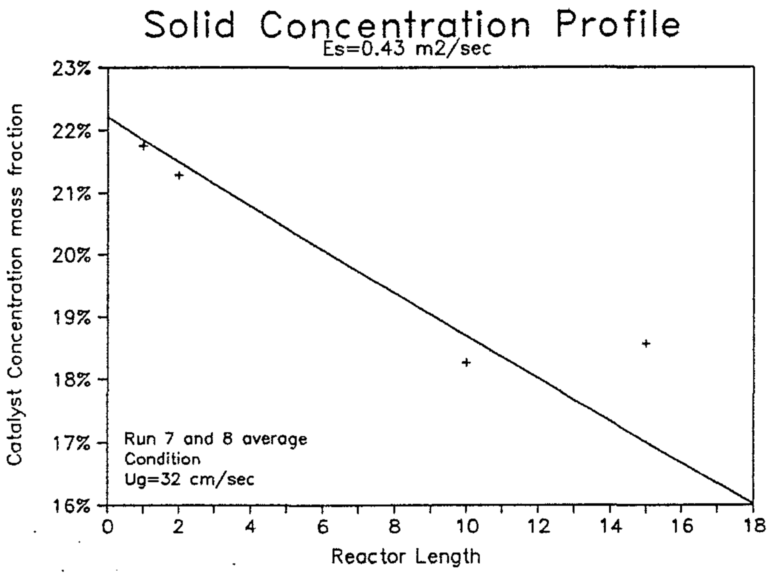

The sedimentation model was applied to our system with the following considerations:

Table 4.6: Physical properties of the Catalyst used.

Particle size	d_p	30 microns	mean particle size at reaction conditions
Density of squeleton	ρ_{Fe}	2.5-2.9 g/cc	$Fe_5C_2, Fe_2O_3, Fe_3O_4$
Porous Volume		0.6 cc/g	Determined by Basic Catalysis by adsortion/desortion of Nitrogen
Wax density	ρ_l	0.7 g/cc	Determined by the CSIR (45)
Particle density	ρ_p	3.72 g/cc	Calculated at reactor conditions, all the porous filled with wax

The calculated effective terminal settling velocity of the SSB catalyst is comparable with previous works (Smuk 1991, Air

Products 1980, Buijn 1989, Imafuku 1968, O'Dowd 1987, Kato 1972). The actual particle size of the catalyst used in the works pilot plant is presented in table 4.7 .

Table 4.7: Particle size distribution of the Slurry Bed Catalyst

Below	Cumulative volume percent	
microns	Arge Crushed	Spray Dried Catalyst
176	100	100
125	100	100
88	82.9	78.3
62	58.6	70
44	30.4	56.2
31	12.3	39.3
22	6.8	35.9
16	4.5	28.9
11	4.1	24.4
7.8		14.5
5.5		9.1

4.7 Liquid velocity

Although the Works pilot plant does not have the capacity to induce net liquid velocity, the location of the filters induce a liquid velocity of 0.25 mm/sec. This is not enough to eliminate the sedimentation tendency of the solid particles. In spite of the low value of this factor, it is necessary to consider it for the reactor modeling.

An assesment of the liquid circulation velocity can be made with the result of the gamma ray test for bubble detection. It was measured velocities about 2 m/sec in the middle of the column (Smith 1991b). This high velocity produces turbulence

PARTICLE SETTLING VELOCITIES

Particle	Size microns	Density g/cc	Liquid Used					Reference
			Water cm/s	R.Wax cm/s	Isoparaffin cm/s	Varsol cm/s	Tricloro–ethylene	
Glass Beads	180	2.55	2.72					Imafuku et.
	111	2.55	1.03					al 1968:
	74.3	2.55	0.463					153
	64.2	2.55	0.346					
Ion Exch.Resin	110	1.2	0.13					
FeSiO2	73.5	7	1.65					
Cu	64	8.8	1.44					
Glass Beads	58		0.3			0.247	0.322	Bruijn et.al
	71		0.443			0.369	0.456	1989: 285
	91		0.69			0.599	0.684	
	122		1.119			1.009	1.085	
	78.5		1.1103			0.901	1.328	
	66		0.394			0.325	0.409	
Glass Beads	96.5		0.8		Without Internals			O'Dowd et al:
	96.5		0.4		With Internals			1987: 1966
Fe Oxide	3	5			0.1			Air Products
	48	5			0.4			Final Report
	100	5			1.9			1990
Silica	48	2.4			0.2			Fig. 9.4.1
	100	2.4			0.6			
Glass beads	1410	2.52	20.24					Smuk et al:
Nickel beads	512	8.9	22.97					1991:1384
Ion exch resin	850	1.35	4.61					
Ottawa sand	725	2.52	10.73					
Fe oxide	30	3.1		0.2				
SSB catalyst	30	3.72		1.36				Our Work
Glass beads	63–88	2.52	0.67					Kato et al
	88–105	2.52	1.36					1972: 113
	125–149	2.52	1.4					
	149–177	2.52	1.85					
Glass beads	774	2.5	11.9					Miyahara et al
	300	2.5	4.86					1989: 1196
Activat. Carbon	778	1.509	5.69					
	912	1.509	4.83					
Acetate	1500	1.252	6.99					
	1000	1.252	4.94					
	1500	1.252	7.4					
Nylon	2500	1.15	8.74					

Liquid Properties							
Density	kg/m3	997	700	740	788	1452	
Viscosity	Pa.sec	0.00089	0.00142	0.0012	0.001236	0.000552	
Surface Tension	N/m	0.072	0.0254	0.022	0.0283	0.029	
Specific Heat	KJ/kg.K	4.187	4.07	1.08			
Thermal Conductivity	W/m.K	0.603	0.147	0.13			

in the filter region. This was used for the disintegration of the filter cake after being dislodged by the backflush (Inga 1991). This was the experience during SSB run 7 and confirmed during run 13.

4.8 Liquid dispersion coefficient

This is the parameter that had the most agreement amongst all the authors. All of them agreed on an expression of:

$$D_l = 2.7 d_c^{3/2} U_g^{0.3} \qquad (*)$$

The first coefficient changes from author to another by up to 10 percent and the exponents almost stay the same.

4.9 Isothermal Behaviour

From run 1 to run 5 in the Works pilot plant, isothermal behaviour was noted. During these runs different configurations of the coils and the filters were tried. A major change was introduced between run 5 and 6. Dummy coils were placed in the coil section in order to have a more even distribution of the coils . The filters were re-positioned above the coil section, in a similar location to the commercial reactor.

A temperature difference was found along the reactor. This temperature increased with catalyst concentration.

Table 4.9: Geometrical difference of the works pilot plant when isothermal behaviour was lost

	Run 5	Run 6,7	Difference
% of open area in coil section	83.14	78.13	-6.0%
Hydraulic diameter	27.16	21.38	-37.02

(*) d_c = cm, U_g = cm/s, D_L = cm²/s

One explanation of this behaviour is the existance of two circulating cells as showed in figure 4.13.

The existance of two different circulation cells is related to the liquid circulation velocity of each one. The bottom cell includes the coil section which has a smaller hydraulic diameter, this means that has a strong wall effect. Bernemann et al (1991:76) showed that the bigger the number of coils in the column the higher liquid circulation velocity. Considering this, it is expected that the liquid carried by the rising gas after leaving the coil section unto a empty column, decreases its velocity, this discontinuity has to be accomodated. So therefore part of the liquid rises and the rest recirculates.

To have an idea of the length of each cell, temperature readings were used to identify the extent of the cells. The lower circulation cell includes the bottom dome up to the upper coil supports. No temperature difference was found in this section except at the gas inlet, which is expected due to the lower temperature of the gas. The top circulation cell starts from the top of the coils and includes the filter section up to the bed level. In this region the temperature difference is minimal.

For modelling purposes, a homogeneous temperature was assumed. Considering that the difference is only about 7 C, this assumption is not far from reality.

A detailed analysis was done by the author (Inga 1992).

LIQUID CIRCULATION PROFILE

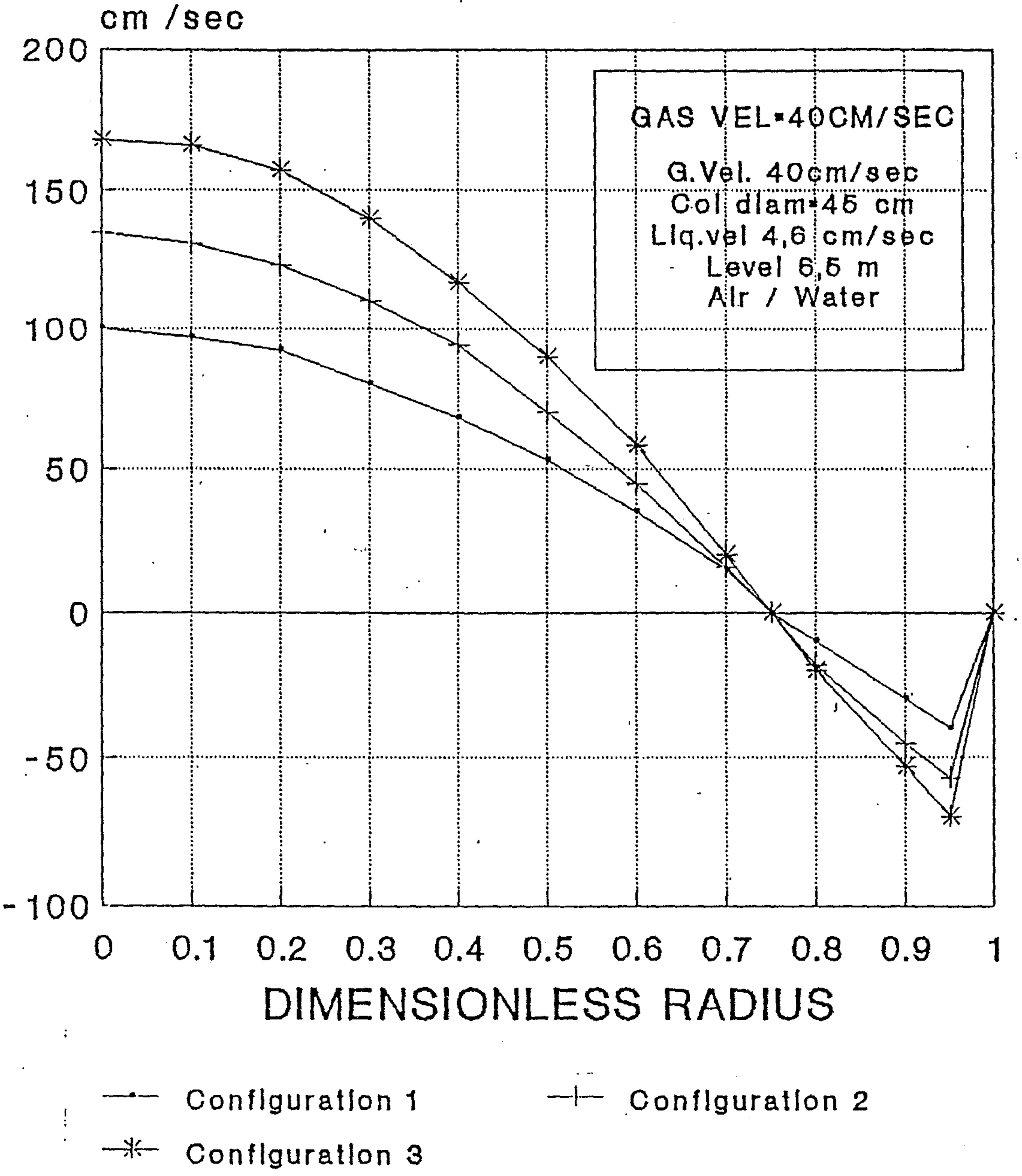

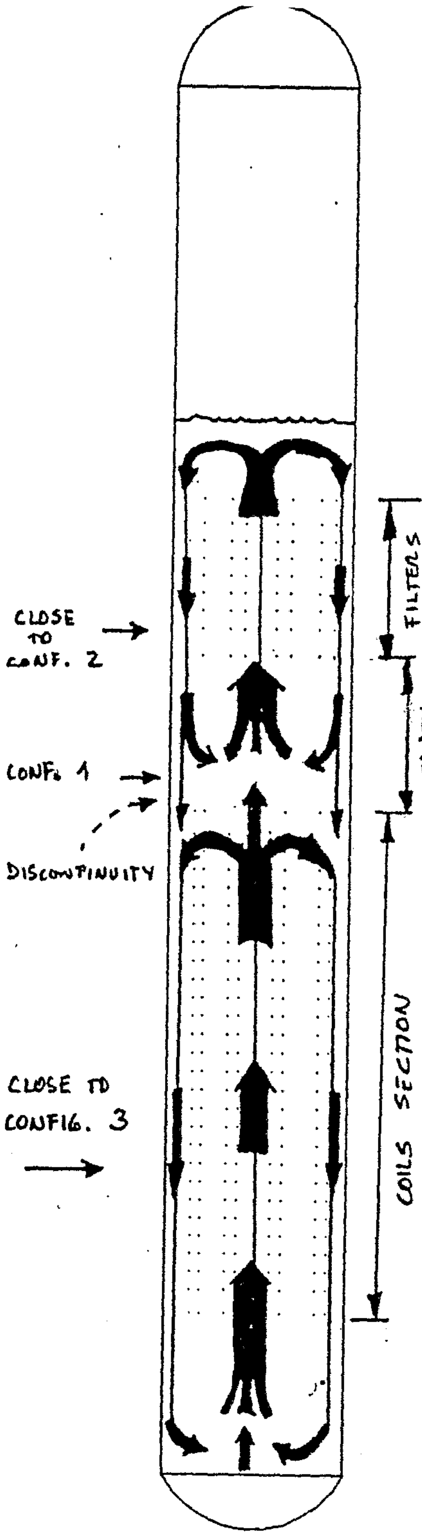

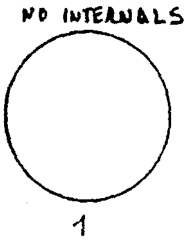

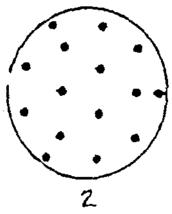

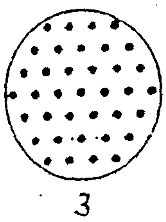

Source: Bernemann K and Steiff A. 1991: 76

4.10 Liquid and Solid Entrainment

During run 7 and 8 liquid and solid entrainment was detected and measured in the first knock-out pot of the slip stream in the demonstration reactor. Calculations were made in order to determine the type of entrainment. It was found that if a mixture of wax/catalyst was entrained as droplets, these droplets should only have a solid concentration of 1.4 kg/m3 . The reactor ran at about 250 kg/m3 of solids.

Although it can be argued that it is a combined effect of thermodynamics (reactor wax condensing in the cooling train) and solids entrainment, it is believed that the mechanism of entrainment is different. The postulated mechanism is divided into two parts. The first part involves a partial solid/liquid separation and the second one a mechanism of droplet disengagement.

The partial solid /liquid separation can be explained by a small layer of foaming. It has been found that even foams of 6 mm can produce a big separation of the solids in a slurry. This theory is based on the observation made by Bruijn et al(1989:283) and explained under **2.4.4**. Bruijn working with varsol (similar properties as reactor wax at reactor conditions) and glass beads and found that the solid concentration of the foam layer was between 1.7 and 4 kg/m3. Atomic Energy in the gamma ray scanning determined that the splashing area of the slurry /gas disengagement was about 25 cm. This would be enough to reduce the solid concentration to levels of 1.4 kg/m3.

The second mechanism is explained by Miyahara et al (1989:1195). Basically the mechanism explains that the wake that follows the ascending bubble is strong enough to carry particles in the freeboard area. Depending on the bubble size and the properties of the particles this solid/liquid mixture would reach a certain height. If the reactor's freeboard is shorter than this required height, the mixture of liquid/solids would end in the coooling train.

4.11 Heat transfer coefficient

4.11.1 Introduction

The heat transfer coefficient for a three phase slurry reactor has been studied extensively due to its importance in the application of slurry bed columns with exothermic reactions. One of the advantages of the three phase slurry reactors over the fixed bed is that this reactor can be considered isothermal due to the easy removal of the generated heat.

The most comprehensive study has been done by Saxena working at Univesity of Illinois at Chicago. Most of his findings are resumed in the final report to the U.S. Department of Energy (Saxena 1991).

Most of the correlations of different researchers can be described by the equation:

$$St=a(Re^{b}Fr^{c}Pr^{d})^{e}$$

Table 4.10: Heat transfer coefficient correlations

Author	a	b	c	d	e
Hikita 1981	0.268	1	1	2.16	-0.303
Deckwer 1980	0.1	1	1	2.00	-0.25
Air Products 1990	0.063	1	2	1.60	-0.25
Shaykhutdinov 1971	0.11	1	1	2.50	-0.223

4.11.2 Measurement in the works pilot plant

In the works pilot plant, the heat is removed by cooling coils inside the reactor. Water is recirculated in these coils and is supplied from and to a steam drum, where flashing occurs. Boiled feed water makeup is fed to the drum to keep a continuous level. Both steam produced and water makeup are measured in order to calculate the heat removed. Knowing this heat removal, the used area, and the temperature difference, it is possible to calculate the overall heat transfer coefficient.

This calculation was made since run 1. The system was designed to have a maximum vaporization rate of 5% inside the tubes. The velocity of the water inside the tubes is high enough to ensure turbulence (Reinolds=600,000)

Using the equation:

$$\frac{1}{U_o}=\frac{1}{h_o}+r_o+r_w\left(\frac{A_o}{A_{avg}}\right)+r_i\left(\frac{A_o}{A_i}\right)+\frac{1}{h_i}\left(\frac{A_o}{A_i}\right)$$

it is posible to calculate the external heat transfer coefficient h_o. For our system it was calculated that the resistance to the heat transfer is as described in figure 4.14.

Figure 4.14: Heat transfer resistances

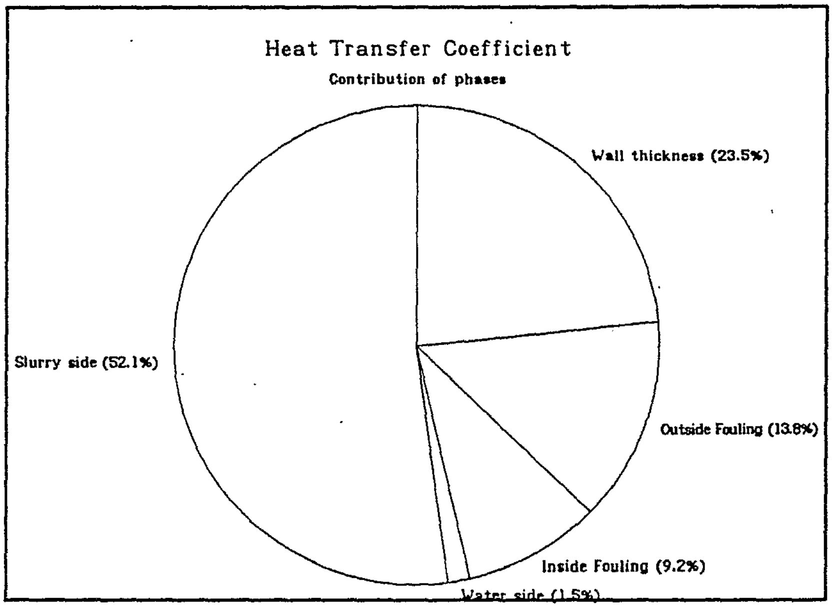

4.11.3 Discussion

The heat transfer coefficient observed in the works pilot plant is in good agreement with the predictions obtained with Deckwer's equation (Inga 1992c). One limitation of these equations is that all of them are related only to the physical properties and the operating conditions of the system. None of them incorporates the effect of column diameter, neither the hydraulic diameter.

Because the main contribution to the heat transfer coefficient is the liquid velocity induced by the rising gas, it is expected that systems with high wall effect would produce more turbulence and therefore higher heat transfer, this would not be reflected in the predicted values.

Another limitation observed is the effect of high solids concentration. There is a point where the viscosity increases so much that the liquid circulation velocity is affected and the heat transfer coefficient drops. This was observed during run 6 (Steyberg 1992).

Figure 4.15: Effect of solids concentration in the Heat transfer coefficient

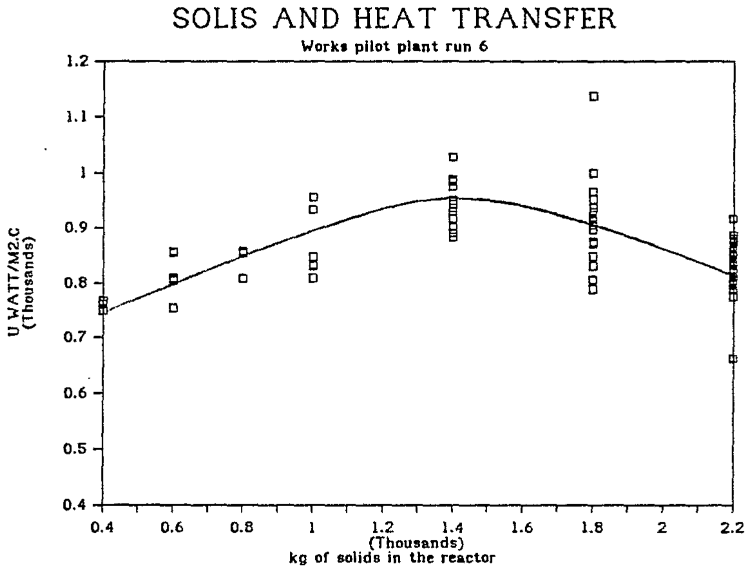

5 MATHEMATICAL MODEL OF THE SLURRY BED REACTOR

5.1 Introduction

The model was based on Stern (1984, 1985a, 1985b) and was initially developed at the University of California at Berkeley USA.

This model was created for the bubbly regime and all the parameter estimation was directed to this hydrodynamic regime. At Sasol the model was set up initially with the existing 2 inch research pilot plant. Most of the correlations were taken from the initial version and applied to our systems working at higher velocities, temperatures and pressures. The intention was to reproduce its performance so well that any discrepancy in the reproduction of the results expected in the demonstration reactor could be attributed to scaleup effect.

The model was linked with flashes subroutines developed by G.Tonsmann. This enabled it to simulate a complete reactor train

Figure 5.1: Slurry Bed Reactor Computer Model

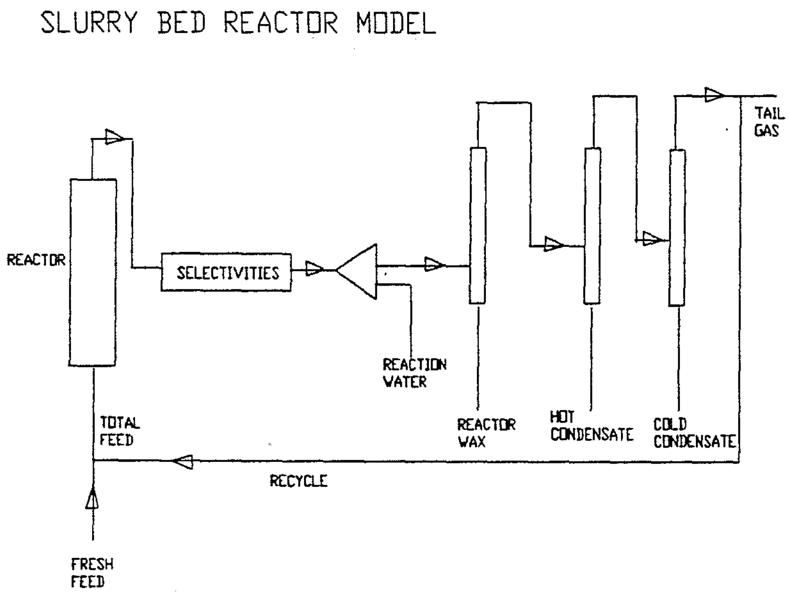

The partial pressure profiles alond the reactor allowed it to be linked to a subroutine developed by Dr. A. Vosloo to calculate the selectivities. The plant computer model was used for the design of the Sasol One commercial plant.

5.2 Reactor Model Description

The mathematical model describes the system with mainly 4 differential equations. The gas and liquid phases are described as second order differential equations and the total mass balance plus the solid phase distribution as a first order differential equation.

The reactor is divided in 21 intervals in which the differential equations (DE) are converged. The expressions for the gas phase are:

$$\frac{\epsilon_g}{Pe_g}\frac{d^2\theta_{g,i}}{d\xi^2} - \frac{d(\nu\theta_{g,i})}{d\xi} - N_{g,i}(\theta_{g,i}-\theta_{L,i}) = 0$$

where the Peclet number is defined as $\frac{U_g L}{D_g}$ and the Stanton Number as $N_{g,i} = \frac{k_{L,i} a L}{m_i U_g}$. The first term considers the gas dispersion effect along the reactor axis and the amount of gas present is expressed by the gas holdup. The gas dispersion coefficient D_g is included here. The Peclet number shows a reverse trend than the gas dispersion coefficient and is very useful for the determination of the degree of mixing inside the reactor. The lower the Peclet number, the closer to a CSTR reactor that means the higher of the gas dispersion coefficient the higher degree of mixing of the gas phase.

The second term $\frac{d(\nu\theta_{g,i})}{d\xi}$ is the effect of the volumetric contraction due to the transfer of the reactants from the gas phase to the liquid phase along the reactor.

The third term $N_{g,i}(\theta_{g,i}-\theta_{L,i})$ is the one that represents the mass trasfer reistance from the gas to the liquid phase through the gas-liquid interfacial area. The Stanton Number includes the $k_{L,i}$ (per component) , the interfacial area defined by the bubble size and the solubility of the reactant.

The expression for the liquid phase is:

$$\frac{\epsilon_L}{Pe_L}\frac{d^2\theta_{L,i}}{d\xi^2} - \frac{d\theta_{L,i}}{d\xi} - N_{L,i}(\theta_{g,i}-\theta_{L,i}) + \frac{m_i w(1-\epsilon)L\overline{w}}{C^{\circ}_{H_2}U_L}r_i = 0$$

where the Peclet number is defined in a similar way as in the gas phase. In the first term the amount of liquid is considered in the liquid holdup, its mixing by the liquid dispersion coefficient and its velocity. For the bench scale reactor the Peclet number of the liquid phase is very high so one can conclude that it is very close to a plug flow reactor. No circulation regime could be expected under these circumstances.

The second term assumes the effect of the total concentration in the liquid phase. The third one is equal to the gas phase only expressed in the liquid side. The fourth is the most important term which assumes all the chemical reactions r_i. Each reaction is defined later by its kinetic expression. This therm also considered the gas solubility, the amount of liquid present, the catalyst present (important factor when the process is kinetically controlled) and the rate of replacement of liquid inventory (liquid velocity).

The overall mass balance of the gas phase can be expressed as:

$$\theta_g \frac{d\nu}{d\xi} + \sum_{i=1}^{n} N_{g,i}(\theta_{g,i} - \theta_{L,i}) = 0$$

with the boundary condition at the initial point, where $\xi = 0$, $\nu = 1$. This only assumes any change in the gas phase.

As it can be seen in this set of equations is not posible to make a direct indication of the effect of a change of one parameter. For example, because the reaction takes place between the liquid and the solid surface, the amount of liquid in a fixed volume should be maximized. This would mean the decrease of the volume of gas in the bed volume (gas holdup), and therefore its interfacial area.

5.2.1 Stoichiometry of the reactions

This model was produced using the theory of Schultz-Flory product distribution. This theory described the growing of the hydrocarbon chain as in polimerization and can be mathematically described with the use of a fixed chain growth probability α. With the use of this parameter only the distribution of carbon numbers in the product is described but not the Hydrogen consumption. Because one of the characteristics of the slurry process is the higher yield of olefins (which is not only a function of the process but also of the catalyst used), the Hydrogen consumed depends also on the ratio of olefins / paraffins produced. Therefore the used on another parameter defined as γ which represents the proportion of the parafins present per carbon number is used. The use of this variable assumes that this ratio is been kept constant with carbon number.

The set of equations used for the Fischer Tropsch synthesis is:

$$\nu_{CO}CO+\nu_{H_2}H_2 \dashrightarrow \nu_{HC}C_xH_y+\nu_{H_2O}H_2O$$

and each coefficient is defined as:

$$\nu_{CO}=-\frac{1}{3+\gamma\alpha(1-\alpha)+(1-\alpha)^2}$$

$$\nu_{H_2}=-\frac{2+\gamma\alpha(1-\alpha)+(1-\alpha)^2}{3+\gamma\alpha(1-\alpha)+(1-\alpha)^2}$$

$$\nu_{HC}=\frac{1-\alpha}{3+\gamma\alpha(1-\alpha)+(1-\alpha)^2}$$

$$\nu_{H_2O}=\frac{1}{3+\gamma\alpha(1-\alpha)+(1-\alpha)^2}$$

$$x=\frac{1}{1-\alpha} \qquad y=2\left(\frac{1}{1-\alpha}+\gamma\alpha+(1-\alpha)\right)$$

The Stern model introduces the water gas shift reaction with the assumption that it reaches equilibrium so rapidly that it is maintained along the reactor. This is true in the case of the Synthol reactor because of its high temperature and catalyst characteristics. It is also important to mention that Stern worked at 268 C. For the introduction of this reaction the use of a proportional parameter is necessary. So β is defined as the ratio of the formation of Water over the formation of CO_2. So that the global expression can be expressed as:

$$\nu'_{CO} = -\frac{1+(1-\beta)^{-1}}{3+\gamma\alpha(1-\alpha)+(1-\alpha)^2}$$

$$\nu'_{H_2} = -\frac{1+\beta(1-\beta)^{-1}+(1-\alpha)^2+\gamma\alpha(1-\alpha)}{3+\gamma\alpha(1-\alpha)+(1-\alpha)^2}$$

$$\nu_{HC} = -\frac{1-\alpha}{3+\gamma\alpha(1-\alpha)+(1-\alpha)^2}$$

$$\nu_{CO_2} = \frac{(1-\beta)^{-1}}{3+\gamma\alpha(1-\alpha)+(1-\alpha)^2}$$

$$\nu_{H_2O} = \frac{\beta(1+\beta)^{-1}}{3+\gamma\alpha(1-\alpha)+(1-\alpha)^2}$$

The relation between this stoichiometric coefficient and the usage ratio is:

$$UR = \frac{\Delta H_2}{\Delta CO} = \frac{1+\beta(1+\beta)^{-1}+(1-\alpha)^2+\gamma\alpha(1-\alpha)}{1+(1-\beta)^{-1}}$$

5.3 Mathematical Solution

For the purpose of this study, the logic used in the development of the model was kept as originally designed by Stern (1985). Changes were required in the assesment of the hydrodynamic characteristics but not for the differential equations or the mathematical solution.

As mentioned in **4.1** the differential equations to solve are the mass balance equations for the liquid and gas phases. These differential equations have to be solved simultaneously with the overall mass balance and should include the axial dispersion term.

To solve this set of equations, it is necessary to use the subroutine COLSYS, developed by Ascher (1981a, 1981b). This subroutine was designed for multipoint boundary value-problems with mixed order systems of ordinary differential equations.

COLSYS follows the method of spline collocation at Gaussian points. The problem is solved on a sequence of meshes until a user specified set of tolerances is satisfied. More detail about the method of mesh generation can be found in Ascher 1981a.

Table 5.1: Differential Equations

z_i	**Component**	**Function**
1		**Volumetric Contraction**
2	**Hydrogen**	**Gas Concentration**
4	**CO**	
6	**CxHy**	
8	**CO2**	
10	**H2O**	
12	**Hydrogen**	**Liquid Concentrations**
14	**CO**	
16	**CxHy**	
18	**CO2**	
20	**H2O**	

The differential equations are supplied in the subroutine FSUB. In the form of:

$$\frac{d^m z_i}{d\xi^m} = \mathrm{Function}_j(z,\xi)$$

here is defined each function in terms of the dimensionless axial position ξ and the value of each function z_i. The function z_i is explained below:

The boundary conditions are supplied in the subroutine GSUB. The variation of the function j with the function z_i is supplied in the subroutine DFSUB. This subroutine evaluates the Jacobian of $\text{Function}_j(z,\xi)$

A more detailed explanation about the mathematical treatment of the COLSYS subroutine can be found in Ascher (1981b.) X

5.4 Catalyst distribution Model

This model is based on the solid dispersion model (Matsumoto 1989). The mass balance around the solid phase is:

$$\phi_s u_p - D_s \frac{d\phi_s}{dz} = \phi_{s,f} \frac{U_{slf}}{(1-\epsilon_g)}$$

The first term represents the settling term, the second one the effect on the solid concentration, and the third the feed to the system.

U_p is not the same as the particle terminal velocity due to the effect of the circulating liquid and the rising gas. It is defined as:

$$u_p = \frac{U_l}{(1-\epsilon_g)(1-\phi_s)} - v_{s,\infty}(1-\phi_s)^{n-1}$$

The first term is the effect of the liquid slip velocity and the second one the effect of the particle terminal velocity.

In a batch operation (no continuous addition or removal of solids), the ϕ_f (solids introduced to the reactor) is zero.

If the aim of the operation is to have an even distribution of the solids in the bed, the optimum would be when $\frac{d\phi}{dz}=0$. Therefore the mass balance equation would be reduced to:

$\phi_p u_p = 0$ meaning that the u_p should be zero.

This requires that the drag effect of the liquid should be equal to the effect of the effective settling velocity of the particle. It is therefore possible to operate a column in such a way that there is not a gradient in solid concentration. This can be done with the liquid velocity.

$$u_l = v_{s,\infty}(1-\phi_s)^n(1-\epsilon_g)$$

Linearizing this expression :

$$u_l = v_{s,\infty}(1-\phi_s)^n - v_{s,\infty}(1-\phi_s)^n \epsilon_g$$

Matsumoto plotted the liquid velocity against $(1-\phi_p)$, keeping the gas holdup constant, in order to get the slope (n).

But not only this arrives from this information: by plotting the liquid velocity vs the gas holdup one can determine the liquid velocity required to operate with an even distribution of the solids at any gas velocity.

Figure 5.2: Conditions for an homogeneous distribution of solids

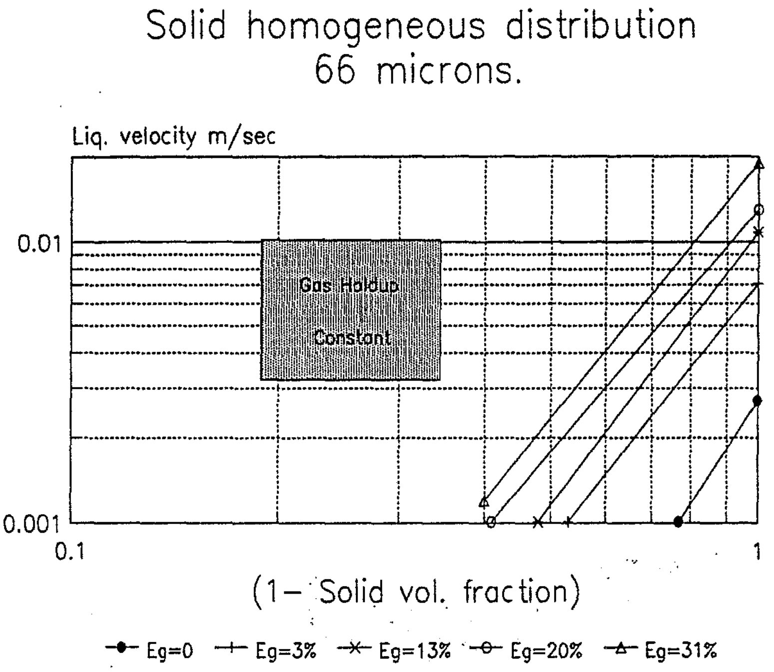

The determination of the required set of velocities for an homogeneous distribution of the solids can be seen in figure 5.4. Matsumoto correlated the n value with the Galilei number. The definition of the Galilei number is:

$$Ga=\frac{d_p^3 g}{\nu^2}\left(\frac{\rho_p}{\rho_l}-1\right)$$

Figure 5.3: Correlation for the exponent n in function of the Galileo number

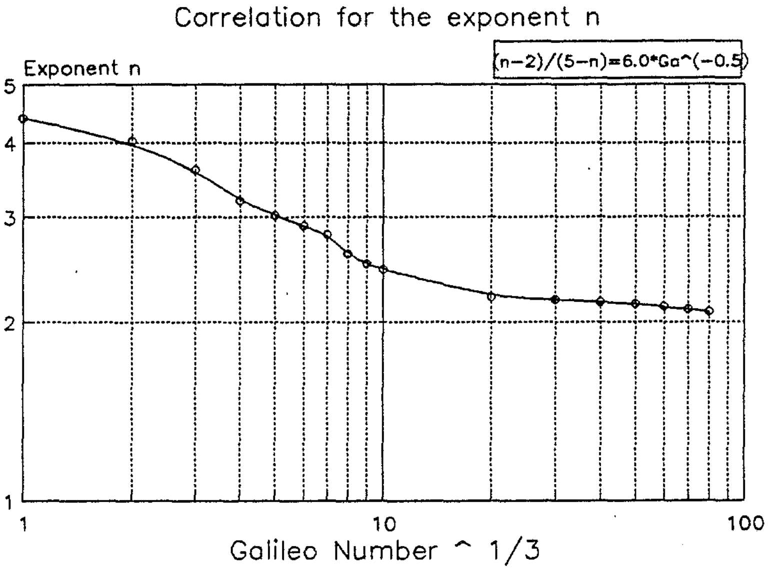

Figure 5.4: Liquid and gas velocities for solid homogeneous distribution

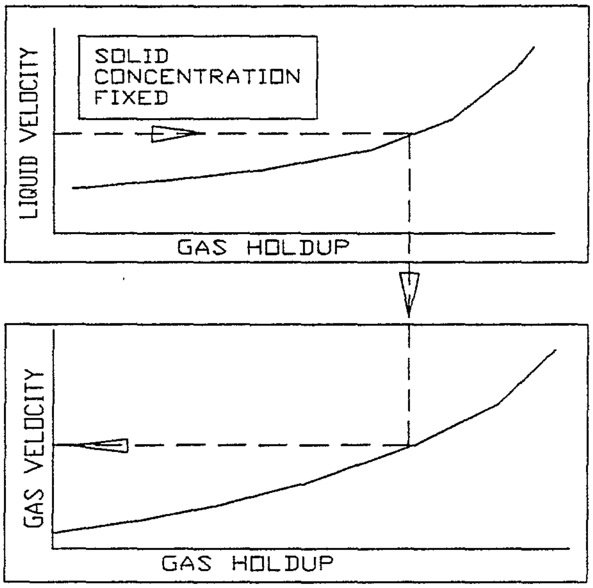

The effective particle settling velocity depends on the particle size and the gas holdup. The calculation of this effective particle settling velocity is done by means of an equation that assumes the Stokes, Allen's and Newton's laws. Due to the fact that this sedimentation effect would take place in a three phase system, a correction factor was required :ζ.

$$\frac{v_\infty d_p}{\nu}=\frac{Ga\zeta}{\left(18^{0.8}+\left(\frac{Ga\zeta}{3.0}\right)^{0.4}\right)^{1.25}}$$

where the correction factor is defined as:

$$\zeta=1+\left\{\frac{6.5(\epsilon_g(1-R))^{0.5}Ga^{0.333}}{1+\left\{(\epsilon_g(1-R))^{0.5}\frac{Ga^{0.333}}{15}\right\}^2}\right\}^{1.5}Ga^{-2/3}$$

5.5 Limitations of the model

The initial model was initially based in Stern (1985) and all his work was done at very low gas velocities (below 5 cm/sec). The hydrodynamics in this region are defined as bubbly regime for the gas phase and a stangnant liquid phase.

The Stern model was tested with results of the two inch pilot plant facility at Research. The model gave meaningless results. Even the trend was not correct. The region where the Research Pilot Plant was working was: U_g about 40 cm/sec, pressures between 20-26 barg in a column diameter of 4.6 cm at temperatures about 240 C with a solid concentration varying from 6 % to 35 % weight and using wax as liquid phase which covers a wide region of carbon number (from $C_{15}-C_{98}$). It is expected that the accuracy of the model should depend on how well all the physical as the hydrodynamic properties can be defined under these conditions. As an example, the gas holdup expression used by Stern was:

$$\epsilon_g = \frac{3U_g}{1.0 + 8U_g}$$

which was found to be a good correlation for gas velocities below 5 cm/sec.

If this equation is used for the conditions of the Research Pilot Plant the gas holdup expected is about 29%. As it can be seen in fig 5.5, at no catalyst concentration the expected value (57%) is almost double. More over, as it can be seen, no solid concentration effect has been taken into account and no temperature or pressure effect was considered in the original equation. As it has been indicated before (Chapter 2) the gas holdup varies with pressure, molecular weight, temperature, liquid velocity, solid concentration and column diameter.

Figure 5.5 : Gas holdup in the Bench Scale Pilot Plant

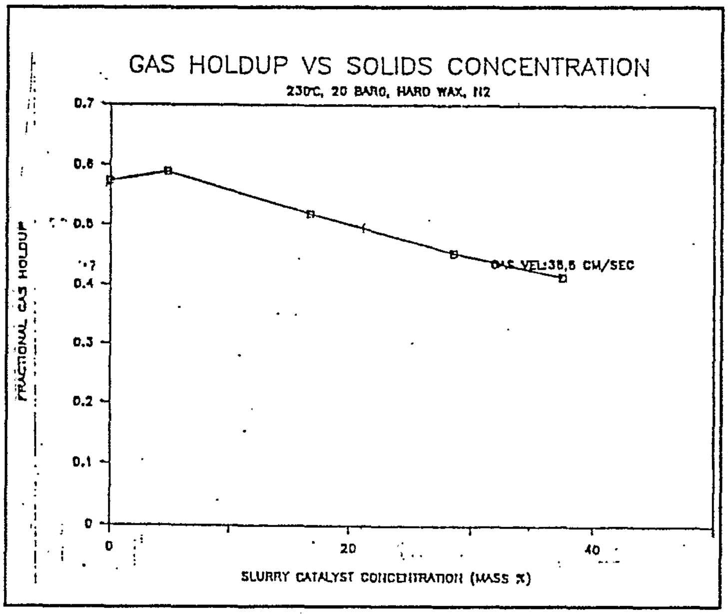

These limitations were overcome by replacing the correlations of the hydrodynamic parameters with the results obtained in the Works Pilot Plant. This would eliminate the effect of the different liquid media and the effect of the operating conditions. With respect to the parameters that we were not able to measured, such as k_L, m_i, D_i, these were obtained from literature. This mean that the results presented in the literature was only considered when similar systems was used under churn-turbulent regime.

The present model does not have a parameter that consider aging of the catalyst. Due to the catalyst addition and removal, this process always is a cycle of catalyst reduction, activity, deactivation and replacement. The effect of the frequency of the catalyst replacement on the reactor performance was addressed in a different study (Inga 1991b).

The main limitation of the model is the unknown effects of scaleup. What would a bigger diameter do to ak_l?. Although it was found by Akita and Yoshida (1973:79), that it would increase, this is the only reference about it, no other authors has confirmed their findings. More over they worked with aquous systems, are their results applicable?.

The effect of internals was addressed in chapter 2. The major effect of their presence is in the degree of mixing. This is expressed in D_L which is a function of the column diameter. This correlation was obtained working with empty columns. The presence of internals decreases the hydraulic diameter, therefore it is expected that the presence of internals should decrease the degree of mixing, which has been demonstrated the opposite by Bernemann and Steiff (1991:76) and O'Dowd et al (1987:1959).

6 Results of the Demonstration Unit

6.1 Introduction

The reactor modelling was done including all the results of the hydrodynamic tests. This has been useful for the separation of the kinetic and mass transfer resistances.

As mentioned in 3.4 the Works Pilot plant operates in a cycle mode. Each cycle is characterised by a online catalyst addition, followed by a reduction period, the peak of activity, deactivation period and finish with catalyst removal. For any model to reproduce the performance of the reactor during these periods, it is necessary to have a very good estimation of the parameters involved.

The catalyst introduced is greencorn (basically Hematite Fe_2O_3). This catalyst in order to react, first has to suffer a reduction step, changing its chemical composition to Fe_3O_4 Magnetite, which is an active site for Water Gas Shift reaction. As the catalyst reduces further, it goes to Iron Carbide Fe_5C_2 where the Fischer Tropsch reaction take place.

The reduction step take place in an Hydrogen rich environment and consumes it, producing water. It has been noted that the activation period is only of 12 hours at the start of run with a reducing gas of 58% Hydrogen, but it takes about 3 days for the subsequent catalyst additions. This difference is because of the reduction of the partial pressure of the Hydrogen due to the Fischer Tropsch reaction and the presence of water in the system, product as well of the Fischer-Tropsch synthesis.

For example, it is known that the last part of the catalyst bed in the fixed tube reactors contains more Magnetite than the average of the tube. And this is because the high partial pressure of water re-oxidize the Fe5C2.

This consideration had to be taken into account in order to evaluate the predictions of the slurry bed computer model.

Another observation made is that the hydrogen of catalyst performance were linked with special events rather than being a continuous process.

Some of the causes that produced these steps changes in the catalyst activity in are listed here. It is important to note them because they are external parameters and the model does not consider their effect in the reactor performance.

Table 6.1: Effect of operating incidents on the reactor performance

Event	Effect in the reactor performance
Slump	If not depressurized and purged with Nitrogen the water dissolved in the wax would re-oxide the catalyst surface
Sulphur	The high reactivity of H2S, produce a permanent deactivation of the catalyst forming FeS.
Oil in Gas	Experience in run 8 showed a drastic fall in catalyst activity. It is believed that the elements contained in the oil (additives) can foul the catalyst surface.
Water	During run 1, water was introduced to the system in the light oil used for filters backflush. The whole catalyst inventory had to be replaced.
Temperature runaway	Temperatures higher than 257 C produce wax craking and higher deactivation rates (run 5).
Bridging	During the inspection after run 5, catalyst bridging was found. This catalyst after being trapped in this bridging, can be consider inert for syntesis purposes.
Entrainment	After run 6, catalyst entrainment was consider an issue. Although the absolute losses is small compared with the inventory, in a continous operation this effect has to be taken in the catalyst balance.
Settling	After run 5, it was found at the reactor bottom a catalyst layer of 15 cm thickness. This amount of catalyst after being compacted with time into this layer was not able to be fluidized again and stayed there for the rest of the run.
Filter Cake	The catalyst trapped in the filter cake does not react while is part of the cake (Inga 1991c). The length of the filtration cycle would affect how much of the catalyst is not utilize for hydrocarbon synthesis.

6.2 Mass Balance

Due to that the demonstration reactor does not have its own cooling train but is linked to the Synthol train for the condensing of products, a mass balance around the reactor is difficult to make. The use of a scale up from the condensates of the slip stream is necessary to calculate conversion, yields and selectivities. A computer program was developed in order to assist the plant personell to evaluate the reactor performance.

The computer programm works with the gas analysis and readings obtained by the plant instruments. The drainnings obtained in the slip stream are accumulated 24 hours and sent for analysis. The moles of liquid products are joined with the moles of gas, calculated by the gas analysis and flowrate, and the sum scaled up with the ratio of the gas flows.

The main limitations of this model are related to human errors (ie: the reliability of the analysis and the operation of the slip stream).

The usual problems when working with waxes is that it congeals. It is a common experience to found some wax blocking the impulse lines of the orifice used for measuring the reactor gas flow. This makes this reading unreliable.

One of the limitations of the slipstream is that it only represent 0.3% of the reactor gas. This gives small drainnings and relative high errors. If one consider that this has to be scaled up 300 times, any error produced in the sampling, or in the measurement of the drainnigs has a enormous effect in the total mass balance. Special effort is being made in order to decrease the number of errors in this operation.

This program is being used daily for internal evaluation and management information.

6.3 Gas-Liquid Mass Transfer in the Slurry Bed

In order to determine the proportion of the mass transfer resistance over the total resistance of the system, a model has to be used. A similar approach to the determination of the heat transfer coefficient need to be done. The equation used should be as well the sum of different resistances, in a similar form as:

$$\frac{1}{U}=\frac{1}{h_i}+\frac{1}{h_{out}}+r_{wall}+r_i$$

The first model used for the determination of the mass transfer resistance was the one proposed by Satterfield (1980). It is a simple model with a number of assumptions described in 2.5.4. The equation that he arrived was:

$$\frac{1}{w(1-\epsilon_g)k_o}+\frac{V_L.S.X_{H2}}{(1+s).X_{H2+CO}.Q.m_H(1-e^{-\alpha_H L})}=\frac{V_L.S}{Qm_H(1+S)X_{H2+CO}}$$

where $\alpha_H=\frac{k_{K.L}a}{m_H.U_g}$

The first term represents the kinetic resistance. As indicated depends on the catalyst activity and the amount of catalyst in the system.

The second term indicates the contribution of the gas/liquid mass transfer to the total resistance. As can be seen it depends on the liquid volume, the gasflow, the solubility of the reactants and the gas/liquid interfacial area. The right side of the equation is the total resistance of the system.

In order to simplified the mathematical treatment, the Fischer Tropsch reaction rate was expressed as:

$$r_{H2+CO} = k_o . W . (1 - \epsilon_g) C_{H,L}$$

This equation comes from the Anderson equation which consider the Fischer - Tropsch reaction rate proportional to the partial pressure of Hydrogen in the system. This equation is being used extensively and is fairly accurate up to conversion levels of 60% per pass.

The results obtained is shown in figure 6.1. For the design case, the mass transfer resistance represents 33% of the total resistance of the system.

Figure 6.1 : Mass transfer and Kinetic Resistances

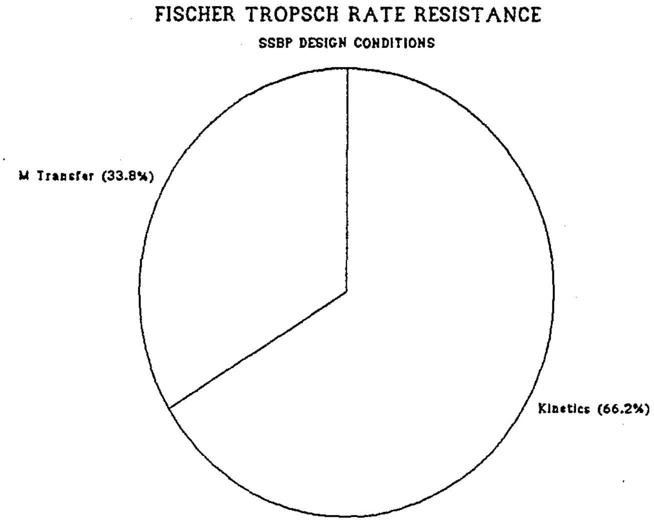

The second method used was based on Bukur (1983:442). He expressed the relative proportion of the mass transfer resistance as:

$$\frac{R_{MT}}{R_{total}}=\frac{\frac{1}{k_L a}}{\frac{1}{k_L . a}+\frac{1}{k_H \epsilon_L}}$$

The results of this method agrees very well with the Satterfield one. An example of the calculation is presented in Appendix 6.

6.4 Reactor Performance Analysis

The slurry bed model was used for the assesment of the catalyst performance. As discussed previously, ther are different events that can affect the catalyst performance. This decay in activity would be reflected in the apparent pre-exponential factor.

The reaction rate used was:

$$r_{FT}=A.e^{-\frac{E}{RT}}w\frac{C_{H,L}C_{L,CO}}{C_{L,CO}+KC_{L,H2O}}$$

The activation energy used was 70,000 kJ/mol. W represent the amount of catalyst in the reactor and the value of K was taken as 3.

During stable operation, the overall reaction rate can be measured by the gas analysis and gas flowrates. The Arhenious factor would take the effect of any temperature difference and the function in terms of the liquid concentration the effect of any change in gas composition. As it can be seen in figure

6.1, there are changes of the pre-exponential factor with catalyst addition or renewals. After a catalyst addition, the first day it decreases indicating that the catalyst just added is inactive. No continuous decay can be observed.

Figure 6.2 :Run 9: Pre-exponential factor

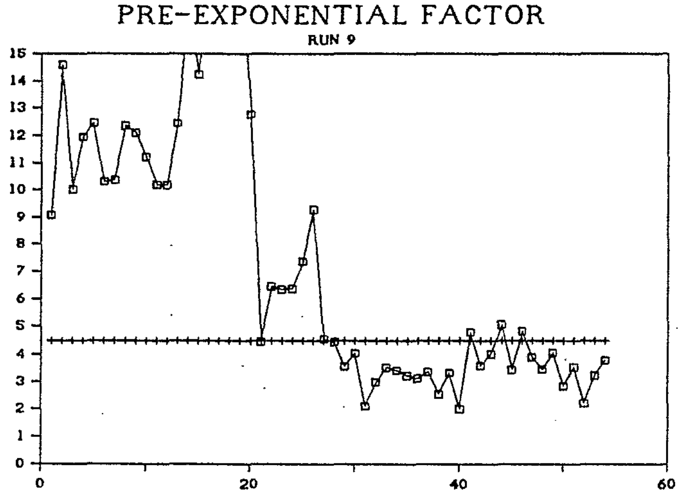

Figure 6.2 shows the effect of the pre-exponential factor in the conversion levels. As can be seen, for the first twenty days, the plant performs better than the model, indicating a very high activity. From day 30 there is a reasonable good agreement between the predicted and the observed performance.

Figure 6.3 : Run 9: H2 + CO Conversion

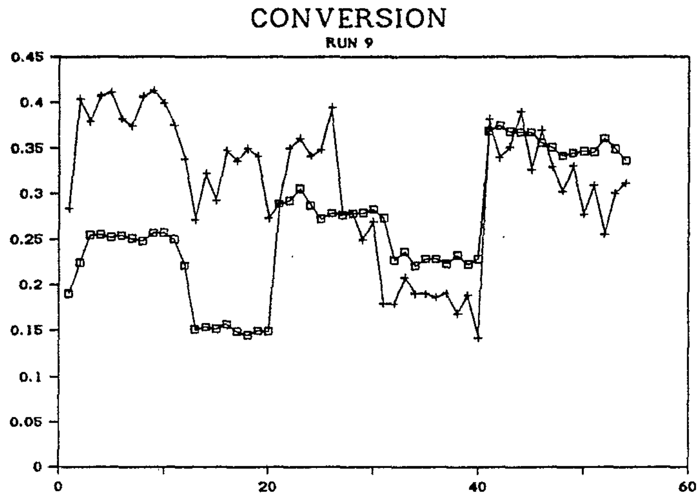

6.5 Discussion

The present model is a theoretical one, therefore the most probable source of error is the estimation of the hydrodynamic parameters. As discussed previously, the estimation of the degree of mixing of the liquid phase is very difficult due to the fact that no study has been conducted with the presence of internals and therefore the present correlation could be inadequated. The importance of the degree of mixing is based on the difference between a CSTR and a plug flow reactor. It is known that for similar reactor volume, a plug flow reactor would give a better performance that a CSTR.

In the Sasol One scenario, where the scaleup is from 86.6 cm to 508 cm, it would mean an increase in the degree of mixing of the liquid phase of 1300 %, moving the system close to a CSTR.

$$\frac{D_{L,\,comm}}{D_{WPP}} = \left(\frac{508}{86.6}\right)^{1.5} = 14.2$$

However, because both of them have internals, and if the degree of mixing depends on the hydraulic diameter, the scaleup would only mean an increase of mixing of 127 %.

$$\frac{D_{L,\,comm}}{D_{L,\,WPP}} = \left(\frac{37}{21.4}\right)^{1.5} = 2.27$$

Another indication of the increase of the degree of mixing is the expected mixing time defined in 2.3.2. A decrease of 50% in the mixing time is expected. This because of the drop in the L/D ratio.

In order to asses the effect of this increase in mixing on the reactor performance, one has to bear in mind the number of CSTR in series represented by the reactor

Using the gas dispersion coefficient D_G, the Peclet number was calculated as well as the number of CSTR's.

Table 6.2 : Number of CSTR's in series

Reactor	D_G	Peclet	# of CSTR
Works Pilot P.	8489	6.8	9.6
Commercial	292111	0.2	1

Figure 6.3 shows that this kind of increase in mixing would imply a significant decrease in the performance per unit volume.

Whereas if the D_L depends on the hydraulic diameter, the expected number of CSTR's would be 8.2 indicating only a drop of performance of 12 %.

The only indication available is the one given by O'Dowd (1987:1961), where he showed the effect of internals on the solid dispersion coefficient (figure 2.19).

Another parameter that we need to asses is the bubble size. It was measured by means of the dynamic disengagement method. In our regime (churn-turbulent), the validity of this method has been questioned due to the liquid recirculation . The reliability of the indicated level and density during the test is also questionable due to settling and disengaging of the gas. However, no alternative method has proven to be succesful in a system similar to ours. Moreover, to obtain bubble sizes from disengaging rates, it is necessary to use correlations of bubble sizes and their rising velocities. Most of these were obtained with water or alcohols. None have been done with Fischer Tropsch wax at our operating conditions.

The effect of scale up on the bubble size is not clear. There is only one study done by Saxena that reports that the bubble size increases with column diameter.

The mass transfer coefficient was estimated by means of a correlation based on diffusivities. Discussion held with proffessor B. Morsi from Pittsburg University showed that the characteristics of the particle used in the slurry could change the liquid properties from a Newtonian fluid to a non-Newtonian one, decreasing k_L by two orders of magnitude. In our system, this would mean that the synthesis rate would be controlled by mass transfer.

The product of the gas/liquid interfacial area and the mass transfer coefficient $a.K_L$ can be addressed jointly. It was found by Yoshida and Akita (1965:11) that it increases with column diameter (figure 6.4), while Sharma and Mashelkar (1968:10) found that aK_L increases when L/D decreases (figure 6.6).

As mentioned before, the scaleup effect would increase the degree of mixing, and this in turn would increase the heat transfer coefficient. Although the correlation that fits our data does not include the column diameter, it has been shown by Saxena that the heat transfer coefficient increases with column diameter (figure 6.5). This was expected due to the increase of liquid circulation velocity at the middle of the column. If one uses the equation proposed in 2.3.3, the expected increase in the liquid velocity would be about 1300 %. This would not be so high if this correlation is also effected by the hydraulic diameter rather than the column diameter. In this case the liquid velocity would only increase by 120%. This would increase the kinetic energy of the bubbles. As discussed in 4.10, the liquid/solid entrainment depends on the kinetic energy of the droplet formed when the gas bubble hits the bed surface. It could be expected that the amount entrained would increase according to the increase in the liquid velocity.

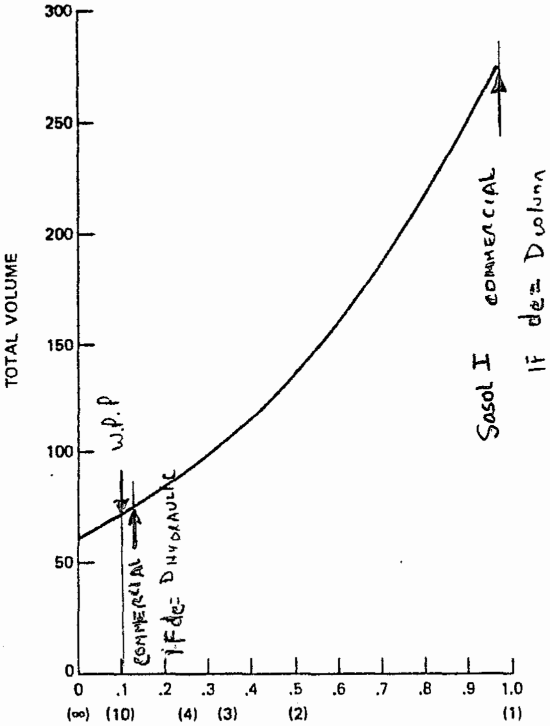

Total volume of CSTRs in series.

FIGURE 6.3

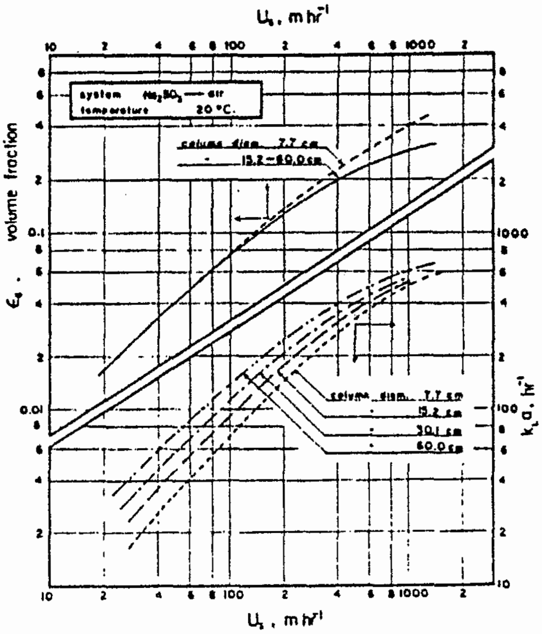

. Effect of column diameter on k_La and gas holdup in sodium sulfite solution.

FIGURE 6.4

FIGURE 6.5

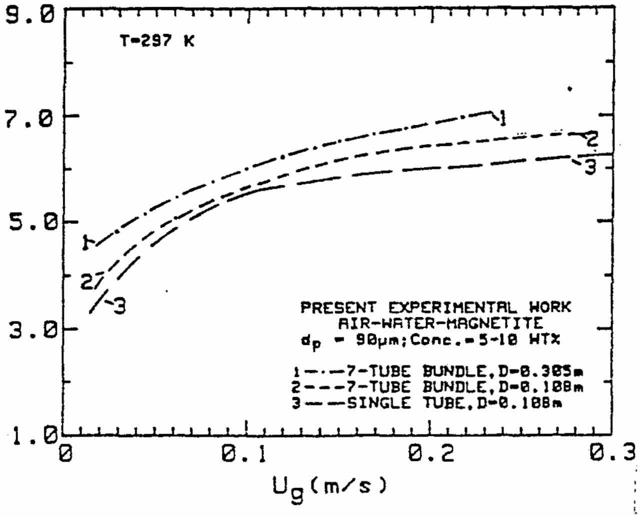

Influence of bubble column diameter and internals on heat transfer coefficient.

FIGURE 6.6

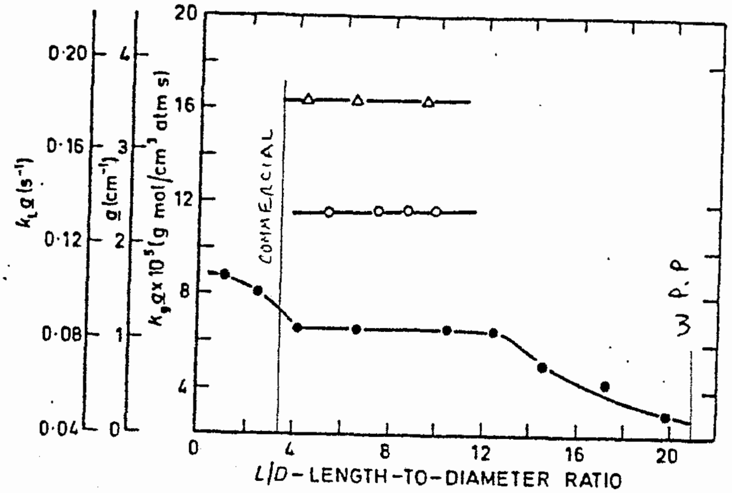

Column diameter = 6·6 cm; Superficial gas velocity ~ 21 cm/s

●: liquid-side mass transfer coefficient

△: gas-side mass transfer coefficient

○: effective interfacial area

—Effect of the length-to-diameter ratio on the liquid-side mass transfer coefficient, the gas-side mass transfer coefficient, and the effective interfacial area

There are a number of parameters that were not addressed during the development of the SSB process due to the tight schedule set by the Sasol One renovation project. Therefore, there is room for improvement of the present situation. It has been said that under our hydrodynamic regime, the gas sparger does not play a role in the bubble size distribution. We have observed catalyst breakage inside the reactor, a phenomena that can affect the filtration. It is likely that the zone of highest shear stress is just below the gas sparger. The present configuration of the sparger (not discussed here) creates high turbulence and the Weber number of the nozzles as described in 2.2.8, is much higher than the minimum of 6. One way to reduce the turbulence at the bottom of the column is to decrease the Weber number of the nozzle to a minimum of 6 below which the initial bubble size could be affected.

It has been observed that the catalyst settles at the bottom of the column when low gas velocities are used. With our present configuration, the minimum gas velocity for total fluidization is 22 cm/sec. This means that the turndown case is only 68% of the design case (32 cm/sec). This indicates a low degree of flexibility of the system. One way to overcome this sedimentation problem is to use conical bottoms. This was discussed under 2.2.12. Abraham et al (1992:1146) showed that the critical gas velocity for the suspension of solid particles was proportional to $d_c^{0.27}$. If this is the case, the minimum gas velocity to fluidize the solids particles in the Sasol One commercial plant would be

$$V_{g,c} = 22 * \left(\frac{508}{86.6} \right)^{0.27} = 35.4 \quad \text{cm/sec}$$

which is very close to the design case. This reduces further the flexibility of the process. If the relationship is ruled by the hydraulic diameter, the expected gas critical velocity would be 25 cm/sec which is only 10% higher than the one required in the Works Pilot Plant.

After the commissioning of the Sasol One commercial Slurry Bed, a new stage of the development would take place, this would include optimization.

The position of the coils divide the reactor in to two main sections, creating the two circulation cells. The isothermal behaviour observed during run 1 to 5 was lost when the filters were placed above the coils and when 5 dummy coils where place in the coil section. It is believed that the latter is the most likely to be the cause of the temperature profile. In any case, the position of such internals have to be investigated in order to ensure high turbulence around them in order to reduce the cake growth, thus improving the filtration rate and to increase the heat transfer coefficient. Another factor to bear in mind is that when producing certain products, isothermal behaviour is essential to avoid side reactions and the formation of by- products.

As mentioned in 6.3, the kinetic resistance represents around 66 % of the total resistance. The kinetic resistance can be expressed as $\frac{1}{k_H \epsilon_L}$. As can be seen, in order to reduce it, it is necessary to increase k_H, meaning a better catalyst, or by increasing ϵ_L, in other words reducing the gas holdup.

It is necessary to bear in mind that any change to the gas holdup would also affect the gas/liquid interfacial area.

$$a = \frac{6\epsilon_g}{d_{b,s}}$$

Also, any change in the sauter diameter would change the gas holdup. In this case one has to determine which is the rate limiting step. If it is mass transfer kL.a should increase irrespective of the gas holdup. But if the system is kinetically controlled, the gas holdup should be decreased.

If one considers the Fischer Tropsch reaction rate, it can be seen that it would increase with pressure. Higher pressure would increase the reactants concentration in the liquid phase, would produce smaller bubbles, decreasing the bubble Sauter diameter, and would increase the gas holdup. This means an increase of the gas/liquid interfacial area.

It is possible to reduce the gas holdup without changing the bubble size, by meanzs of liquid velocity. Air Products reported this finding in 1989 (Roberts 1989). This would also help to keep the catalyst particles in suspension and therefore the gas turndown could be lowered giving the system higher flexibility.

As discussed before, the bigger the column diameter, the higher the energy of the bubbles due to the high liquid circulation velocity and therefore higher the liquid/solid entrainment. One way to control this entrainment is to stabilize the top bubble layer. This can be done by installing a sort of mesh that can reduce the turbulence or by introducing large particles of low density into the bed, so that they always float on the surface. This would not create pressure drop and would eliminate the first step of the droplet formation.

In order to improve the filtration performance, bigger particles can be tested. It is known that particles smaller than 200 microns have an effectiveness factor of 1. So therefore there is no reason to go to smaller sizes.

Here are discussed only a few alternatives for improvement of the present situation. The slurry bed reactor has inherent limitations that defined the maximum output obtainable under certain conditions. Simulations were done in order to assess whether a better catalyst would improve the reactor performance. As can be seen in figure 6.7 the contribution of the mass transfer resistance increases continuously, up to levels of 80%. At this point the system is controlled by mass transfer and the improvement of the catalyst would be insignificant.

Other simulations were done. It was assumed that the a.KL could be increased without changing the gas holdup. As can be seen in figure 6.8, the mass transfer resistance decreases down to levels of 24%. At this stage the sytem is kinetically controlled.

Figure 6.7 :Effect of catalyst activity on the rate controlling step

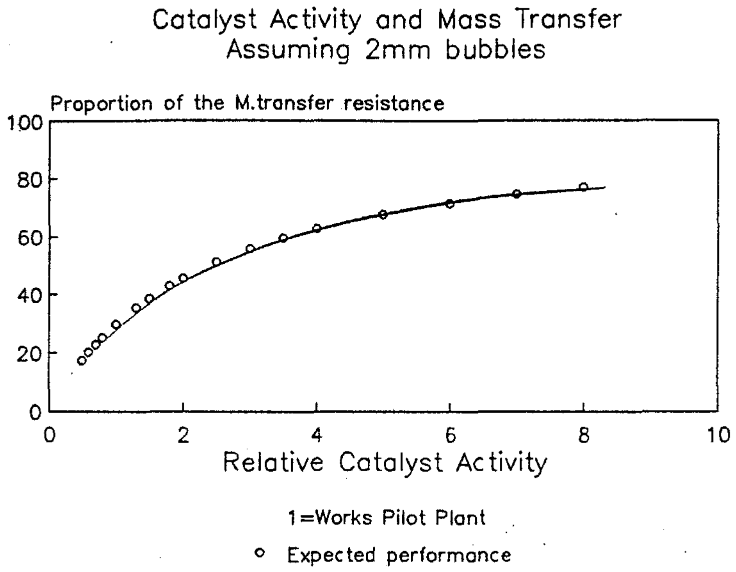

Figure 6.8 :Effect of Mass transfer on the rate controlling step.

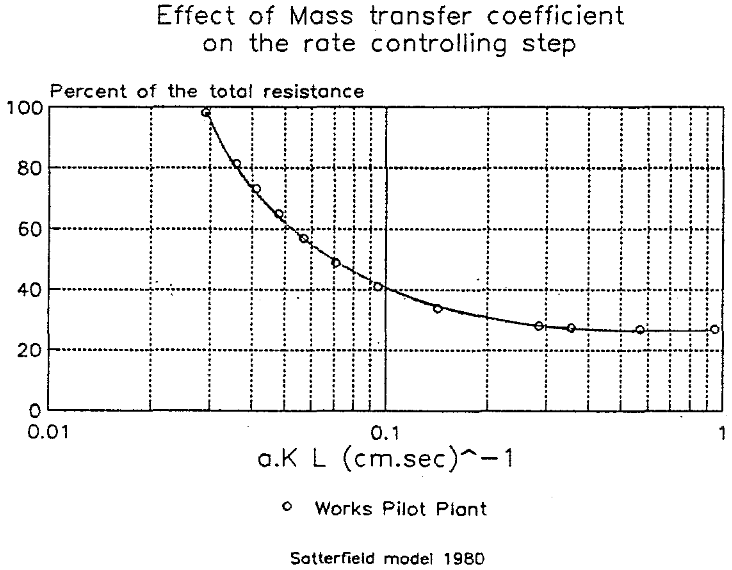

7 Conclusions

* Sasol has developed enough knowledge to confidently scaleup and design slurry bed type reactors.

* A computer model that can predict reactor performance working in the churn-turbulent regime is available. It is believed that this is the first of its kind.

* Due to the high online factor, unavoidable cycles are necessary to occur. This would affect the reactor performance but the model is able to do it knowing the frequency of the replacement and the amounts.

* The reactor is a useful tool to monitor the reactor performance while online. This can be use to determine whether or not catalyst should be replaced or not.

* The reaction in the conditions of the demonstration reactor is controlled by kinetics and not by mass transfer.

* Solid concentration profiles were predicted inside the bed. The observations fit very well the predictions.

* There is a maximum solids loading which beyond it the reactor is controlled by mass transfer. This limit is 37 % mass greencorn.

* Catalyst deactivation occurs in step changes rather than being a continuous process

* The reactor internals increase the degree of mixing.

* The gas phase behaves very close to plug flow. The reactor can be represented by 12 CSTR's in series

* Due to the scaleup effect, it is expected that the Sasol One commercial reactor compared with the Work Pilot plant would have

higher wax/solid entrainment
higher degree of mixing
higher heat transfer coefficient
higher mass transfer coefficient aK_L
smaller mixing time
higher turbulence due to high liquid circulation
higher gas critical velocity for solid fluidization
lower temperature difference along the reactor

8 Recomendations for future work

The state of knowledge of the parameters in the slurry bed process is listed in Appendix 9. One can see that there is a number of variables that have not investigated. Some of them only the trend is known but to quantify them, cold model studies are required. Some of the recommendations are not applicable for the present Sasol I Renovation project but for future projects. It is recommended the study of these hydrodynamic parameters for the improvement of the reactor performance

The study of the interfacial area between the gas bubbles and the slurry.

The effect of column diameter and the effect of the hydraulic diameter

The decrease of the coalescence tendency by means of surface tension agents

The production of a bigger amount of secundary bubbles product of the breakage of the initial ones, by varying the Weber number of the gas distributor nozzles.

The effect of semi-wettable particles to break bubbles

The effect of different cooling coils arrangement in order to reduce coalescence.

The study of the gas holdup (bearing in mind that the lower the gas holdup the bigger the amount of slurry per volume) and the effect of:

Different particle size distribution

Liquid velocity

Cooling coils arrangement in order to increase the fraction of the gas holdup that recirculates.

Surface tension agents either for stabilizing or destroying the presence of foam in order to reduce the entrainment material.

Different gas spargers (at low velocities)

It is possible also to optimize the reactor operation. The demonstration reactor gave a good understanding were our weak points lay. It is possible to study those parameters in order to improve the flexibility of the reactor. It is therefore recommeded to study the:

The effect of the shape of the bottom in order to:

reduce the critical fluidization velocity (giving the slurry a very high turndown capacity).

reduce the catalyst laydown after slumps or periods of low gas velocities

increase the mixing capacity (isothermal behaviour)

avoid excessive shear stress that could be the reason of particles breakage

have a more even distribution of the catalyst

The study of the coils and filters configuration in order to :

increase the turbulence around the filter region in order to reduce the cake growth and to destroy the cake after been dislodge by the backflush

increase the heat transfer coefficient, reducing the cooling area required.

avoid bridging

optimize the filtration rate putting the filters were the gas holdup values are not at maximum.

limit the growing of the bubbles to a practical minimum

The wax and solid entrainment can be addressed and various possibilities tested. It is recommended the study of:

demisters and meshes in the disengagement zone

centrifugal separators

foam stabilizers at the bed surface

the introduction of large particles with low density so they can float in the bed surface and reduce entrainment.

The study of the hydrodynamic parameters in the homogeneous regime because higher conversion can be achieved. Potential problems that could be present is the solid suspension due to low gas velocities, low turbulence, coalescence etc.

The study of change of intrinsic properties of the liquid phase, such as:

solubility of reactants, therefore changing the H_2/CO ratio disolved in the liquid phase for the selection of certain product distribution

solubility of water in the system, the lower the less effect it has on the kinetic of the process

the introduction of small particles of activated carbon, to be used as carrier of reactants from the gas/liquid interfacial film to the bulk of the liquid.

The use of inert particles to enhance filtration. This particles should be non-wettable, attrition resistant, heat resistant with sizes bigger than the filter gap with settling velocities lowere than 10 cm/sec in order to be fluidized.

REFERENCES

Abraham M, Khare A.S., Sawant S.B and Joshi J.B : 1992 "Critical gas velocity for suspension of solid particles in three phase bubble columns", Ind. Eng Chem. Res. vol 31, 1136-1147

Air Products and Chemicals Inc. "Slurry reactors Hydrodynamic studies" Final Report DOE Contract No DE AC 22 80 PC 30021

Air Products and Chemicals Inc. " Liquid Phase Methanol Laporte Process Development Unit: Modification, Operation and support studies. U.S. DOE DE 91-005732. Topical Report Task 2.3 Tracer studies in the La Porte LPMEOH PDU August 31, 1990

Akita K., Yoshida F. 1973: "Gas holdup and volumetric mass transfer coefficient in bubble columns". Ind. Eng Chem. Proc.Des.Dev., Vol 12, No 1

Ascher U., Cristiansen J and Russell R.D. 1981: "Collocation Software for Boundary Value ODEs", ACM Trans on math softw, vol 7, No 2, 209-222

Ascher U., Cristiansen J and Russell R.D. 1981: "Algorithm 569: COLSYS :Collocation Software for Boundary Value ODEs", ACM Trans on math softw, vol 7, No 2, 223-229

Bernermann K., Steiff A, Weinspach P.M. 1991:" Zum Einflus von langsamgestromten Rohrbudeln auf die grosraumige Flussigkeitsstromun in Blasensaulen" Chem.Ing. Tech. 63 , No 1, pp 76-77

Bhavarajir S.J., Russels F., Blanch H. 1978: "The design of gas sparger for viscous liquid systems" Aiche J. 24,454-466

Blass E. 1990: "Formation and coalescence of bubbles and droplets" Int. Chem Eng , vol 30, No 2, 206-221

Bolder F.H.A. 1990: "Effect of catalyst concentration in slurry bed reactor performance" SASOL Arge Pilot Plant Report 205

Bruck F.J. and Hammer H. 1986: "Intensification of mass transfer in bubble column reactors by suspended solids" Ger. Chem. Eng. 9, 382-390

Bruijn T.J de, Reilly I.G., Mac Intyre D and Scotts D.S. 1989: "Solid exit discontinuity in slurry bubble column" Can. J. of Chem Eng. (Vol 67) 283-289

Bukur D and Daly J 1982: "Gas holdup in bubble column for Fischer Tropsch synthesis" Chem Eng Sci ,vol 42, 2967-2969

Bukur D. 1983: " Some comments on models for Fischer Tropsch reaction in slurry bubble column reactors" Chem Eng Sci. Vol 38, No 3

Bukur D.B., Petrovich D, Daly J. 1987: "Flow regime transition in a bubble column with a paraffin wax as a liquid medium" Ind. Eng Chem Res.(26) 1087-1092

Bukur D.B. and Patel S.A. 1989: "Hydrodynamic studies with foaming and non-Newtonian solutions in bubble columns" Can J.of Chem Eng. Vol 67, 741-751

Bukur D.B. Patel S.A. and Daly J.G. 1990a: "Gas holdup and solid dispersion in a three phase slurry bubble column" AIChE J. Vol 36, No 11

Bukur D, Daly J and Patel S.A. 1990b: "Hydrodynamics of three phase slurry Fischer Tropsch bubble column reactors" Final Report., DOE Contract No. DE AC 22-86 PC 90012

Calderbank P.H. and Moo Young M.B. 1961:" The continuous phase heat and mass transfer properties of dispersions" Chem Eng. Sci. Vol 16, 36-54

Calderbank P.H , Evans F, Farley R , Jepson G., Poll A. 1963: "Rate process in the catalyst slurry Fischer Tropsch reaction" Cat. in practice , 66-74

Clark K.N.1990: "The effect of high pressure and temperature on phase distribution in a bubble column" Chem Eng Sci. Vol 45, No 8, 2301-2307

Clift R., Grace J.R., Weber M.E. 1978: "Bubble drops and particles". Academic Press New York, p 35, 171-176

Deckwer W.D. 1980: "On the mechanism of heat transfer in bubble column reactors", Chem Eng Sci, vol 35, 1341-1346

Deckwer W.D. Serpemen Y, Ralek M and Schmidt B. 1981: "On the relevance of mass transfer limitations in the Fischer Tropsch slurry process" Chem Eng, Vol 36

Deckwer W.D. Serpemen Y, Ralek M, Schmidt B 1982: "Modeling the Fischer Tropsch synthesis in the slurry phase" Ind.Eng.Chem.Proc.Des.Dev , 21, No 2, 231-241

Fan L.S. 1989: "Gas-Liquid-Solid Fluidization Engineering" Butterworth Publishers USA

Field R.W. and Davidson J.F.1980: "Axial dispersion in bubble column" Trans.Int Chem.Eng , vol 58, 228-235

Fujimoto K and Kunugi T. 1982: "Review of Slurry Phase Fischer Tropsch Synthesis" Pan Pac Synfuels Conf., 167-175

Ganguly U.P. 1990:"On the prediction of terminal settling velocities of solid in liquid solid systems" Int. J.Miner. Proces 29 , 235-247

Godbole SP, Joseph S, Shah YT, Carr NL,1984: "Hydrodynamics and mass transfer in a bubble column with an organic liquid" Can. J. of Chem Eng. Vol 62

Godbole SP, Schumpe A, Shah YT 1990:"The effect of solid wettability on gas - liquid mass transfer in a slurry bubble column" Chem Eng Sci, Vol 45, No. 12

Guy C., Carreau P.J. and Paris J.1986: "Mixing characteristics and gas holdup of a bubble column" Can. J of Chem Eng vol 64, 23-35

Hakita H, Asai S, Kikukawa H., Zaalke T and Ohue M, 1981: "Heat transfer coefficient in bubble columns" Ind Eng Proc. Des. Dev. vol 20, 540-545

Hills A.E., Vermeulen A., Kotze W.S. 1992: " Gamma ray scans on empty slurry bed reactor" Atomic Energy Corporation AEK 92/07 (B/R)

Imafuku K., Wang T, Koide K and Kubota H.1968:" The behaviour of suspended solids particles in the bubble column", Journ Chem. Eng of Japan vol 1, No. 2

Inga J.R., Theron D.M., Dancuart L.P., Steynberg A.P. 1990: " Slurry bed works pilot plant runs 1&2 " SASOL R&D Report No. FT/04/90 Dec 1990

Inga J.R. 1991a: "Filters Backflush effectiveness" Memo to L.P. Dancuart 2 Dec

Inga J.R. 1991b: " Online Catalyst Replacement for the slurry bed reactor: A mathematical model for design and optimization" SASOL Process Development report No. FT/04/91 August 91

Inga J.R. 1991c:"Effect of Filtration cycles on reactor performance" SASOL memo to R.C. Kelfkens, 21 Nov 1991. Ref.PS/3358

Inga J.R. 1991d: "Reply on Badger comments (BAC/RDS F-007)" Sasol memo to R.C. Kelfkens, 12 Dec 1991 ref. 3475

Inga J.R. 1992a:"Deviation of the SSB reactor from Isothermal Behavior" SASOL, Memo to A.P.Steynberg 30 Jan 1992, Ref. 3427/eb

Inga J.R. 1992b:" Wax/Catalyst entrainment studies in the SSB reactor" Memo to A.P. Steynberg 28 April, Ref eb/3792 File 540600/3.3.8, RDS /BAC /M-011

Inga J.R. 1992c:"Heat transfer coefficient for the Sasol Slurry Bed (SSB) Reactor- Analysis of Work Pilot Plant runs 5, 6 and 7" Report No. FT/08/92 s8 February

Kabel R.L. 1985: "Homogenous reaction systems" in chapter 4 of Scaleup of Chemical Processes, Bisio A. and Kabel R. John Wiley and Sons Inc.

Kastanek F. 1977: "The volume mass transfer coefficient in a bubble bed column" Collect.Czechos. Chem Commun (Vol 42)

Kato Y, Nishiwara A, Fukuda T and Tanaka S.H. 1972: "The behavior of suspended solids particles and liquid in bubble column" J. of Chem. Eng. of Japan , Vol 5, No 2, 112-118

Kawase Y and Moo Young M. 1986: "Liquid phase mixing in bubble columns with Newtonian and non-Newtonian fluids" Chem Eng Sci, No 8, 1969-1977

Khare A.S. and Joshi J.B. 1990; "Effect of fine Particles on gas holdup in three phase sparged reactors" Chem Eng. Journ. 44 , 11-25

Kim V. H., Tsutsumi A. and Yoshida K. 1987:" Effect of particle size on gas holdup in three phase reactors" Sadhara vol 10, 261-268

Kojima H., Okumura B and Nakamura A. 1991: "Effect of pressure on gas holdup in a bubble column" J.of Chem. Eng of Japan , Vol 24, No 1, 115-117

Kuo J.C.W. 1983: "Slurry Fischer Tropsch/ Mobil two stage Process of converting syngas to high octane gasoline" US DOE Final Report N.DOE/PC/30022-ID, Dec 83

Lee Y.H., Kim Y.J., Weinberger C.B., 1991:"Analysis of Dispersion structure of fermetation media by dynamic disengagement method" Biotechnology and bioengineering vol 37, 288-291

Levenspiel 1966: "Chemical Reaction Engineering" John Wiley and Sons, London.

Mangartz K.H. and Pilhofer Th. 1980:"Untersuchungen zu Gasphasen dispersion in Blasensaulen reaktoren" Vt.Verfahrenstechnik 14, No 1

Maruyama T., Yoshida S. and Mirushina T. 1985: "The flow transition in a bubble column" Journ. of Chem Eng. of Japan, vol 14 No. 5

Mashelkar R.A. 1970: "Bubble columns", British Chem. Eng. Vol 15, No 10

Matsumoto T., Hidaka N. and Mooroka Sh. 1989: "Axial distribution of solid holdup in bubble colum for gas-liquid-solid systems" AICHE J. vol 35, No 10, 1701-1709

Mill G.A.1991: "Liquid Fuels from syngas ", DOE progess report, Indirect Liquefaction contractor meeting.

Miyahara T, Tsuchiya K, Fan L.S. 1989: " Mechanism of particle entrainment in a gas - liquid - solid Fluidized Bed", AICHE J, Vol 35, No 7,1195-1198

Molerus O. and Kurtin M. 1986: "Hydrodynamics of bubble columns in the liquid circulation regime" Chem Eng. Sci. vol 41, 2685-2692

Neubauer G. 1977: Dissertation, TU Munich SFB 153

O'Dowd W, Smith D. N. Ruether J.A. and Saxena S.C. 1987: "Gas and solid behaviour in a baffled and unbaffled slurry bubble column" AICHE J. vol 33, No 12, 1959-1970

Prakash A., Briens C.L. 1990: "Porous Gas Distributors in bubble columns. Effect of liquid presence in distributor pressure drop. Effect of startup procedure on distributor performance". The Can. J of Chem Eng. vol 68, 204-210

Roberts G.W. 1989: "Methanol as an alternative fuel" for Air Products and Chemicals Testimony before the Subcommittee on Energy Research and Development, June 8

Saxena S.C. and Rosem M. Smith D. N. Ruether J.A.1986: "Mathematical Modeling of Fischer Tropsch slurry bubble column reactors", Chem. Eng. Commun. Vol 40, 97-151

Satterfield C.N. and Huff G.A. 1980: "Effects of Mass transfer on Fischer Tropsch synthesis in slurry Reactors" Chem Eng Sci. 35, 195

Saxena A.C., Rao N.S. Saxena S.C. 1990 :"Bubble size distribution in bubble columns" Can. J of Chem Eng, vol 68, 159-161

Saxena S.C., Rao N.S., Saxena A.C. 1991a: "Heat transfer and holdup studies in a three phase slurry bubble column with internals" AICHE Symp. series 87 (281, Adv. Fluid Syst) 101-10

Saxena S.C.1991b:Department of Energy "Heat transfer investigation in a slurry bubble column", Final Report, Univ. of Illinois at Chicago

Saxena S.C., Rao N.S.,Saxena A.C. 1991c:"Heat transfer and holdup studies in a three phase slurry bubble column with internals", AICHE symp. series 199,87, (281, Adv. Fluid. Syst.) 101-110

Sharma M.M. and Mashelkar R.A. 1968:"Absortion with reaction in bubble columns", I.Chem Eng. Symp.Series No 28, 10-21

Shaykhutdinov A.G., Bakirov N.U., Usmanov A.G. 1971:" Determination and mathematical correlation of heat transfer coefficient under conditions of bubble flow, cellular and turbulent foam", Intern Chem Eng , vol 11, No. 4

Smith S.W., Hills A.E., Vermeulen A. , Laesecke W.F. 1991: "The measurement of the residence time distribution of gas in the SASTECH Works Pilot Plant at Sasol One" Atomic Energy Corporation of South Africa AEK -91/58 (B/R)

Smith S.W., Hills A.E., Kotze W.S. 1991:" Density measurements on the pilot slurry bed reactor at Sasol One " Atomic Energy Corporation of S.A. AEK 91/70 (B/R)

Smith S.W., Hills A.E., Vermeulen A. 1991: "Density measurements and bubble detection in the pilot Slurry Bed reactor at SASOL ONE" Atomic Energy Corporation of S.A. AEK 91/77 (B/R)

Smith S.W., Hills A.E., Vermeulen A. , Kotze W.S.1992: " Bubble and droplet detection in the pilot slurry bed reactor at Sasol One (Third Series) Atomic Energy Corporation of S.A. I.S. 181

Smuk D. Scotts and Mac Intyre 1991:" Settling velocities of particles in bubbly gas-liquid mixtures" The Can. J. of Chem. Eng. Vol 69, 1382-1388

Stern D, Bell A.T. Heinemann H. 1983:" Effect of mass transfer on the performance of slurry reactors used for Fischer Tropsch synthesis" Chem Eng. Sci. Vol 38, 597

Stern D., Bell A.T. Heinemann H 1985:" A theoretical model for the performance of bubble column reactors used for Fischer Tropsch synthesis" Chem Eng. Sci. 40, N.9

Stern D., Bell A.T. Heinemann H. 1985: "Analysis of the design of Bubble column reactors for Fischer Tropsch synthesis" Ind Eng Chem Proc Des Dev, Vol 24 No 4

Stern D. 1984: "Experimental and theoretical studies of bubble column slurry reactors used for Fischer Tropsch synthesis" Phd. Thesis University of California

Steynberg A.P., Inga J.R. Scaife T.L., Van Antwerpen JAC, Bolder F. 1992: "Slurry Bed Report of Run 6". SASTECH R&D January 92

Steynberg A.P., Inga J.R. 1991: "Analysis of the second set of gamma ray scanning test on the Sasol Works Pilot Plant Slurry Bed reactor" in the Fax transmital No. SAS/SAC-F0095 to Badger September

Steynberg A.P., Inga J.R., Scaife T.L., van Antwerpen J.A.C., Bolder F., Dancuart L.P., Kelfkens R.C. :1992 "Works Pilot Plant Report of Run 6"

Suh I.S., Deckwer 1989: "Unified correlation of heat transfer coefficient in three phase fluidized beds", Chem Eng Sci, vol 44, No. 6, 1455-1458

Tinje J.T. and Drikenburg A.A.H.:1992 "Absorption of gases into activated carbon water slurries in a stirred cell" Chem Eng. Sci vol 4, No 6

Towell G.D. Strand C.P. and Ackermann G.H. 1965: " Mixing and mass transfer in large diameter bubble column" Aiche Int.Chem Eng.Symp.Series No 10

Ueyama K, Tsuru T., Furusaki S. 1989:"Flow transition in a bubble column" Int Chem Eng Vol 29, No 3

Van Berge P.J.1989: "Detail description of slurry micro reactor", Sasol: Basic Catalysis Report No 96 February.

Van Vuuren D.S.1987: "Slurry reactors for Fischer Tropsch synthesis" CSIR, progress report May 1986- May 1987. CENG MEMO 87/14

Van Vuuren D.S. 1988: "Hydrodynamic studies on slurry bubble column" CSIR, CENER 8840

Van Vuuren D.S. 1986: "Slurry reactor for Fischer Tropsch synthesis" CSIR, Progress Report June 1985-May 1986. CERG MEMO 86/10

Van Vuuren D.S. 1988: "Hydrodynamiss studies on Slurry reactors" CSIR Contract N. 342/86

Van Vuuren D.S. 1989: "The evaluation of distributor design for Fischer Tropsch slurry reactors" CSIR Contract Report ENERC 89074, July

Wilkinson P.M. and Dierendonck L.L. 1990: "Pressure and gas density effect on bubble breakup and gas holdup in bubble column" Chem. Eng.Sci.Vol 45, No 8

Wilkinson P.M. 1991: "Physical Aspects and scaleup of high pressure bubble columns", Phd thesis, Rijksuniversiteit Groningen.

Wachi S and Nojima Y. 1990: "Gas phase dispersion in bubble column" Chem Eng. Sci Vol 4, 901-905

Wallis G.B.1969: " One dimensional two phase flow" Mc Graw Hill New York

Yoshida F and Akita K:1965 "Performance of gas bubble column: Volumetric Liquid phase mass tranfer coefficient and gas holdup" AICHE J vol 11, No 1, 9-13

Zahradnik J, Kastanek F and Kratochvil J. 1982:" Hydrodynamic and mass transfer in uniformerly aerated bubble columns reactors". Collect. Czechoslovak Chem. Commun. Vol 47

Appendix 1

The measurement of the residence time distribution of the gas in the slurry bed reactor by Atomic Energy Corporation of S.A.

Gas tracer used : Argon 41

Intensity : 300-400 MBq

The tracer gas was injected each time in the form of an impulse by means of nitrogen pressure. The inlet point was situated on the gas feed line just before the grid and the detector was placed on the gas outlet pipe. Pulses from the detectors were processed by conventional electronics and accumulated in successive time intervals by means of a microcomputer. The mean residence time was calculated as follows:

$$\bar{t} = \frac{\sum t.C_t \Delta t}{\sum C_t \Delta t}$$

The axial flow model described by the equation:

$$C_t = \left\{\frac{Pe}{4\pi t \bar{t}_m}\right\}^{\frac{1}{2}} .\exp\left(\frac{-Pe(t-\bar{t}_m)^2}{4t\bar{t}_m}\right)$$

was fitted to the actual data by changing $\bar{t}_m$ and the Peclet number. These was done by means of a least-squares regression method.

Gas Flow nm3/h	Temp in oC	Temp bed oC	Press out bar	Gas cm/s	cat. g/l	$\bar{t}$ sec	σ^2 s^2	$\bar{t}_m$	Pe
4892	148	233	17.86	23	140	80.2	536	72.9	26.7
4924	141	234	17.86	23	140	79.5	564	71.9	23.8
3071	139	233	17.86	13	140	125.6	1670	112.9	19.1
6760	141	235	15.86	37	140	50	240	44.9	26.6
7681	141	236	10.86	62	140	31.9	109	28.2	28.2

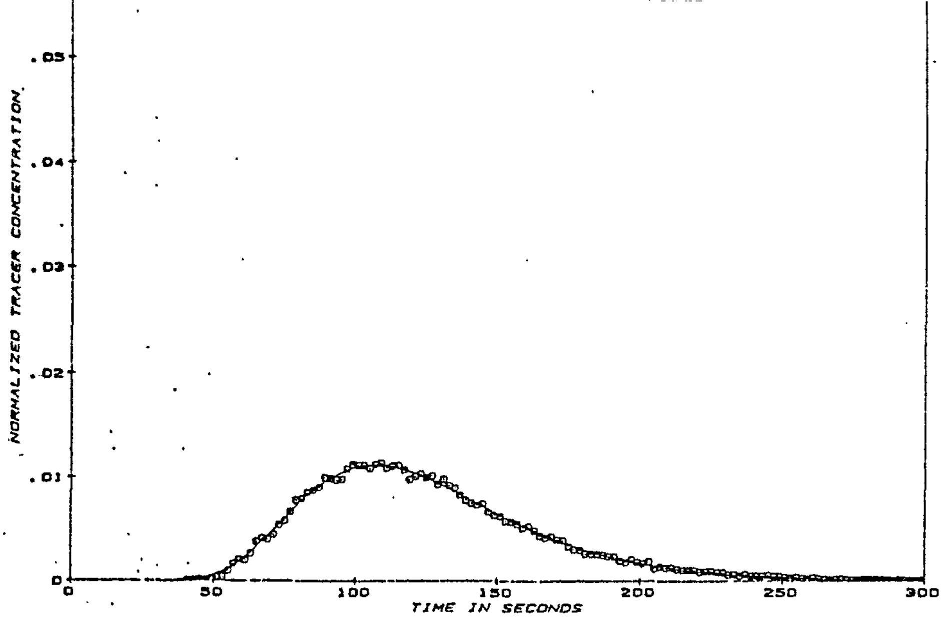

FIG. 3: RESPONSE AT OUTLET OF REACTOR DURING RUN 3

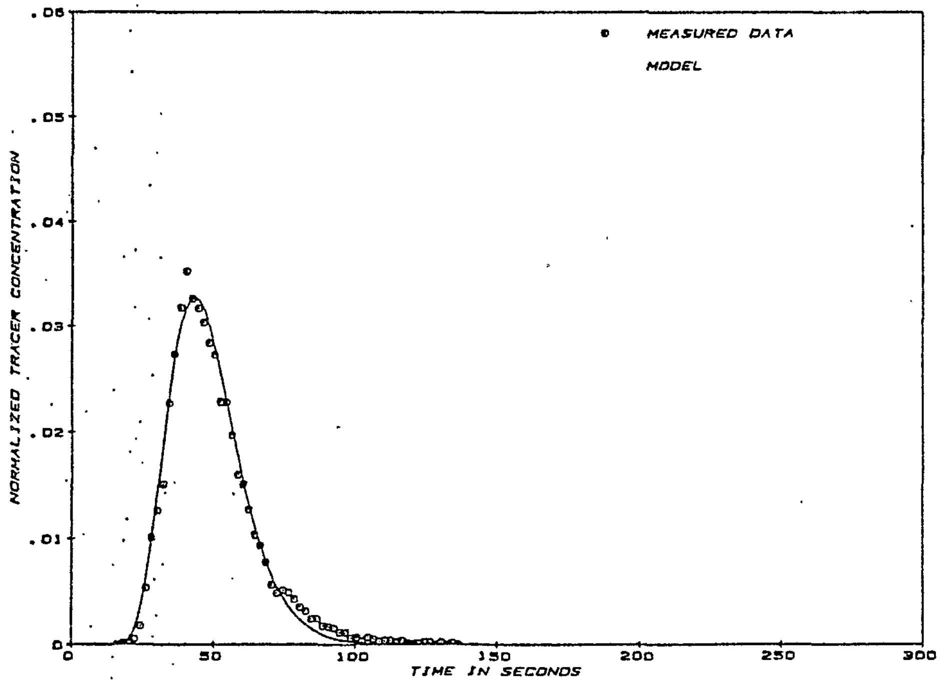

FIG. 4 RESPONSE AT OUTLET OF REACTOR DURING RUN 4

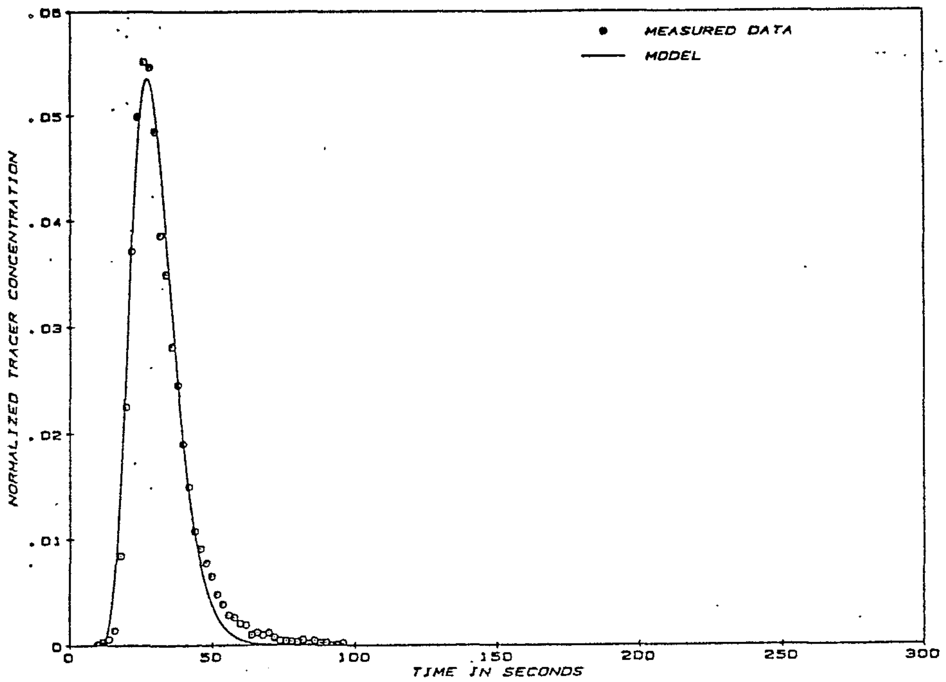

FIG. 5: RESPONSE AT OUTLET OF REACTOR DURING RUN 5

Appendix 2

Calculation of the equivalent number of CSTR in series

The gas phase mixing is quantified by the residence time distribution (RTD) or exit age distribution E(t). To calculate the number of equivalent CSTR in series it is necessary to fit the measured E (t) to a tanks in series model. The number of tanks and the tank residence time are used as adjustable parameters in fitting the model to the data. If the reactor behaves as a CSTR, then the model will predict one tank. If the reactor behaves as a Plug Flow reactor, then there will be an infinite number of tanks in series. The tanks in series model is based in these equations:

$$\frac{dC_{i,n}}{dt}=\frac{C_{i,n-1}-C_{i,n}}{\tau_n}-\frac{dC_i}{dt} \qquad n=1,\ 2....N$$

with $\tau_n=\frac{V_n}{Q}$

The translation of a plug flow dispersion model to a series of CSTR's is given by Levenspiel (1966)

$$\frac{1}{n}=\frac{1}{Pe}-\frac{2}{Pe^2}.(1-\exp(-Pe))$$

Appendix 3

CSIR results of the dynamic disengagement tests

Column diam. cm	Temperat deg C	Pressure bar	Column gas velocity cm/sec	Fraction of big bubbles	Fraction of small bubbles
15	214	3.26	22.47	75	20
15	214	3.26	22.39	75	20
15	200	4.45	18.34	86	11.6
45	206	3.19	14.49	73	25
45	244	3.46	11.52	41	29
15	193	5.23	20.08	60	30.6
45	225	4.31	12.19	53	36.4
45	182	12.31	12.61	58	38.2
45	235	4.6	13.7	61	35.2
45	239	12.11	12.87	52.9	45.3

Appendix 4

Dynamic disengagement method for the determination of the buble size distribution in the slurry bed.

The dynamic disengagement involves a interruption of the gas supply and the subsequent decay of the dispersion height as a function of time. From the transient height profile obtained, bubble rise velocities and holdups for each bubble size can be estimated. The assumption that has to be made is that no coalescence occurred after the cutting of gas and that the circulation in the bed stop at the time the gas supply was cut.

The method is fairly simple compared with probes techniques. It has been used for the analysis of fermentation media (Lee et al, 1991: 288) and to determine the bubble size distribution in wax (Bukur 1990: 215). Some researchers (Van Vuuren 1988:3, Molerus et al 1986:2689) instead of determining the bubble size distribution only quantified the proportions of the so call "big bubbles" and "small bubbles". This is ussually done due to the difficulty to get accurate correlations between the bubble size and it's rising velocity. This simplification assumes a bimodal distribution of the bubbles.

The following figure, shows the actual data from the works pilot plant. The dynamic dysengagement method is ruled by a number of equations .

$$L_i.Area = L_{i-1}.Area - \sum_{i}^{N} Q_i t$$

where t_i is the time when i th stage of disengagemnet is completed.

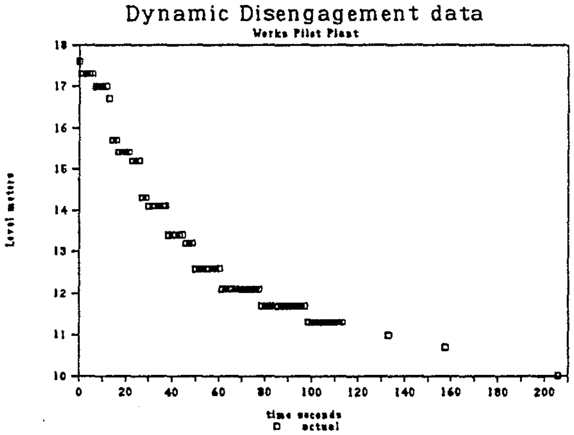

The rest of the method considers fit slopes in the curve. The fraction of the gas holdup that representes the small bubbles is defined as:

$$\epsilon_i = \frac{t_i}{L_o}(S_{i+1} + S_i)$$

The bubble rise velocity can be obtained by calculations using different correlations. In this method, the relationship between the bubble size and the rising velocity can be described as follows $u_i = \frac{H_i}{t_i}$

One of the most commonly used correlation is the one obtained by Clift et al (1978):

$$u_b = \left\{ \frac{2.14.\sigma_l}{\rho_l.d_b} + 0.505 g d_b \right\}^{0.5}$$

Appendix 5

Determination of the maximum bubble size in the Works Pilot Plant by means of gamma ray.

Gamma ray sources and detectors were placed at different elevation of the reactor. Each one of the detectors were reading the count at a frequency of once every 20 miliseconds for a period of 50 seconds. The readings of counts can be transformed into density by the following relationship:

$$I = I_o . \exp(-\mu \rho x)$$

where I= transmitted radiation intensity

I_o = radiation intensity through empty reactor

μ gamma absortion coefficient of slurry

ρ bulk density of slurry

x = distance through the slurry that the radiation travels

In order to determine the constant parameters (eg: μ, I_o) measurements where done through an empty part of the reactor. After being the detectors calibrated the test was done. The detection of one bubble passing through the detectors is shown here.

The actual drop of the calculated density during these events give us the idea of the size of the bubble. This bubble diameter was calculated by the following equation:

$$\rho_{obs} = d_c . \rho_{sl} . (1 - \epsilon_g) - \rho_g . d_b$$

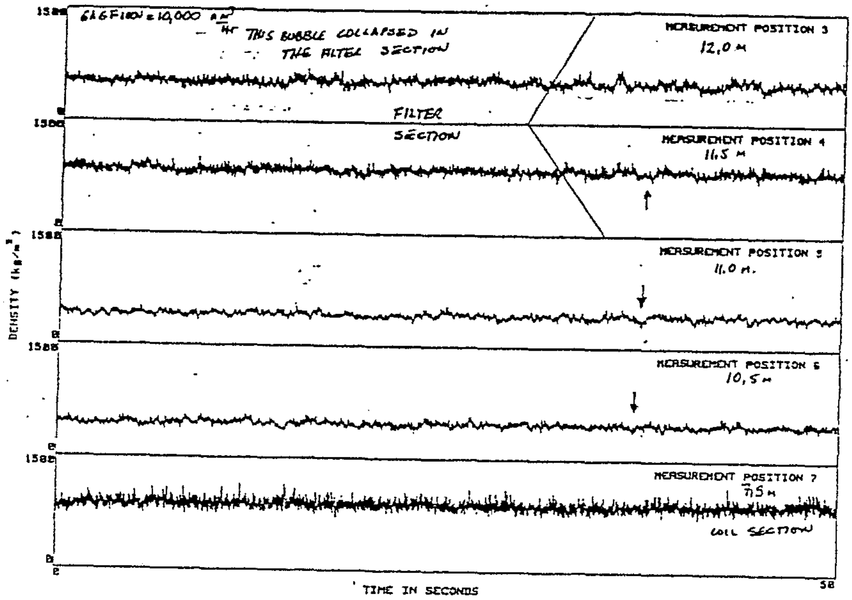

[illegible]: BUBBLE-TEST DATA (COND II, CONFIG C, RUN 4)

APPENDIX 6

Calculation of the contribution of mass transfer to the total resistance

Method Bukur 1983:441

The proportion of the mass transfer is defined as

$$\frac{R\ \text{mass.transf}}{R\ \text{total}}$$

so in therms of the hydrodynamic parameters would be:

$$\frac{R_m}{R_T} = \frac{\frac{1}{k_L a}}{\frac{1}{k_L a} + \frac{1}{k_H \epsilon_L}}$$

At design conditions:

Gas flow = 8800 nm3/h

Cat. inventory= 950 kg

Bed Level = 18 meters

Temperature = 240 C

Pressure = 21.5

H2 % in gas = 58%

Gas holdup = 60%

Bubble diameter= 2mm

viscosity = 1.42 cPo

density of slurry= 800 kg/m3

The calculation of $k_{H,L}$ is done with the correlation presented by Satterfield and Huff (1980:197)

$$k_{L,H} = \left\{ 3.08 D_{L,H}^2 \frac{\rho_L}{\mu_L} \right\}^{\frac{1}{3}}$$

The calculation of the diffusion coefficient of Hydrogen is done by

$$D_{L,H} = 7.35x10^{-3} e^{-\frac{2285}{T}} \quad cm^2/s$$

$D_{L,H}$ =0.00008547 cm^2/s

$k_{H,L}$ =0.0108 cm/s

a=30 cm-1

$a.k_{H,L}$ =

0.324 sec^{-1}

The calculation of the kinetic constants is:

Carbon to Fischer Tropsch=33.3 kg mol/h = 9.26 mol/sec
The concentration of Hydrogen in the gas phase is 2.96E-4 mol/cm3
The concentration of Hydrogen in the liquid phase is 1-0.74 E-5 mol/cm3
The rate constant as defined by Bukur is

$r_{FT} = k_H . \epsilon_L C_{H,L} V_L$ mol/sec

giving a:

$k_H =$

0.24-0.32 sec-1

so $\frac{1}{k_H \epsilon_L} = 7.81$ and $\frac{1}{a k_{L,H}} = 3.08$

Therefore the contribution of the mass transfer over the total resistance of 28.8%.

```
            SLURRY BED REACTOR PROGRAMM
             JUAN R. INGA
            SATTERFIELD EQUATION DATE OF STORAGE 18/01/91
            INCLUDES INPUT/OUTPUT TO BE USED AS A SUBROUTINE
       DIMENSION M(11),IPAR(11),ZETA(21),LTOL(11),TOL(11)
       DIMENSION ISPACE(3200),FSPACE(200000),S(5),SL(5),V(5),CL(5)
       DIMENSION CG(5),SO(5),Z(21),ROLD(5),FCG(5)
       REAL LIQDSP,FACTIV
       COMMON /RATE/ A,B,C,D,ALPHA,GAMMA
       COMMON /APPR/ NS,NOLD,NMAX,N1,N2,N3,N4,N5
       COMMON /MINE/S,SL,PEG,PEL,EPS,CL,CG,V,CTOT,SO,EQ,T,PTOT,FCG,RRAT
       COMMON /LC/ FSPACE
       COMMON /REP/ RL,DCOL,UG,UL,WR,WAV,SN(5),ICALL,FUDGE1,FUDGE2,UINIT
       COMMON /JUAN/CSCAL,AREA,TRANSV,LIQDSP,GASDSP,CONTRAC,FACTIV,RMANI
       COMMON /JUAN2/THERM,HCAP,RMUL,RHOL,GEE,HYDR

       OPEN (1,FILE='SBR.DAT',STATUS='OLD')
       OPEN (2,FILE='SBR.PRN',STATUS='UNKNOWN')
       OPEN (3,FILE='SFLORY.DAT',STATUS='OLD')

       EXTERNAL FSUB,DFSUB,GSUB,DGSUB,SOLUTN
       READ(1,*)NNPT,NNINT,TTOL
       READ(3,*)ALPHA,GAMMA
       CLOSE(3)
       WR = 0.5
       ICALL = 0
           READ (1,*) UINIT,UL,RL,DCOL,T,PTOT,WAV
           READ (1,*) FUDGE1, FUDGE2, RRAT,CONTRAC,RMANI,HYDR
C ------------------------------------------------
              DO 11 J=1,5
              READ(1,*) FCG(J),CL(J)
              IF (J.EQ.1) HTEMP=FCG(J)
11            FCG(J)=FCG(J)/HTEMP

C        WRITE(6,*)'CALLING PECLET ...READ AND CALCULATE  PROPERT'
        CALL PECLET
        ICALL = 1
C -----------------ASUMING C5 IS THE CARBON NUMBER AVERAGE-----------
       NC = 5
C -----------------MOLES OF HYDROGEN CONSIDERING OLEFINS-----------
       NF = 2*NC+1
C-------------------------------------------------------------------
       DO 12 J=1,NF
           M(J) = 2
           ZETA(J) = 0.0
           L = J+10
            IF ( J .EQ. 1 )  L = 12
                ZETA(L) = 1.0
            IF ( J .GT. 1 )  LTOL(J) = 2*(J-1)
               TOL(J) = TTOL
12     CONTINUE

       LTOL(1) = 1
       M(1) = 1

C  IPARM(1)= NUMBER OF COLLOCATION POINTS PER INTERVAL
C  IPARM(2)=NUMBER OF COLLOCATION INTERVALS
C  IPARM(3)= COLSYS PRINT SWITCH
C  RPARM(1)=K' IN FT RATE EQUATION
C  RPARM(2)=REACTOR VOLUME
C  RPARM(3)=REACTOR TEMPERATURE
C  RPARM(4)=CATALYST CONCENTRATION (WT FRACT)
C  RPARM(5)=FT RATE PARAMETER
C  RPARM(6)=WGS RATE PARAMETER
C  RPARM(7)=TEMP.OF REACTOR OUTLET STREAM
C  RPARM(8)=TEMP.OF REACTOR OUTLET STREAM
```

```
C  SUPPLE(1)= REACTOR HYDRAULIC DIAMETER
C  SUPPLE(2-31) = SELECTIVITIES
      IPAR(1) = 1
      IPAR(2) = NNPT
      IPAR(3) = NNINT
      IPAR(4) = 11
      IPAR(5) = 200000
      IPAR(6) = 3200
      IPAR(7) =  1
      IPAR(8) = 0
      IPAR(9) = 0
      IPAR(10) = 0
      IPAR(11) = 0
C -----------------------------------------------------------------
      CTOT=0.
      DO 110 I=1,5
          CG(I)=FCG(I)
          CTOT=CTOT+FCG(I)
          ROLD(I)=0.0
 110  CONTINUE

C--------------INLET SPACE VELOCITY (INCLUDING RECYCLE EFFECT--
 120  UG=UINIT*(1.+RRAT)*T/273/PTOT/.0036/TRANSV/0.9869233
      CALL COLSY2(11,M,0.,1.,ZETA,IPAR,LTOL,TOL,DUMMY,ISPACE,FSPACE,
    $     IFLAG,FSUB,DFSUB,GSUB,DGSUB,SOLUTN)
C --------------------------------------------------------------------
 21   IF ( IFLAG .NE. 1 )  GOTO 14
      X = 1.0
      CALL APPSLN(X,Z,FSPACE,ISPACE)

C----------------   KNOCK OUT H20--------------------------------
      Z(10)=0.0
C------------- KNOCK OUT 50% OF HYDROCARBONS FORMED IN REACTOR----
      DHC=Z(6)*Z(1)-CG(3)
      Z(6)=Z(6)-DHC/Z(1)*0.50
C ------------------------------ CHECK IF CONVERGED-------------
      DO 130 I=1,5
          IF(ABS(ROLD(I)-Z(2*I)).GT.0.001)GOTO 140
130   CONTINUE
      GOTO 15
C-----------------------------------------------------------------
140   RTOT=0.0
      CTOT=0.0
      DO 145 I=1,5
          ROLD(I)=Z(2*I)
          RTOT=RTOT+ROLD(I)
          CTOT=CTOT+FCG(I)
145   CONTINUE
C--------------------------------GAS CONC. AT INLET--------------
      DO 150 I=1,5
          CG(I)=(FCG(I)/CTOT+RRAT*ROLD(I)/RTOT)/(1+RRAT)
150   CONTINUE
C-------------------HYDROGEN CONC. AT INLET --------------------
      CSCAL=CG(1)
C-------------------TRANSFORMING ALL CONC. TO DIMENSIONLESS EXP.---
      CTOT=0.0
      DO 160 I=1,5
          CG(I)=CG(I)/CSCAL
          CTOT=CTOT+CG(I)
160   CONTINUE
C------------------------------------------------------------------
      IPAR(3)=NS
      IPAR(9)=3
      GOTO 120
14      WRITE(2,*)'SLURRY BED COULD NOT CONVERGE FOR GIVEN INPUT'
        WRITE(2,*)'SO SOLUBILITY        ',SO(1),SO(2),SO(3),SO(4),SO(5)
```

```
       WRITE(2,*)'SN VOLUME RATIO ^0.6',SN(1),SN(2),SN(3),SN(4),SN(5)
       WRITE(2,*)'STN H2,CO,C5,CO2,H2O',S(1),S(2),S(3),S(4),S(5)
       WRITE(2,*)'ST.LIQUID           ',SL(1),SL(2),SL(3),SL(4),SL(5)
       WRITE(2,*)'   CG   .AT  MOMENT ',CG(1),CG(2),CG(3),CG(4),CG(5)
       WRITE(2,*)'UG,EPS,AREA,Z(1)    ',UG,EPS,AREA,Z(1)
       WRITE(2,*)'USAGE RATIO   XCOH  ',UR,XCOH
       WRITE(2,*)'FRESHC FEED AT INLET',UINIT
       WRITE(2,*)'CTOT      AT  MOMENT ',CTOT
       WRITE(2,*)'PTOT,T,DCOL, WAV    ',PTOT,T,DCOL,WAV
       WRITE(2,*)'PECLET NUMBER GAS   ',PEG
       WRITE(2,*)'PECLET NUMBER LIQUID',PEL
       WRITE(2,*)'THE VALUE CSCAL     ',CSCAL
       WRITE(2,*)'THE VALUE OF UG     ',UG
       WRITE(2,*)'             COH2   ',COH2
       STOP

     X = 0.0

     DO 16 J=1,21
         CALL APPSLN(X,Z,FSPACE,ISPACE)
          X = X+0.05
       CONTINUE
----------------------CONC OF REACTANTS H2 + CO ------------
     TF=CG(1)+CG(2)
-----------------------OVERALL CONVERSION (RELATED TO REACTANTS-----
     XCOH = (TF-Z(1)*(Z(2)+Z(4)))/TF
-------------------------------------USAGE RATIO -- H2/CO----------
     UR = (CG(1)-Z(1)*Z(2))/(CG(2)-Z(1)*Z(4))
-----------------------------TOTAL GAS CONC. AT INLET--------------
     CINTOT=0.0
     DO 777 I=1,5
         CINTOT=CINTOT+FCG(I)
7    CONTINUE
     TINH2=FCG(1)/CINTOT*100.0
     TINCO=FCG(2)/CINTOT*100.0
     TINC5=FCG(3)/CINTOT*100.0
     TINCO2=FCG(4)/CINTOT*100.0
     TINH2O=FCG(5)/CINTOT*100.0
-------------------------------LINEAR EXIT VELOCITY-------------
     OUTUG=UG*Z(1)
------------------------------EXIT COMPOSITION----------
     OUTH2=Z(2)/CTOT*100
     OUTCO=Z(4)/CTOT*100
     OUTC5=Z(6)/CTOT*100
     OUTCO2=Z(8)/CTOT*100
     OUTH2O=Z(10)/CTOT*100
-----------------------------DIMENSIONLESS ANALYSIS ----
        REINOL=(UG/100)*(DCOL/100)*RHOL/RMUL
        FROUD=(UG/100)**2/(GEE*(DCOL/100))
        PRANDT=RMUL*HCAP/THERM
        STANTO=0.1*(REINOL*FROUD*PRANDT**2)**(-0.25)
         HINTER=STANTO*RHOL*HCAP*UG/100
------------------YIELDS CALCULATIONS---------------
    FTCNV=UINIT/22.414*(TINCO+TINH2)/100*XCOH/3
    WGSCNV=Z(1)*UINIT*OUTCO2/100/22.414-UINIT*TINCO2/100/22.414
    WATER=(FTCNV-WGSCNV)*18
    YH2O=WATER*1000/UINIT
-----------------HEAT GENERATED---K WATTS--AND KG/H-------------
    TOTH=(159.106*FTCNV+41.2*WGSCNV)/3.6
    STEAM=TOTH/1950*3600
------------------------SUBROUTINE OUTPUTS----------------------
     DH2CO=UINIT/2241.4*(TINH2+TINCO)*XCOH
     EXITH2=UINIT/2241.4*TINH2-DH2CO*UR/(1+UR)
     EXITCO=UINIT/2241.4*TINCO-DH2CO/(1+UR)
     EXITRS=UINIT/2241.4*TINC5+DH2CO/3/5
```

```
      EXICO2=UINIT/2241.4*TINCO2+DH2CO*(2-UR)/(UR+1)/3
      EXIH2O=UINIT/2241.4*TINH2O+DH2CO*(0.6666-1/(1+UR))
      WRITE(2,*)
      WRITE(2,*)'VERSION 1 SLURRY BED MODEL'
      WRITE(2,*)'ANY QUERIES TO J.R.INGA 2815'
      WRITE(2,*)'LAST MOD. 12:30 OF 4 NOVEMBER 1992'
      WRITE(2,*)
      WRITE(2,*)'FRESH FEED(NM3/H)     ',UINIT
      WRITE(2,*)'LIQUID VELOCITY(CM/S)=',UL
      WRITE(2,*)'REACTOR LENGTH(CM)   =',RL
      WRITE(2,*)'REACTOR DIAMETER(CM) =',DCOL
      WRITE(2,*)'TEMPERATURE     (K)  =',T
      WRITE(2,*)'PRESSURE       (BAR) =',PTOT
      WRITE(2,*)'CATALYST CONCENT(WT%)=',WAV*100
      WRITE(2,*)'RECYCLE RATIO        =',RRAT
      WRITE(2,*)'CAT FTS RATE PARAMETR=',FUDGE1
      WRITE(2,*)'CAT WGS RATE PARAMETR=',FUDGE2
      WRITE(2,*)'INLET VELOCITY (CM/S)=',UG
      WRITE(2,*)'H2   CONC AT INLET=     ',TINH2
      WRITE(2,*)'CO   CONC AT INLET=     ',TINCO
      WRITE(2,*)'REST CONC AT INLET=     ',TINC5
      WRITE(2,*)'CO2  CONC AT INLET=     ',TINCO2
      WRITE(2,*)'H2O  CONC AT INLET=     ',TINH2O
    SOLO IMPRIME SI EXISTE RECYCLE
      IF (RRAT.NE.0.0) THEN
        WRITE(2,*)'TOTAL  VELOCITY (CM/S)= ',UG
        WRITE(2,*)'H2   CONC AT TOT.FEED   ',FCG(1)
        WRITE(2,*)'CO   CONC AT TOT.FEED   ',FCG(2)
        WRITE(2,*)'REST CONC AT TOT FEED   ',FCG(3)
        WRITE(2,*)'CO2  CONC AT TOT FEED   ',FCG(4)
        WRITE(2,*)'H2O  CONC AT TOT FEED   ',FCG(5)
      ELSE
        WRITE(2,*)'ONCE THROUGH OPERATION............'
      ENDIF
        WRITE(2,*)'EXIT VELOCITY(CM/S)=    ',OUTUG
        WRITE(2,*)'H2   CONC AT EXIT=      ',OUTH2
        WRITE(2,*)'CO   CONC AT EXIT=      ',OUTCO
        WRITE(2,*)'REST CONC AT EXIT=      ',OUTC5
        WRITE(2,*)'CO2  CONC AT EXIT=      ',OUTCO2
        WRITE(2,*)'H2O  CONC AT EXIT=      ',OUTH2O
        WRITE(2,*)'PER PASS CONV=      ',XCOH
        WRITE(2,*)'USAGE RATIO=        ',UR
      TOTCNV=XCOH*(1+RRAT)*(CG(1)+CG(2))/(FCG(1)+FCG(2))
      WRITE(2,*)'OVERALL CONV      =',TOTCNV
      WRITE(2,*)'F ACTIVITY=         ',FACTIV
      WRITE(2,*)'THERMAL CONDUCTIVITY     W/M.K        ',THERM
      WRITE(2,*)'HEAT CAPACITY            J/KG.K       ',HCAP
      WRITE(2,*)'REINOLDS NUMBER BASED IN GAS VELOCITY',REINOL
      WRITE(2,*)'FROUD NUMBER                         ',FROUD
      WRITE(2,*)'PRANDT NUMBER                        ',PRANDT
      WRITE(2,*)'H STANTON NUMBER                     ',STANTO
      WRITE(2,*)'H INTERNAL              W/M2.K       ',HINTER
      WRITE(2,*)'WATER PRODUCTION        KG/H    ',WATER
      WRITE(2,*)'THEORETICAL WATER YIELD  G/M3 N  ',YH2O
      WRITE(2,*)'FISCHER-TROPSCH RATE   KGMOL/HR  ',FTCNV
      WRITE(2,*)'WATER GAS SHIFT RATE   KGMOL/HR  ',WGSCNV
      WRITE(2,*)'HEAT OF REACTION       K Watts   ',TOTH
      WRITE(2,*)'STEAM PRODUCE AT 15 BAR KG/H     ',STEAM

      WRITE(2,*)
      WRITE(2,*)'OUTPUT OF SUBROUTINE SLURRY'
      WRITE(2,*)'KG MOL OUT H2 =',EXITH2
      WRITE(2,*)'KG MOL OUT CO =',EXITCO
      WRITE(2,*)'KG MOL OUT C+ =',EXITRS
      WRITE(2,*)'KG MOL OUT CO2=',EXICO2
      WRITE(2,*)'KG MOL OUT H2O=',EXIH2O
```

```
      WRITE(2,*)'H2+CO CONVERTED=',DH2CO


         STOP
C                        ____________________
C_____________________________________________________________________

100   FORMAT ( 3F10.4, I10, F10.4 )
200   FORMAT ( 5X, 5( 2X, E12.4 ), I10 )
201   FORMAT ( 5X, '   S = ', 7X, '  SL = ', 7X, '  CL = ',
     $            7X, '  CG = ', 7X, '  SO = ', 7X, 'COMPONENT' )
299   FORMAT ( ' DIMENSIONLESS CONCENTRATIONS RELATIVE TO H2 AT INLET'/
     $    '      Z     ',
     $    '       U         H2         CO        REST       CO2        H2O' )
300      FORMAT ( 2X, 12( F8.4, 1X ) )

330      FORMAT ( 5X, 'IFLAG = ', I10 )
      END
C
C-----------------------------------------------------------FSUB--------
      SUBROUTINE FSUB ( X, Z, F )

      COMMON /RATE/ A,B,C,D,ALPHA,GAMMA
      COMMON /MINE/S,SL,PEG,PEL,EPS,CL,CG,V,CTOT,SO,EQ,T,PTOT,FCG,RRAT
      COMMON /REP/ RL,DCOL,UG,UL,WR,WAV,SN,ICALL,FUDGE1,FUDGE2,UINIT
      COMMON /JUAN/CSCAL,AREA,TRANSV,LIQDSP,GASDSP,CONTRAC,FACTIV,RMANI
      COMMON /JUAN2/THERM,HCAP,RMUL,RHOL,GEE,HYDR

      DIMENSION Z(21),F(11),R(5)
      DIMENSION S(5),SL(5),CL(5),CG(5),V(5),SO(5),FCG(5)
      DIMENSION SN(5)

C--------------------GASDSP---------GAS DISP COEFFICIENT-----
      GASDSP=1.9*HYDR**2*UG**(5/11)
C--------------------LIQDSP---------LIQ DISP COEFFICIENT-----
      LIQDSP=2.7*HYDR**1.4*((UG)**0.3)
C---------------------PEG  PECLET NUMBER FOR GAS PHASE--------------
      PEG=RL*UG/GASDSP
C---------------------PEL  PECLET NUMBER FOR LIQ PHASE--------------
      PEL=RL*UL/LIQDSP
C------DEFINITION OF THE INTERFACIAL AREA AT ACTUAL CONDITIONS---
      AREA=0.31*UG**0.603*RMANI
C---------------------------------STANTON NUMBER FOR GAS AND LIQUID--
      DO 11 J=1,5
          S(J)  =AREA*SN(J)*RL/(UG*SO(J))
          SL(J) =AREA*SN(J)*RL/UL
11       CONTINUE
C-----------------------------------------------------GAS HOLDUP EXP.-------
C       NEW EQUATION INTRODUCED ON THE  18/01/91

       EPS=0.21*(Z(1)*UG)**0.3*(1+(T-518)*0.008)*(1+(PTOT-20)*0.01)

      IF (EPS.EQ.0.0)EPS=1E-6

---------------------EQUATION 6 (STERN-1985) OVERALL MASS BALANCE--
      F(1) = -(S(1)*(Z(2)-Z(12))+S(2)*(Z(4)-Z(14))
     $                +S(3)*(Z(6)-Z(16))+S(4)*(Z(8)-Z(18))
     $                +S(5)*(Z(10)-Z(20)))/CTOT
----------------------------GAS PHASE MASS BALANCE (STERN 85 EQ 3)---
      DO 22 J=1,5
          K = J+1
          L = 2*J
          I = L+10
          M = L+1
          F(K) = (PEG/EPS)*(Z(1)*Z(M)+F(1)*Z(L)+S(J)*(Z(L)-Z(I)))
2        CONTINUE
```

```
-------------------------------------SCHULTZ FLORY DISTRIBUTION----
      DENOM = 3.0+(1.0-ALPHA)**2.0+GAMMA*ALPHA*(1.0-ALPHA)
      DEN = Z(14)+Z(20)
      COH2=PTOT/CTOT*273/T/22400
      IF ( DEN .LT. 0.00001 )  DEN = 0.00001
-------------CAMBIO-----------------FISCHER TROPSCH RATE EQUATION------
       FACTIV=1.0
       FACTIV=3.683045-15.453*WAV+22.25*WAV**2

      AA = RL*(1-EPS)*WAV*2595.6*Z(14)*Z(12)**2*CSCAL**2*FUDGE1*FACTIV
      BB = UL*(Z(20)*CSCAL+2.06E4*Z(14)*Z(12))
      IF (BB.EQ.0.0) THEN
            RR=0
      ELSE
            RR=AA/BB*EXP(-7500/T)*2E6

      RR = RL*(1-EPS)*WAV/UL/COH2*PTOT/CTOT*EXP(8.194-7500/T)*
     1   Z(12)*SO(1)/(1+7*(Z(20)*SO(5))/(Z(14)*SO(2)))*FUDGE1

      ENDIF
      IF (Z(20).EQ.0.0) THEN
          RW=0
      ELSE
-----------------------------WATER GAS SHIFT EQUATION-----------
        I HAVE INCLUDE AN 1000 FACTOR TO MANIPULATED BY SCREEN

      RW = RL*(1-EPS)*WAV/UL/COH2*SQRT(PTOT)/CTOT*EXP(1.716-7650/T)*
     1  (Z(14)*SO(2)-Z(12)*Z(18)/Z(20)/SO(5)*SO(1)*SO(4)/EQ)*
     1     FUDGE2*FACTIV

      ENDIF
 -----------------------------STOICHIOMETRIC COEFFICIENTS---------
      R(1) = (DENOM-1.0)/DENOM*RR-RW
      R(2) = RR/DENOM+RW
      R(3) = -(1.0-ALPHA)*RR/DENOM
      R(4) = -RW
      R(5) = -RR/DENOM+RW
----------------------------LIQUID PHASE MASS BALANCE FOR EACH COMP-
      DO 33 J=1,5
          L=2*J
          I=L+10
          K=L+11
          M = J+6
          F(M) = (PEL/(1.0-EPS))*(Z(K)-SL(J)*(Z(L)-Z(I))+R(J)*SO(J))
        CONTINUE
         FORMAT ( 2X, 12( F8.3, 1X ) )
      RETURN
      END
-------------------------------------------------GSUB-----------------
      SUBROUTINE GSUB ( I, Z, G )

      COMMON /RATE/ A,B,C,D,ALPHA,GAMMA
      COMMON /MINE/ S,SL,PEG,PEL,EPS,CL,CG,V,CTOT,SO,EQ,T,PTOT,FCG,RRAT
      COMMON /REP/ RL,DCOL,UG,UL,WR,WAV,SN(5),ICALL,FUDGE1,FUDGE2,UINIT
      COMMON /JUAN/CSCAL,AREA,TRANSV,LIQDSP,GASDSP,CONTRAC,FACTIV,RMANI
      COMMON /JUAN2/THERM,HCAP,RMUL,RHOL,GEE,HYDR

      DIMENSION Z(21)
      DIMENSION S(5),SL(5),CL(5),CG(5),V(5),SO(5),FCG(5)
--------------------GASDSP----------GAS DISP COEFFICIENT-----
      GASDSP=1.9*HYDR**2*UG**(5/11)
--------------------LIQDSP----------LIQ DISP COEFFICIENT-----
      LIQDSP=2.7*HYDR**1.4*((UG)**0.3)
---------------------PEG  PECLET NUMBER FOR GAS PHASE--------------
      PEG=RL*UG/GASDSP
---------------------PEL  PECLET NUMBER FOR LIQ PHASE--------------
```

```
      PEL=RL*UL/LIQDSP

      MT = 2*I-21
      M = I-1
      L = 2*M
      N = L+1
      J = I-6
C-------------------------------------GAS HOLD UP EXP--------------
       EPS=0.21*(Z(1)*UG)**0.3*(1+(T-518)*0.008)*(1+(PTOT-20)*0.01)
C ------------------------------------------------------------------
      IF ( I .EQ. 1 ) THEN
          G = Z(1)-1.0
      ELSE IF ( I .LE. 6 ) THEN
          G = Z(L)-CG(M)-Z(N)/PEG*EPS
      ELSEIF ( I .LE. 11 ) THEN
          G = Z(L)-CL(J)-Z(N)*(1.0-EPS)/PEL
      ELSE
          G = Z(MT)
      ENDIF
      RETURN
      END
C----------------------------------------------------------DGSUB---------
      SUBROUTINE DGSUB ( I, Z, DG )

      COMMON /RATE/ A,B,C,D,ALPHA,GAMMA
      COMMON /MINE/ S,SL,PEG,PEL,EPS,CL,CG,V,CTOT,SO,EQ,T,PTOT,FCG,RRAT
      COMMON /REP/ RL,DCOL,UG,UL,WR,WAV,SN(5),ICALL,FUDGE1,FUDGE2,UINIT
      COMMON /JUAN/CSCAL,AREA,TRANSV,LIQDSP,GASDSP,CONTRAC,FACTIV,RMANI
      COMMON /JUAN2/THERM,HCAP,RMUL,RHOL,GEE,HYDR

      DIMENSION DG(21),Z(21)
      DIMENSION S(5),SL(5),CL(5),CG(5),V(5),SO(5),FCG(5)

C--------------------GASDSP----------GAS DISP COEFFICIENT-----
      GASDSP=1.9*HYDR**2*UG**(5/11)
C--------------------LIQDSP----------LIQ DISP COEFFICIENT-----
      LIQDSP=2.7*HYDR**1.4*((UG)**0.3)
C---------------------PEG  PECLET NUMBER FOR GAS PHASE--------------
      PEG=RL*UG/GASDSP
C---------------------PEL  PECLET NUMBER FOR LIQ PHASE--------------
      PEL=RL*UL/LIQDSP

      K = 4*5+1

      DO 11 J=1,K
          DG(J) = 0.0
11      CONTINUE

      M = I-1
      MT = 2*I-21
      L = 2*M
      N = L+1
C------------GAS HOLD UP-----
       EPS=0.21*(Z(1)*UG)**0.3*(1+(T-518)*0.008)*(1+(PTOT-20)*0.01)

C ------------------------
      IF ( I .EQ. 1 ) THEN
          DG(1) = 1
      ELSEIF ( I .LE. 6 ) THEN
          DG(L) = 1
          DG(N) = -EPS/PEG
      ELSEIF ( I .LE. 11 ) THEN
          DG(L) = 1
          DG(N) = -(1.0-EPS)/PEL
      ELSE
          DG(MT) = 1
```

```
      ENDIF
      RETURN
      END
--------------------------------------------------------DFSUB-------
      SUBROUTINE DFSUB ( X, Z, DF )

      COMMON /MINE/ S,SL,PEG,PEL,EPS,CL,CG,V,CTOT,SO,EQ,T,PTOT,FCG,RRAT
      COMMON /RATE/ A,B,C,D,ALPHA,GAMMA
      COMMON /REP/ RL,DCOL,UG,UL,WR,WAV,SN,ICALL,FUDGE1,FUDGE2,UINIT
      COMMON /JUAN/CSCAL,AREA,TRANSV,LIQDSP,GASDSP,CONTRAC,FACTIV,RMANI
      COMMON /JUAN2/THERM,HCAP,RMUL,RHOL,GEE,HYDR

      DIMENSION DF(11,21),Z(21),FB1(11),FB2(11)
      DIMENSION S(5),SL(5),CL(5),CG(5),V(5),SO(5),FCG(5)
      DIMENSION SN(5)
      DIMENSION DS(5),DSL(5)

      DO 11 J=1,21
          CALL FSUB(X,Z,FB1)
          ZSAVE=Z(J)
          Z(J)=Z(J)*1.01
          IF(ABS(Z(J)-ZSAVE).LT.0.000001)Z(J)=ZSAVE+0.000001
          ZDIF=Z(J)-ZSAVE
          CALL FSUB(X,Z,FB2)
          Z(J)=ZSAVE
          DO 22 K=1,11
             DF(K,J) = (FB2(K)-FB1(K))/ZDIF
          CONTINUE
      CONTINUE
      RETURN
      END
  ----------------------------------------------------PECLET---------
      SUBROUTINE PECLET

      COMMON /RATE/ A,B,C,D,ALPHA,GAMMA
      COMMON /MINE/ S,SL,PEG,PEL,EPS,CL,CG,V,CTOT,SO,EQ,T,PTOT,FCG,RRAT
      COMMON /REP/ RL,DCOL,UG,UL,WR,WAV,SN,ICALL,FUDGE1,FUDGE2,UINIT
      COMMON /JUAN/CSCAL,AREA,TRANSV,LIQDSP,GASDSP,CONTRAC,FACTIV,RMANI
      COMMON /JUAN2/THERM,HCAP,RMUL,RHOL,GEE,HYDR

      DIMENSION S(5),SL(5),CL(5),CG(5),V(5),SO(5),FCG(5)
      DIMENSION SN(5)
        DO 11 J=1,5

---------------------------TRANSVERSAL AREA----------------------
           TRANSV=0.25*3.14159*DCOL**2
------------------------INLET LINEAR VELOCITY--------------------
          UG=UINIT*(1.+RRAT)*T/273/PTOT/.0036/TRANSV/0.9869233
--------------------------------FISCHER TROPSCH COEFFICIENT------
      EQ = .00938*EXP(4777.4/T)
-----------TOWEL AND ACKERMAN 269--GAS DISPERSION COEFFICIENT--
      GASDSP=1.9*HYDR**2*UG**(5/11)
-------------------------------------LIQUID DISPERSION COEFFICIENT----
      LIQDSP=2.7*HYDR**1.4*(UG**.3)
---------------------------------------PECLET NUMBER FOR GAS PHASE---
      PEG = RL*UG/GASDSP
---------------------------------------PECLET FOR LIQUID PHASE
      PEL = RL*UL/LIQDSP
-----------------------------INTERFACIAL AREA (CM2)-AKL (CO)----------
      AREA = 0.31*UG**0.603*RMANI
----------------------------------------GAS HOLD UP VALUE-------
       EPS=0.21*(UG)**0.3*(1+(T-518)*0.008)*(1+(PTOT-20)*0.01)

-----------------------------------WAX DENSITY
      RHOL = 965.72-0.5322*T
-----------------------------WAX THERMAL CONDUCTIVITY----- W/ M.K------
```

```
      THERM=0.221707-1.4602E-4*T
-----------------------------WAX HEAT CAPACITY ----------J/KG.K--------
      HCAP=2090.2+3.86*T
----------------------------------------MOLAR VOLUME RATIOS
      SO(1) = 4.02E5*EXP(740.3/T)/(T*RHOL)
      SO(2) = 4.99E5*EXP(458.3/T)/(T*RHOL)
      SO(3) = 1.78382E7*EXP(-427.218*5*(1/T-1.03E-3))
    #         /(8.31434*T*(3000-1.79*T))
      SO(4) = 1.23E6*EXP(-373/T)/(T*RHOL)
      SO(5) = 4.05E6*EXP(-1229/T)/(T*RHOL)

-----------------------------------------------HYDROGEN MOL VOL
      DLH2 = 7.35E-7*EXP(-2285/T)

------------------------------GRAVITY FACTOR
      GEE = 9.81
---------------------------------WAX VISCOSITY
      RMUL = 1.8664E-5*EXP(2222.22/T)

------------------------MOLAR VOLUME RATIOS
      ----------------------VALUES--------------------
       SN(1) =1.35744
       SN(2) =1.0
       SN(3) =0.581616
       SN(4) =0.959983
       SN(5) =1.2114145
----------------------------------------STANTON NUMBERS
          S(J) = AREA*SN(J)*RL/(UG*SO(J))
          SL(J)= AREA*SN(J)*RL/UL
         ---------------------------------
      CONTINUE
      RETURN

         FORMAT ( 7F10.4 )
         FORMAT ( 4F10.4 )

      END
----------------------------------------------------------SOLUTN----

... SUBROUTINE SOLUTN PROVIDES AN APPROXIMATION TO THE SOLUTION
... TO THE PROBLEM. THE APPROXIMATION IS VERY SIMPLISTIC, WITH
... CONCENTRATIONS AT ALL POINTS BEING GUESSED AT THEIR INPUT
... VALUES, AND THE VELOCITY DECLINING LINEARLY BY 20% OVER THE
... LENGTH OF THE REACTOR. IT DOES, HOWEVER, KEEP THE DIVIDE-BY-
... ZEROES AWAY FROM THE DOOR.

     SUBROUTINE SOLUTN(X,Z,DMVAL)
     DIMENSION Z(21),DMVAL(11)
       COMMON/ZZZ/CI(5),INXR(5)
       COMMON /JUAN/CSCAL,AREA,TRANSV,LIQDSP,GASDSP,CONTRAC,FACTIV,RMANI
       COMMON /JUAN2/THERM,HCAP,RMUL,RHOL,GEE,HYDR
     Z(1)=1-CONTRAC*X
     DO 10 I=1,5
         TEMP=CI(I)

.. VERY SMALL CONCENTRATIONS CAUSE NUMERICAL INSTABILITY

         IF ( TEMP .LT. 1E-3 ) TEMP = 1E-3
         Z(2*I)=TEMP
         Z(2*I+10)=TEMP
         Z(2*I+1)=0.
         Z(2*I+11)=0.
     CONTINUE
     DO 20 I=1,11
         DMVAL(I)=0.
     CONTINUE
```

Appendix 8

Physical properties used in the slurry computer model

$$C_p = 2090.2 + 3.86\ T \quad (J/kg.K)$$

$$\mu_{wax} = \exp\left(\frac{20000}{9T} - \frac{98}{9}\right) \quad (Pa.s)$$

$$\rho_{wax} = 820.43 + 0.5322 * T \quad (T\ in\ C) \quad (kg/m3)$$

$$\sigma_{wax} = 0.576 - 6.2727 * T \quad (kg/s2)$$

$$\lambda_{wax} = 0.221707 - 1.4602E-4 * T \quad (W/m.K)$$

$$r_{FT} = K's \frac{C_{H,L} C_{CO,L}}{C_{CO,L} + 7 C_{H2O,L}}$$

$$r_{wgs} = K's * C_{CO,L} - \frac{C_{H2,L} * C_{CO2,L}}{K C_{H2O,L}}$$

$$D_G = 1.894 U_G^{\frac{5}{11}} d^2 \qquad cm^2/s$$

$$D_L = 2.7 d^{1.4} U_G^{0.3} \qquad cm^2/s$$

$$M_{H2} = 4.02 X 10^5 \frac{e^{\frac{740.3}{T}}}{T\rho}$$

$$M_{CO} = 4.99 X 10^5 \frac{e^{\frac{458.3}{T}}}{T\rho}$$

$$M_{CO2} = 1.23 X 10^6 \frac{e^{-\frac{373}{T}}}{T\rho}$$

$$M_{H2} = 4.05 X 10^6 \frac{e^{-\frac{1229}{T}}}{T\rho}$$

$$k_H = 7.35 x 10^{-7} e^{-\frac{2285}{T}}$$

The molar volume ratios to use in the calculation of the mass transfer coefficient of the other component are (relative to CO):

```
for Hydrogen = 1.35744
for C2H5 = 0.581616
for CO2= 0.959983
for H2O= 1.2114
```

STATE OF KNOWLEGDE OF THE SLURRY BED REACTOR
AT APRIL 1992

PARAMETER	EFFECT OF	LITER. INFORM	FROM ARGE	FROM CSIR	FROM BENCH SCALE	FROM MICRO REACTOR	FROM DEMONST. REACTOR	FUTURE WORK W.P.P.	COLD MODEL FUTURE	OPTIMIZE ?
GAS HOLDUP										
	Pressure			B			A2	Y		Y
	Temperature			B			A1			
	Gas velocity			B			A1			
	Liquid velocity	B							Y	Y
	Column diameter						A2			
	Particle size	B							Y	Y
	Solid Concentration	D		B	D		A1			
	Surface tension	B							Y	Y
	Radial & axial	B		B				Y	E	Y
	Sparger design	B						Y	Y	Y
GAS DISPERSION										
	Pressure	C								C
	Temperature	C								C
	Solid concentration	C						E	E	
	Internals	C					A2		Y	Y
	Column diameter	B					A1			
	Gas velocity	B					A1			
	Reactor Geometry	B					B	Y	Y	Y
LIQUID DISPERSION										
	Pressure	C								
	Temperature	C								
	Solid Concentration	B								
	Internals	B					A1			Y
	Column diameter	A2					A1			
	Gas velocity	A2					A1			
	Reactor Geometry	B					A2			Y
SOLID DISPERSION										
	Pressure	C								
	Temperature	C								
	Solid Concentration	B					A2		Y	
	Internals	B					A2		Y	Y
	Column diameter	C								
	Gas velocity	A2		B			A2			
	Reactor Geometry	B							Y	Y
GAS/LIQ.INTERFACIAL AREA (BUBBLE SIZE)										
	Pressure	B						Y		
	Temperature	C						Y		
	Solid Concentration	D						Y		
	Internals	B							Y	
	Column diameter	A2								
	Gas velocity	B					A2		Y	
	Reactor Geometry	C							Y	Y
	Gas density	B					A2	Y		
	Coalescence	B					A2		Y	Y
	Breakage	B					A2	Y	Y	Y
	Sparger design	B		B					Y	Y
	Liquid velocity	C							Y	Y
	Max.bubble size	C					A1			
	Solid surf. wettability	B							Y	Y
CATALYST										
	Ageing				B		A1			
	Poisoning		B					E		
	Particle size		B			B	A2			Y
	Temperature		B			B		Y		Y
	Gas/catalyst					B		Y		Y
	Partial Pressure					B		Y		
	Attrition						A1		Y	Y
ISOTHERMAL BEHAVIOR										
	Gas velocity	C					A1	Y		Y
	Liquid velocity	C							Y	Y
	Internals orientation	C					A2		Y	Y
	Coils position	C							Y	Y
	Column diameter	C								
	Solid concentration	C					A2	Y	Y	Y
HEAT TRANSFER COEFFICIENT										
	Gas velocity	B					A2	Y	Y	Y
	Liquid velocity	C							Y	Y
	Internals	C							Y	Y
	Coils position	C							Y	Y
	Coils pitch	C							Y	Y
	Solid concentration	B					A2	Y	Y	Y
	Fouling	C							Y	
GENERAL										
	Foaming	D		B	B	B	E	Y		Y
	Wax entrainment	C					A2	Y	Y	Y
	Solid entrainment	C					A2	Y	Y	Y
	Critical Gas velocity for solid suspension	B					A2	Y	Y	Y

A1: Enough for design purposes	D: Conflicting Data
A2: Enough for extrapolation	E: Require information
B: Trends	Y: Yes
C: Unknown	

DAILY MANAGEMENT REPORT

SASOL SLURRY BED PILOT PLANT MASS BALANCE

DATE: 23-Oct-92 RUN 13 DAY 25 SSBP MB MODEL: VERSION 4

DISTRIBUTION LIST

R.Espinoze
J.Inge
R.C.Keifkens
FEJ Malherbe
T. Shingles

GAS FLOWS

	units	TOTAL FEED	REACTOR EXIT GAS
Uncorrected	m3n/h	8862	8690
TG Corrected	m3n/h	8862	8282
CH4 Tracer	m3n/h	8862	8098

CONVERSION

	H2+CO	CO+CO2	Usage Ratio
Uncorrected	10.6%	10.2%	1.59
TG Corrected	14.8%	14.4%	1.78
CH4 Tracer	15.8%	15.4%	1.79

LIQUID PRODUCT DRAININGS

	kg/day	Ratio
Reactor Wax	2044	1.00
Hot Condensate	508	0.25
Cold Condensate	2284	1.12
Reaction Water	7931	3.88

BALANCE ACCURACY

CARBON	105%
HYDROGEN	106%
OXYGEN	109%

PRODUCT DISTRIBUTION

	TOTAL FEED	PRODUCTS - TG CORRECTED			TAIL GAS
		YIELD	MASS SELECTIVITIES		
	%	g/m3n	%	CH4 fixed	%
CO2	1.45	11.4	▨	▨	2.18
Methane	14.50	8.40	4.3	4.13%	16.64
Ethylene	0.05	0.42	1.5	1.47%	0.09
Ethane	0.13	0.25	0.6	0.59%	0.16
Propylene	0.03	1.18	4.3	4.34%	0.10
Propane	0.03	0.32	1.1	1.06%	0.05
Butylene	0.02	0.43	1.5	1.52%	0.04
Butane	0.03	-0.29	0.7	0.00%	0.02
Pentanes	0.03	-0.07	0.9	0.00%	0.03
Hexenes	0.02	-0.05	0.0	0.00%	0.02
Cold Condensate	0.00	10.76	40.1	40.22%	0.00
Hot Condensate	0.00	2.38	8.9	8.91%	0.00
Reactor Wax	0.00	9.61	37.9	37.78%	0.00
Hydrogen	56.58	▨	▨	▨	55.03
Inerts (N2+Ar)	1.50	▨	▨	▨	1.78
Carbon Monoxide	25.69	▨	101.6	100.0%	24.00
H2 / CO RATIO	2.20	▨	▨	▨	2.29

ISOTHERMAL BEHAVIOUR

T-PROBE level (m) No	TEMP °C
GAS OUT	232
▨	▨
22.7 -> T16	232
16.0 -> T21	231
13.1 -> T19	244
9.4 -> T11	238
6.5 -> T9	▨
3.7 -> T7	232
2.3 -> T6	238
1.3 -> T5	237
0.1 -> T1	235
▨	▨
GAS IN	188

DESIGN & OPERATING DATA

Variable	Unit	
Reactor Pressure	Barg	19.6
BFW makeup/steam	kg/h	396
Overall H.T.Coeff	W/m2-K	379
Reactor Bed Level	m	17.3
Cat.Concentration	% mass	10.3
Slip stream flow	m3n/h	24.3

Checked: ______________

Approved ______________

ASSUMPTIONS

Rev. 03-Jan-1992

M.W. Hot Condensate:	278
M.W. Cold Condensate:	145
Water in Cold Condensate	0.00%